STUDY OF GLYCATION AND DRUG INDUCED PROTEIN CROSSLINKING

A THESIS SUBMITTED TO THE

UNIVERSITY OF PUNE

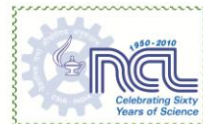FOR THE DEGREE OF

DOCTOR OF PHILOSOPHY

IN

BIOTECHNOLOGY

BY

Ms. SNEHA BALASAHEB BANSODE

UNDER THE GUIDANCE OF

Dr. MAHESH J. KULKARNI

DIVISION OF BIOCHEMICAL SCIENCES

CSIR-NATIONAL CHEMICAL LABORATORY

PUNE-411008, INDIA

JULY 2014

CERTIFICATE

Certified that the work in Ph.D. thesis entitled '**Study of glycation and drug induced protein crosslinking**' submitted for the award of Ph.D. degree by Ms. Sneha Balasaheb Bansode was carried out by the candidate under my supervision. The material obtained from other sources has been duly acknowledged in this thesis.

Date: Dr. Mahesh J. Kulkarni

Place: (Research Guide)

CANDIDATE'S DECLARATION

I hereby declare that the thesis entitled "**Study of glycation and drug induced protein crosslinking**" submitted for the degree of Doctor of Philosophy in Biotechnology to the University of Pune has not been submitted by me to any other university or institution. This work was carried out at CSIR-National Chemical Laboratory, Pune, India.

Sneha B. Bansode   **Date:**

Senior Research Fellow   **Place:**

Biochemical Sciences Division

CSIR-National Chemical Laboratory

Pune-411008, India

Dedicated to

My Beloved Family

Table of Contents

ACKNOWLEDGEMENTS

Abbreviations

AChE	:	Acetylcholinesterase
ACN	:	Acetonitrile
AD	:	Alzheimer's disease
ADH	:	Alcohol Dehydrogenase
AFM	:	Atomic Force Microscopy
AGE	:	Advanced Glycation End Product
Aβ	:	Amyloid β
ANS	:	1-Anilino-8-Naphthalene Sulphonate
ATCI	:	Acetyl Thiocholine Iodide
BBB	:	Blood Brain Barrier
BSA	:	Bovine Serum Albumin
CBB	:	Coommassie Brilliant Blue
CD	:	Circular Dichroism
CHAPS	:	3-[(3-cholamidopropyl) dimethylammonio]-1-propanesulfonate
Da, kDa	:	Dalton, Kilodalton
DAB	:	Diaminobenzidine
DTNB	:	5, 5-dithiobis (2- nitrobenzioc) acid
EDTA	:	Ethylenediamminetetraacetate
ENO	:	Enolase
ESI MS	:	Electro Spray Ionisation Mass Spectrometry
FBS	:	Fetal Bovine Serum
FDA	:	Food and Drug Administration

g	:	Relative centrifugal force
g, mg, μg, ng	:	Gram, milligram, microgram, nanogram
GAPDH	:	Glyceraldehyde 3-Phosphate Dehydrogenase
GST	:	Glutathione S-Transferase
HbA1c	:	Glycated haemoglobin
HDMS	:	High Definition Mass Spectrometry
HSA	:	Human Serum Albumin
HSP	:	Heat Shock Protein
IAA	:	Iodoacetamide
ICDH	:	Isocitrate Dehydrogenase
ITC	:	Isothermal Titration Calorimetry
LDH	:	Lactate Dehydrogenase
MALDI MS	:	Matrix Associated Laser Desorption Ionisation MS
MD simulation	:	Molecular Dynamic Simulation
MDH	:	Malate Ddehydrogenase
MRE	:	Mean Residual Ellipticity
MSE	:	MS at elevated energy
MTDLs	:	Multi-Target-Directed Ligands (MTDLs)
PLGS	:	Protein Lynx Global Server
PRPs	:	Protease Resistant Proteins
PVDF	:	Polyvinylidene fluride
RAGE	:	Receptor for Advanced Glycation End Products
RMSD	:	Root Mean Square Deviation

SASA	:	Solvent Accessible Surface Area
SOD	:	Superoxide Dismutase
STZ	:	Streptozotocin
TBS	:	Tris buffered saline
ThT	:	Thioflavin T
V, kV	:	Volt, kilovolt
XIC	:	Extracted Ion Chromatogram
ΔM	:	Mass Increase

List of Tables

List of Figures

Thesis Abstract

Crosslinking and aggregation of proteins has been related to several disorders such as diabetes, Alzheimer's and other neuronal diseases. Glycation is known to accelerate protein cross-linking and aggregation. The crosslinked and aggregated proteins plays a major role in the pathogenesis of diseases. Therefore this thesis mainly focuses on the identification, characterisation of crosslinked proteins and inhibition of this process. In addition to glycation, drugs that promote glycation were also studied.

Proteomic analysis of cross-linked protein aggregates in diabetes

Glycation induced protein aggregation has been implicated in the development of diabetic complications and neurodegenerative diseases. These aggregates are known to be resistant to proteolytic digestion. Here we report the identification of protease resistant proteins from the streptozotocin induced diabetic rat kidney, which included enzymes in glucose metabolism and stress response proteins. These protease resistant proteins were characterized to be advanced glycation end products modified and ubiquitinated by immunological and mass spectrometry analysis. Further, diabetic rat kidney exhibited significantly impaired proteasomal activity. The functional analysis of identified physiologically important enzymes showed that their activity was reduced in diabetic condition. Loss of functional activity of these proteins was compensated by enhanced gene expression. Aggregation prone regions were predicted by *in silico* analysis and compared with advanced glycation end products modification sites. These findings suggested that the accumulation of protein aggregates is an inevitable consequence of impaired proteasomal activity and protease resistance due to advanced glycation end products modification.

Protriptyline, an anti-depressant inhibits protein cross linking and multiple targets of Alzheimer's disease

Alzheimer's disease (AD) is a complex neurodegenerative disorder involving multiple cellular and molecular processes. The discovery of drug molecules capable of targeting multiple factors involved in AD pathogenesis would greatly facilitate in improving therapeutic strategies. The repositioning of existing non-toxic drugs could dramatically reduce the time and costs involved in developmental and clinical trial stages. In this study, preliminary screening of 140 FDA approved nervous system drugs by docking suggested the viability of the tricyclic group of antidepressants against three major AD targets, viz. Acetylcholinesterase (AChE), β-secretase (BACE-1), and amyloid β (Aβ) aggregation, with one member, protriptyline, showing highest inhibitory activity. Detailed biophysical assays, together with isothermal calorimetry, fluorescence quenching experiments, kinetic studies and atomic force microscopy established the strong inhibitory activity of protriptyline against all three major targets. The molecular basis of inhibition was supported with comprehensive molecular dynamics simulations. Further, the drug inhibited glycation induced amyloid aggregation, another important causal factor in AD progression. This study has led to the discovery of protriptyline as a potent multi target directed ligand and established its viability as a promising candidate for AD treatment.

Tolbutamide, an anti-diabetic drug promotes glycation

In this study, we have investigated the effect of tolbutamide on albumin confirmation using BSA as a model protein. We have found that the binding of tolbutamide, a first generation sulfonylurea, induces significant conformational change in the albumin, which was proved by Thioflavin T assay, ANS assay, and CD analysis. Molecular dynamic simulations suggested that the binding of tolbutamide increases the solvent accessibility of lysine residues, the hotspots of glycation of albumin. Furthermore, the change in conformation of albumin facilitates increased glycation, which was observed by AGE fluorescence and the results were corroborated by mass spectrometric analysis. This study suggested

that tolbutamide enhances albumin glycation by inducing conformational change in the protein and hence it could be a risk factor if used for prolonged period.

CHAPTER I

Introduction

I.1. Diabetes:

Diabetes is a metabolic disorder characterized by high blood glucose level. The disease results due to defects in insulin secretion, insulin action, or both (Expert Committee 2003). Typical symptoms of diabetes include polyuria, blurred vision, thirst and weight loss. Prolonged glucose in diabetes mellitus causes various complications including retinopathy, nephropathy, neuropathy and cardiovascular diseases.

I.1.1. Classification of diabetes

Broadly, diabetes mellitus can be classified into three main types: (a) type 1 diabetes which results from failure in insulin secretion, (b) type 2 diabetes which is a result of insulin resistance and (c) gestational diabetes which is observed among pregnant women, who never had diabetes before but have a high blood glucose level during pregnancy.

I.1.1.a. Type 1 diabetes

Type 1 diabetes was formerly known as insulin-dependent diabetes mellitus (IDDM). It is characterized by autoimmune destruction of the β-cells of the islets of pancreas, with consequent insulin deficiency. It is often associated with elevated blood glucose levels including symptoms like polyuria, polydipsia, and unexplained weight loss (Rother, 2007).

I.1.1.b. Type 2 diabetes

Type 2 diabetes is also known as non-insulin-dependent diabetes mellitus (NIDDM), adult-onset diabetes or obesity-related diabetes. It is often caused by insulin resistance which may be combined with relatively reduced insulin secretion. Although patients with type 2 diabetes may appear to have normal insulin levels, however their levels are relatively low in relation to elevated plasma glucose levels (Ward et al., 1984). Type 2 diabetes accounts for 90 percent of all people diagnosed with diabetes

I.1.1.c. Gestational diabetes

Gestational diabetes occurs in ~5% women during pregnancies but the condition may improve or disappear after delivery. Thirty to forty percent of women experiencing gestational diabetes develop type 2 diabetes within five to ten years. It is fully treatable only if critical medical supervision is achieved effectively throughout the pregnancy (Homko et al., 1996). Weight gain and production of hormone Resistine are the two main factors responsible for the onset of gestational diabetes (Saldana et al., 2006; Kuzmicki et al., 2009).

I.2. Global burden and prevalence of diabetes

The prevalence of diabetes is increasing due to population growth, aging, urbanization, obesity and physical inactivity (Wild et al., 2004). The number of people suffering from diabetes will rise from 151 million in the year 2000 (Amos et al., 1997), to 221 million by the year 2010, and to 300 million by 2025 (King et al., 1998). The top three countries for estimated number of adults with diabetes between 2000 and 2025 are India, China, and the U.S.A. with India alone having 31 million diabetic people at present. The number might increase to 79 million by 2025 which is more than double (Wild et al., 2004) (Table 1.1).

Table 1.1 List of countries with the highest numbers of estimated cases of diabetes for 2000 and 2030. (*Table adopted from Wild S et al., 2004*)

	2000		2030	
Ranking	**Country**	**People with diabetes (millions)**	**Country**	**People with diabetes (millions)**
1	India	31.7	India	79.4
2	China	20.8	China	42.3
3	U.S.A.	17.7	U.S.A.	30.3
4	Indonesia	8.4	Indonesia	21.3
5	Japan	6.8	Japan	13.9
6	Pakistan	5.2	Pakistan	11.3
7	Russian Federation	4.6	Russian Federation	11.1
8	Brazil	4.6	Brazil	8.9
9	Italy	4.3	Italy	7.8
10	Bangladesh	3.2	Bangladesh	6.7

I.3. Diabetes and glycation

Prolonged exposure of plasma proteins to the elevated blood glucose has been observed in diabetic patients with poor glycemic control (Austin et al., 1987). Several plasma proteins including hemoglobin, serum albumin and transferrin are known to undergo glycation, a post translational modification (PTM) caused by non-enzymatic reaction between glucose and protein (Ulrich et al., 2001). During glycation, condensation reaction between carbonyl group of glucose and free amino group of protein lead to the formation of Schiff's base. This is the first step of glycation reaction and is reversible in nature. The next step involves conversion of thermodynamically unstable Schiff's base into a stable irreversible Amadori product. Finally, the Amadori product undergoes a series of dehydration and fragmentation reactions and results into a variety of carbonyl compounds including methylglyoxal, glyoxal, glucosones, 3-deoxyglucosone (3-DG) etc (Thornalley, 1999). These carbonyl compounds are more reactive than glucose or other reducing sugars, and act as propagators of reaction leading to the formation of advanced glycation end products (AGEs). Further, AGEs have known to interact with the amino groups of several other proteins like collagen thus resulting in the formation of protein cross-linkings (Reddy et al., 2004) (Figure 1.1).
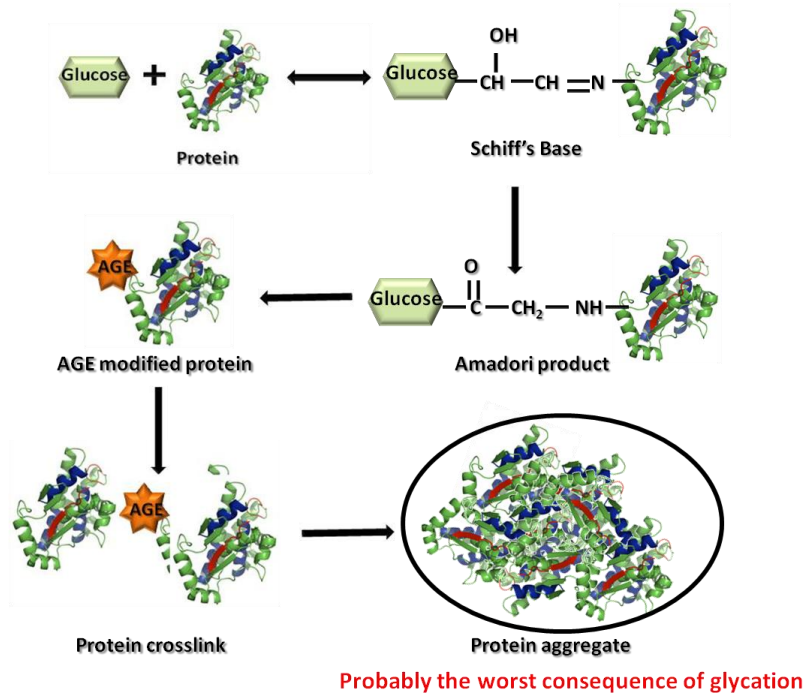
Figure 1.1 Mechanism of formation of advanced glycation end products (AGEs).

Different modifications have been reported on glycated proteins and have been characterized with mass spectrometric analysis. For example, Table 1.2 depicts glycation modification at lysine residue with a corresponding increase in mass of 162.0258 Da. Some of these modifications namely carboxymethyllysine (CML), carboxyethyllysine (CEL) and pyrraline have been reported in the previous studies (Wa et al., 2007; Thornalley et al., 1990; Biemel et al., 2001).

Table 1.2 Glycation modifications with mass increase (ΔM) for different AGEs.

S. No	Abbreviations	Modification	ΔM (Da)
1	FL	Fructosyl-lysine	162.0528
2	CEL	N_ε-carboxyethyl-lysine	72.0211
3	CML	N_ε-carboxymethyl-lysine	58.0055
4	PYR	Pyrraline	108.0211
5	FL-2H$_2$O	Fructosyl-lysine- 2H$_2$O	126.0317
6	IMI-A	Imidazolone-A	144.03
7	IMI-B	Imidazolone-B	142.0266
8	ARGPYR	Argpyrimidine	80.0262
9	MG-H1	Nε-(5-hydro-5-methyl-4-imidazolon-2-yl)ornithine	54.0106
10	G-H1	Nε-(5-hydro-4-imidazolon-2-yl)ornithine	39.9949
11	AFGP	1-alkyl-2-formyl-3,4-glycosyl-pyrrole	270.074
12	MOLD	Methyl Glyoxal Lysine Dimer	49.0078
13	CROSSLINE	Crossline	252.11

I.4. Glycation induced protein crosslinking

One of the major and worst consequence of glycation reaction is generation of covalently cross-linked proteins. There are several cross-links

reported to date. For example, Pentosidine, MOLD (Methylglyoxal Lysine dimer) and GOLD (Glyoxal Lysine dimer) (Wellsknecht et al., 1995), cross-lines (Nakamura et al., 1992), vesperlysine (Nakamura et al., 1997), glucosepane and DOGDIC (Biemel et al., 2001). These are glyction crosslinks reported to be present in vivo and their structrures are given in the Figure 1.2.

A. Lysine-Arginine crosslinks

Pentosidine

Glucosepane

DOGDIC

B. Lysine-Lysine crosslinks

GOLD

MOLD
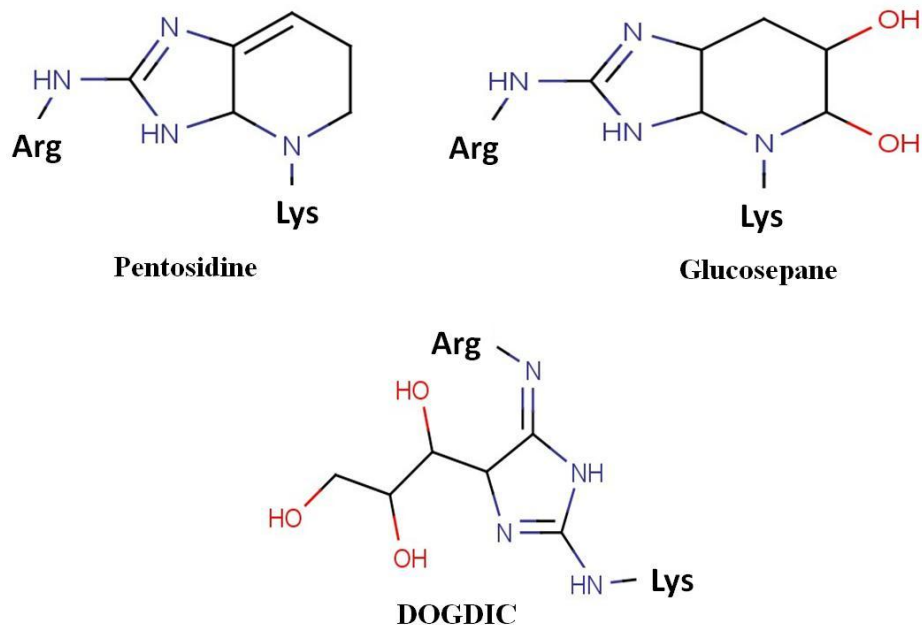
Figure 1.2 Glycation crosslinks reported to be presenet *in vivo.* **A.** Lysine-Arginine crosslinks **B.** Lysine-Lysine crosslinks

Generally, proteins which are stable and long lived such as collagen, lens crystallin, serum albumin are affected by this process. It is thought that lysine residues are involved in cross-link formation (Monnier et al., 1996). AGE induced crosslink formation increases the stiffness of matrix proteins, hence affecting function and increasing resistance to removal by proteolytic system which finally affects the tissue remodelling. This condition enhances with age and in diabetes (Dyer et al., 1993). Physiological consequence of crosslinking is sclerosis of renal glomeruli, thickening of the capillary basement membrane and atherosclerosis development (Monnier et al., 1996). Crosslinking of proteins by glycation may acts as a nucleation site for protein aggregation (Münch et al., 1997). Glycation of lens crystallins by various sugars and sugar phosphates results in its crosslinking and ultimately causes formation of insoluble aggregates of cataract (Swamy et al., 1993; Seidler et al., 2004). Collagen being a long lived extracellular matrix protein, undergoes glycation mediated crosslinking and aggregation (Mentink et al., 2002), which ultimately leads to premature stiffness of arteries and joints (Ricard-Blum et al., 1988). Additionaly, there are many age-related neurodegerative disorders such as Alzheimer's, Parkinson's, Huntington's and prion diseases which are affected due to the accumulation of AGEs (Li et al., 2012) (Figure 1.3.). These diseases are associated with misfolding and deposition of specific proteins either intracellularly or extracellularly in the nervous system. In addition to familial mutations, other factors that contribute to the onset and progression of these diaseses. Several proteins linked to neurodegenerative

diseases such as amyloid, tau, synuclein, prions, transthyretin were found to be glycated and this is thought to be associated with increased protein stability through the formation of protein crosslinks that stabilizes protein aggregates. If the etiology of these aggregation related diseases is considered, diabetes and alzheimer's are the most prevalent diseases worldwide.
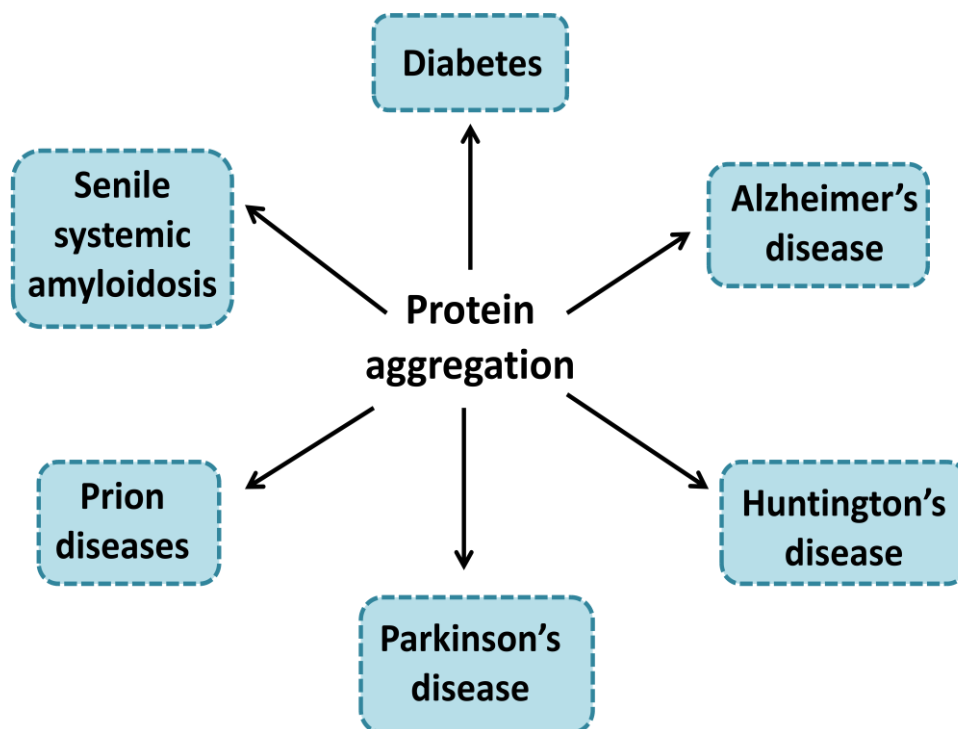
Figure 1.3 Protein aggregation associated diseases.

I.5. Glycation in Alzheimer's

Alzheimer's is the most prevalent neurodegenerative disease, affecting ~35 million people worldwide. This number is expected to double by 2030 and more than triple by 2050 (World Health Organization, news release, 2012). Its symptoms are memory loss, followed by confusion, motor dysfunction and disorientation, and disordered thinking. Degeneration of neurons occurs in several brain areas such as nucleus basalis, amygdale, entorhinal cortex and hippocampus. Only 6% AD cases are genetic, while most are sporadic (Campion et al., 1999). The presence of ε4 allele of the apolipoprotein E (APOEε4) and mutations in APP (amyloid precursor protein) are the genetic causes (Rademakers et al., 2009). The

major hallmarks of AD are the presence of amyloid β (Aβ) plaques and neuro-fibrillary tangles (NFTs) (Cummings et al., 1998). Glycation of these proteins plays an important role in formation of senile plaques and NFT formation (Vitek et al., 1994; Smith et al., 1994). Glycation of tau increases the paired helical filament formation and decreases its ability to bind to microtubules *in vitro* (Ledesma et al., 1996). AGE modified tau increases the production and secretion of Aβ (Yan et al., 1995). Glycation of Aβ by methylglyoxal elevates the formation of β-sheets, oligomers, protofibrils and also enhances the aggregate size. It is also supported by the lower expression levels of glyoxalase I, an enzyme required for detoxification of methylglyoxal, in the brain of AD patients (Kuhla et al., 2007). Hyperglycemia plays an important role for carbonyl stress in AD suggesting a link between diabetes and AD. Diabetic patients are 2-5% more susceptible to Alzheimer's than non-diabetic patients (Haan et al., 2006). Impairment of insulin signaling, inflammation, oxidative stress, mitochondrial dysfunction, advanced glycation end products, APOEε4 and cholesterol in diabetes mellitus appear to be important mediators and are likely to act synergistically in promoting AD pathology (Yang et al., 2013). AGEs derived from glyceraldehydes which are present in the cytosol of neurons in the hippocampus and parahippocampal gyrus, also enhances carbonyl stress (Choei et al., 2004). There are 3-fold higher levels of AGEs in AD as compared to normal patients (Vitek et al., 1994). Receptor for Advanced Glycation End product (RAGE) also plays an important role in AD, since it also recognizes Aβ in addition to AGEs (Li et al., 2009). Presence of AGEs in cerebrospinal fluid (CSF) of AD patients suggests that this may be investigated as a biomarker for AD.

I.6. Glycation and crosslink inhibitors

As cross-linking of proteins by glycation is probably the worst consequence of Maillard reaction, many researchers attempted to find out the drugs that would inhibit glycation and hence protein crosslinking and aggregation in diseases such as diabetes and Alzheimer's. A number of natural or synthetic compounds as AGE inhibitors have been proposed, discovered or currently being advanced. One of the most studied AGE and crosslink inhibitor is

aminoguanidine. It is a nucleophilic hydrazine derivative, which acts by scavenging intermediates in the advanced glycation reaction. The accumulation of AGEs in blood vessels and associated aortic collagen insolubility was decreased in the presence of aminoguanidine (Brownlee et al., 1986). Although this drug had reached clinical trials, due to its side effects such as non-specificity towards AGE inhibition, development of glomerulonephritis, it couldn't be continued for the diabetic treatment (Coughlan et al., 2007). Metformin, an oral hyperglycemic drug also reduces AGEs by trapping methylglyoxal and other dicarbonyl compounds (Ruggiero-Lopez et al., 1999). 2-AG, semicarbazide and OPD are dicarbonyl reactive compounds which inhibits 50% crosslinking at 1-2 mM concentration. Most of the studies have selected collagen as model protein to study crosslinking and its inhibition. Administration of green tea to diabetic rats significantly decreased the AGE fluorescence and increased the collagen solubility which indicates the reduced AGE formation and collagen crosslinking. Hence, green tea may provide a therapeutic option in the treatment of diabetes (Babu et al., 2007). Inhibition of collagen crosslinking in skin and tail of diabetic rats was also shown by curcumin (Sajithlal et al., 1998). Other compounds showing AGE inhibitory activity are D-penicillamine, desferoxamine, acetylsalicylic acid, ibuprofen, and indomethacin may be due to their antioxidant activity (Keita et al., 1992; Jakus et al., 1999). Thiamine pyrophosphate and pyridoxamine were found to be inhibitors of post-amadori products (Booth et al., 1997). Diclofenac, a non-steroidal anti-inflammatory drug, inhibits AGE formation through non-covalent interaction with serum protein (Boekel et al., 1992). *In vitro* studies showed that Inositol inhibits glycation through quenching of reactive oxygen species (Ramakrishnan et al., 1999). Additionally, a series of other compounds, such as calcium antagonists (Sobal et al., 2001), amlodipine (Akira et al., 2006), kinetin (Verbeke et al., 2000), quinine155 (Jung et al., 2005) and synthesized 6-dimethylaminopyridoxamine (Culbertson et al., 2003) decrease AGE formation through radical scavenging property. Benfotiamine, a lipid soluble compound, blocks 3 major pathways of hyperglycaemic damage and prevents diabetic retionopathy in rats (Hammes et al., 2003). There are reports of some natural compounds showing AGE-inhibitory activity as they are proven to be relatively safe for human comsumption as compared to synthetic compounds. Resveratrol (3, 4, 5-trihydroxystilbene), curcumin has found to be potent inhibitors of glycation and AGE-induced

crosslinking of collagen in diabetic rats (Sajithlal et al., 1998). The methanolic extracts of Finger millet (Eleusine coracana) and Kodo millet (Paspalum scrobiculatum) were found to be useful for protection from glycation and cross-linking of collagen (Hegde et al., 2002). G-rutin is a potent glycation inhibitor, especially for kidney proteins and collagen (Nagasawa et al., 2003). Among its metabolites those containing vicinyl dihydroxyl groups had stronger inhibitory effects on the formation of some AGEs including crosslink pentosidine and fluorescent adducts than metabolites without vicinyl dihydroxyl groups. All the five metabolites of rutin were effective to prevent the formation of N3-carboxymethyllysine (CML) adducts (Cervantes-Laurean et al., 2006). AGE derived crosslinked protein aggregates also contribute to neuronal dysfunction and death. Assuming that 'carbonyl stress' contributes significantly to the progression of Alzheimer's disease, AGE-inhibitors might also become interesting novel therapeutic drugs for treatment of AD. Hence, AGE inhibitors including aminoguanidine, carnosine, tenilsetam, OPB-9195 and pyridoxamine can be studied for the treatment of AD (Dukic-Stefanovic et al., 2001).

I.7. Repositioning of drugs

Discovery of drug for any disease condition is a lengthy process taking 10-17 years with a success rate around 0.01% (Ashburn et al., 2004; Hurle et al., 2013; Swamidass et al., 2011). It starts from target identification, lead compound identification and optimization, ADMET studies and finally to market. These molecules have to go through number of toxicity and pharmacokinetic studies in cell and animal models before release into the market. Even after systematic evaluation of drug activities, several drug molecules may have to drop due to their undesired toxicity and bio-distribution. For example, AstraZeneca's NXY-059 showed promising result in the first clinical trial for improvement of stroke induced injury, but failed in the next trial (Feuerstein et al., 2008). Sometimes drugs show toxicity long after the approval of drug which causes its withdrawal from market (Furberg et al., 2001). Therefore a new concept has emerged called "drug repositioning". Drug repositioning is the application of known drugs and compounds for new indications (Tobinick et al., 2009). A repositioned drug

reduces risk, cost and time needed for the development of new drug (Harrison et al., 2011) (Figure 1.4). Drug repositioning requires understanding of molecular mechanism of action and identification of interacting proteins of the drug. In case of many drugs, mechanism of drug action is less understood. The usability of a drug can be enhanced by 1] finding new indications or 2] formulation of new delivery system either to enhance bio-availability or to avoid drug induced toxicity (Qu et al., 2009).
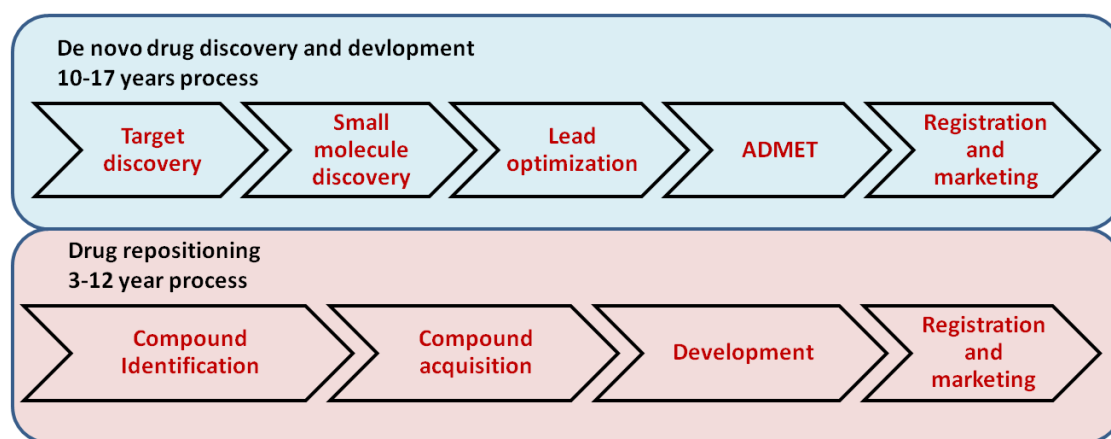
Figure 1.4 Classical Vs Repositioning Drug Discovery Pipeline: Classical drug discovery may take 10-17 years to bring a drug into the market with high risk of failure while drug repositioning takes 3-12 years with reduced cost and assured biosafety

I.8. Drug induced glycation/aggregation

Aggregation of protein occurs naturally through aging and it increases in some disease conditions. There are also some chemicals which are toxic to proteins and induce crosslinking. As we have mentioned earlier that various reactive dicarbonyls or lipid peroxidation product 4-hydroxynonenal are involved in protein crosslinking (Carbone et al., 2005). A chemically similar compound to 4-hydroxynonenal i.e acrolein also reacts extensively with proteins and forms carbonyl-retaining Michael adducts which may be attacked by adjacent protein nucleophiles to form cross-links (Burcham et al., 2007). Similarly, there are few chemicals such as cerium (III) and lanthanum (III) induce protein aggregation not only by lanthanide cation non-covalent binding and cross-linking, but also by

oxidative cross-linking through disulfide bond formation. The aggregation was accompanied by the conformational changes with tryptophan residues exposing to more hydrophobic environment and the decreasing α-helix and β-sheet contents (Du et al., 2000). Furthermore, researchers have also studied the effect of formaldehyde, a common environmental contaminant and a metabolite of methanol, on tau protein. Tau is a microtubule associated protein and is a principle component of neurofibrillary tangles in AD; similar lesions are also observed after chronic alcohol abuse. Neuronal tau aggregates in formaldehyde solution and the aggregated tau induces apoptosis of SH-SY5Y and hippocampal cells. Likewise, the drugs used in the chronic disease treatment may have harmful effects. Hence, we have hypothesized that the drugs which are used in the treatment of chronic diseases may cause conformational change in the proteins which further leads to protein aggregation.

I.9. Genesis and organization of thesis

Crosslinking of proteins by glycation and other chemicals has an adverse effect on the proteins. It is associated with many diseases related to protein aggregation and misfolding such as diabetic complications, Alzheimer's and many other neurodegenerative diseases. As these crosslinked and aggregated proteins play a pivotal role in the pathogenesis of diseases, we realized that the identification, characterization and inhibition of these proteins as an important question to address. The crosslinked aggregates are known to be resistant to the proteolytic damage due to hindrance to the cleavage site of the protease. Hence, we thought to utilize this property of aggregated proteins to identify and characterize them. An increased plasma glucose level during diabetes makes the proteins susceptible to undergo crosslink formation through glycation reaction. Therefore, diabetic rats were used as a model system to study glycation induced protein crosslinking. As the accumulation of these proteins is harmful, inhibition of the crosslink and aggregate formation is good strategy to prevent the progression of these diseases. Thus, it is important to find a molecule which will inhibit the protein crosslinking. Furthermore, any drugs used for treatment of chronic diseases can have damaging or toxic effect on the body. There could be

certain drugs which may induce protein aggregation or may accelerate glycation reaction after binding to proteins, which ultimately results in increased protein crosslinking and aggregation.

Major objectives of the thesis are as follows

- Identification and characterisation of crosslinked proteins

- To screen inhibitors for protein cross links

- To study drug induced protein crosslinking

This thesis is organized in the following manner

Chapter 1: Introduction

Chapter 2: Proteomic analysis of cross-linked protein aggregates in diabetes

Chapter 3: Protriptyline, an anti-depressant inhibits protein cross linking and multiple targets of Alzheimer's disease

Chapter 4: Tolbutamide, an anti-diabetic drug promotes glycation

CHAPTER II

Proteomic analysis of cross-linked protein aggregates in diabetes

II.1. Introduction

One of the foremost causes of diabetic complications is formation of sugar-derived substances called advanced glycation end products (AGEs), which affects target cell through altered protein structure- function, matrix-matrix/matrix-cell interaction, and by activation of receptor for AGE (RAGE) signaling pathway (Brownlee, 2001). Although the accumulation of AGEs is a slow process in healthy individuals, their formation is markedly accelerated in diabetes due to hyperglycaemia (Peppa et al., 2003). AGE-modified proteins are thermostable and resistant to denaturation. The thermal and proteolytic stability of highly oxidized proteins has been studied extensively by different groups. The stability of proteins is believed to be due to additional negative charge (Highly oxidized state) brought by AGE modification of proteins, which may contribute to protease resistance (Bulteau et al., 2001). Glycation induced protease resistance has been studied in long lived proteins such as collagen (Monnier et al., 1984; Reddy et al., 2002; Schnider et al., 1981) and amyloid (Smith et al., 1994).

In addition to glycation, impairment in the proteasomal function may facilitate accumulation of protease resistant protein aggregates in diabetes. Proteasome mediated protein degradation is a central quality control mechanism in the cell. Activity of proteasome is affected during aging (Vernace et al., 2007) and physiological disorder like diabetes (Portero-OtÃn et al., 1999) resulting in accumulation of ubiquitinated protein aggregates. In muscle extract of diabetic rats, accumulation of toxic glycated proteins was observed due to decreased proteasomal activity (Schnider et al., 1981; Smith et al., 1994; Vernace et al., 2007; Portero-OtÃn et al., 1999). This proteolytic system is of particular importance in protecting cells against adverse conditions, such as heat shock, glycation or oxidative stress. However, when the generation of damaged proteins exceeds the capacity of the cell to degrade them, they are progressively accumulated leading to cytotoxicity (Goldberg, 2003). Severely aggregated, cross-linked and oxidised proteins are poor substrate for degradation and actually inhibit the proteasomal activity (Davies et al., 2006).

The kidney is one of the main organs affected in diabetes due to accumulation of AGEs. Proteins of extracellular matrix, kidney, as well as proteins from circulation, get AGE modified and trapped in the kidney (Chougale et al., 2012). Both intracellular and extracellular AGEs have been observed in the diabetic kidney. Extracellular AGEs interact with the RAGE leading to apoptosis and inflammation (Figueroa-Romero et al., 2008), whereas intracellular AGEs are formed due to various dicarbonyls. Eventually, both types of the AGEs contribute to kidney damage (Ahmad et al., 2008). Furthermore, methyl glyoxal, a highly reactive dicarbonyl covalently modifies the 20S proteasome, decreasing its activity in the diabetic kidney (Queisser et al., 2010). Together AGE modification and decreased proteasomal function may be responsible for the accumulation of protease resistant proteins (PRPs) in the diabetic kidney. In our previous study, we have reported the presence of AGE modified proteins in the kidney of streptozotocin (STZ) induced diabetic rat (Chougale et al., 2012). The current work is inspired by a DARTS (drug affinity responsive target stability) approach, wherein the drug targets are relatively less susceptible to protease action upon drug binding (Lomenick et al., 2009). A similar approach was used here to identify protease resistant proteins from the diabetic kidney. These proteins were characterized to be AGE modified and ubiquitinated by western blot analysis and mass spectrometry. Functional characterisation and expression analysis of some of the identified proteins was done to gain insight into the consequences of these modifications in diabetes. Further, aggregation prone regions in these proteins were predicted by *in silico* approach. These findings shed light on the role of identified PRPs in diabetic complications.

II.2. Materials and methods

All chemicals were procured from Sigma unless otherwise stated. All the primary antibodies were purchased from Abcam (UK) except for anti-AGE, which was purchased from Millipore (MA). The secondary antibody-biotin conjugate and streptavidin-HRP was purchased from Bangalore Genei (India)

II.2.1. Induction of Diabetes and Kidney Sample Collection. All animal experiments were carried out at Poona College of Pharmacy, Bharati Vidyapeeth University, Pune. The research protocol was approved by the Institutional Animal Ethics Committee (IAEC) of the Poona College of Pharmacy, Pune, India, constituted under the Committee for the Purpose of Control and Supervision of Experiment on Animals (CPCSEA). (Approval No.: CPCSEA/45/2010). Adult male Wistar rats weighing approximately 180-220g were purchased from National Biosciences, Pune, India. The animals were housed in a room at an ambient temperature of $25\pm2°C$. A 12 ± 1 h light and dark schedule was maintained in the animal house. Before the study began, all the animals were received standard rodent chow *ad libitum* and had free access to water. Diabetes was induced by injecting Nicotinamide (110 mg/kg) followed by a single intra-peritoneal injection of streptozotocin 65 mg /Kg body weight dissolved in 10 mM sodium citrate buffer (pH 4.0) to the overnight fasting Wistar rats. Blood glucose level of animals from all the groups was measured using Eco-Pak glucose kit (Accurex Bio Medical Pvt. Ltd., Mumbai, India), according to manufacturer's instructions. After 15 days of administration of STZ, stable hyperglycaemia was confirmed. The animals were considered diabetic if the blood glucose values were > 250 mg/dl. Animals surviving after diabetes induction were maintained for 100–120 days. Glycated haemoglobin (HBA1c) was measured by using HBA1c Analyzer (In2it, Bio-Rad). Control (HbA1C $\leq$ 5.5) and diabetic kidney tissues (HBA1c $\geq$8%) were collected after sacrificing the respective animals. The tissue was washed with cold saline for three to four times and stored at -80º C.

II.2.2. Sample Preparation. The kidney was perfused with cold phosphate buffer saline to remove blood stains prior to homogenization. The tissue was homogenized to fine powder in liquid nitrogen and washed two to three times with chilled acetone. Then, the acetone powder was dissolved in buffer consisting of 7 M urea, 2 M thiourea, 2% CHAPS, 1% DTT, 40 mM Tris, and centrifuged at 14,000 g for 30 min at 4ºC . The supernatant was collected and stored in aliquots

at -80°C. For enzyme assays, protein was extracted in phosphate buffer saline. The extract was centrifuged at 6000 rpm for 30 min at 4°C. Supernatant was collected and re-centrifuged at 14000 g for 30 min at 4°C. Again the supernatant was collected and stored in aliquot at -80°C. Protein concentration was estimated by using Bio-Rad protein assay kit (Bio-Rad, Hercules, CA).

II.2.3. Analysis of protease resistance. As a proof of concept, an *in vitro* glycated and ribosylated BSA was synthesized by incubating 50 mg/ml BSA with either 0.5 M glucose or 0.5 M ribose in 0.2 M phosphate buffer, pH 7.4 at 37°C for 30 days, respectively. Afterwards, 10 μg of control, glycated and ribosylated BSA was subjected for in-solution digestion by using 1 μg of trypsin in 25 mM ammonium bicarbonate buffer pH 8.4, without prior reduction and alkylation with dithiothritol (DTT) and iodoacetamide respectively, to simulate *in vivo* conditions of proteolysis. The reaction was performed at 37°C for 1 h and stopped by 10% formic acid. The samples were air-dried, reconstituted in Laemmli sample buffer (60mM Tris-HCl pH 6.8, 2% SDS, 10% glycerol, 5% β-mercaptoethanol, 0.01% bromophenol blue) and boiled for 5 min. Further, these samples along with respective undigested samples were subjected for 12% SDS-PAGE and proteins were visualised by Coomassie Brilliant Blue (CBB-R250) staining. The same approach was used for kidney protein lysate except the protein quantity used was 20 μg. The experiments were performed in triplicates.

II.2.4. Western blotting. Control and diabetic kidney protein samples, before and after Trypsin digestion, were separated on 12% SDS-PAGE. Proteins were transferred onto PVDF membrane and incubated overnight at 4°C in blocking buffer containing 5% skimmed milk powder dissolved in TBS (20 mM Tris-HCl (pH 7.5), 0.15 M NaCl). The membranes were incubated for 1 h at 37°C and then probed with different primary antibodies in blocking buffer and kept for incubation at 37 °C for 1 h. Following antibodies were used: anti-AGE antibody (1:2500), anti-ubiquitin antibody (1:2000), anti-GAPDH (1:10000), anti-SOD (1:10000), anti-HSP (1:10000), anti-GST (1:2000), anti-LDH (1:1000), anti-ADH

(1:500). After one wash with TBS and two washes with TBS-T (TBS containing 0.05% Tween 20), the membranes were incubated with secondary antibody conjugated with biotin conjugate (Bangalore Genei) at a dilution of 1:2000 for 30 min at room temperature. After one wash with TBS and two washes with TBS-T, membranes were incubated with streptavidin-conjugated horse radish peroxidise (HRP) at dilution 1:2000 for 30 min at RT. Immunodetection was carried out in the dark by adding Diaminobenzidine (DAB), the substrate for HRP. The experiment was repeated independently three times.

II.2.5. In-gel trypsin digestion. The Comassie-stained gels and western blots were scanned using a densitometer GS-800 (Bio-Rad Laboratories). The trypsin resistant proteins, which were detected by Anti-AGE as well as anti-ubiquitin antibody were excised and destained with 100 µl of destaining solution (50 mM ammonium bicarbonate/acetonitrile mixed 1:1 v/v). After thorough rinsing with 100 mM ammonium bicarbonate, the gel pieces were dehydrated in 100% ACN, which was removed by air drying. Proteins were reduced and alkylated by 10 mM DTT for 30 min and 55 mM iodoacetamide for 45 min respectively. Again gel pieces were dehydrated with 100% ACN and kept for rehydration with 15-20 µl of 20 ng/µl trypsin solution in 25 mM ammonium bicarbonate buffer pH 8.4 overnight at 4°C. Further rapid trypsin digestion was done at 58°C for 1 h (HavliŠ et al., 2003). Peptides from the gel were extracted with 5% formic acid in 50% ACN, and were reconstituted in 10 µl of 0.1% formic acid in 3% ACN.

II.2.6. Liquid Chromatography–Mass Spectrometry Analysis. Tryptic peptides were analyzed by nano LC–MS^{E} (MS at elevated energy) using a Nano Acquity UPLC system (Waters Corporation) coupled to a Q-TOF, SYNAPT-HDMS (Waters Corporation). The nano-LC separation was performed using a BEH-C18 reversed phase column (1.7 µm particle size) with an internal diameter of 75 µm and length of 150 mm (Waters Corporation). The binary solvent system used comprised 99.9% water and 0.1% formic acid (mobile phase A) and 99.9% acetonitrile and 0.1% formic acid (mobile phase B). Peptides were initially

preconcentrated and desalted online at a flow rate of 5 μL/min using a Symmetry C18 trapping column (internal diameter 180 μm, length 20 mm) (Waters Corporation) with a 0.1% B. After each injection, peptides were eluted into the NanoLockSpray ion source at a flow rate of 300 nl/min using a gradient of 2–40% B for 35 min, and then the column was washed and equilibrated. All mass spectrometric analysis was performed using positive mode ESI using a NanoLockSpray source. Mass spectrometer was resolved to at least 9000 full width half maximum (FWHM) in V-mode. The instrument was calibrated with a MS/MS spectra of glu-fibrinopeptide B (600 fmol/μL), and the lock mass correction was done every 30s by the same peptide delivered through the reference sprayer of the NanoLockSpray source. MS^E was performed by acquiring the spectra at constant low collision energy (4eV) to generate intact peptide masses, and the collision energy was elevated (20 to 40e V) to get product ions at an alternative 1s scan. The radio frequency voltage applied to the quadrupole mass analyser was adjusted such that ions from m/z 50 to 2000 were efficiently transmitted.

II.2.7. Data Processing and Database Searching. The LC–MS^E data was analyzed by Protein Lynx Global Server 2.4 (PLGS; Waters Corporation) software. The ion accounting search parameters used to search included precursor and product ion tolerance 25 ppm and 100 ppm respectively, minimum number of peptide matches [1], minimum number of product ion matches per peptide [3], minimum number of product ion matches per protein [5] and the number of missed tryptic cleavage sites were 3. The false positive rate was 4%. Ion intensity threshold was set at 1000 counts. A preliminary search was performed for protein identification using UniProt rat database updated with Ensembl release 66 available at the end of February 2012 containing 7773 reviewed protein entries. LC–MS^E data were searched with a fixed carbamidomethyl modification for Cys residues, along with a variable modification for oxidized Met residues. For identification AGE and ubiquitin modifications, a targeted search was performed involving variable glycation modifications specific to lysine residues were carboxymethyllysine (CML) (+58.0055 Da); carboxyethyllysine (CEL) (+72.0211

Da); pyrraline (+108.0211 Da) and ubiquitin (114.02 Da). Those involving both lysine and arginine residues were 1-alkyl-2-formyl-3, 4-glycosylpyrrole (AFGP) (+270.074 Da); Schiff's base/Amadori modification (+162.02); imidazolone-A (144.03 Da); methylglyoxal lysine dimer (MOLD) (49.0078 Da); Pentosidine (58.03 Da) and crossline (252.11 Da). Glycation and ubiquitin modifications identified by PLGS were manually validated as described by Bhonsle et al., 2012. Brifly, the PLGS identified glycated peptides were manually validated with following criteria. a) All glycated peptides (identified by PLGS) should have a corresponding unglycated peptide with/without missed cleavage in MS^E analysis. b) All glycated peptides should have a minimum of 5 fragment ions matching with the sequence d) all glycated peptides should exist at least in two replications.

II.2.8. Semi-Quantitative RT–PCR. Total RNA was isolated from diabetic and control rat kidney using TRIzol reagent (Invitrogen, Carlsbad, CA) according to the manufacturer's instructions. First strand cDNA was reverse-transcribed from 1 μg of total RNA in a final volume of 20 μL using reverse transcriptase and random hexamer primers from eurofins^{TM} reagent kit according to the manufacturer's instructions. PCR was performed with rTaq (BlackBio) in a Veriti thermocycler (Thermo Scientific) according to a standard protocol as follows: one cycle of initial denaturation at 94 ^{0}C for 5 min; 35 cycles of 94 ^{0}C for 30 s, annealing for 45 s, and 72 ^{0}C for 1.30 min; a final extension at 72 ^{0}C for 10 min; and holding at 4 ^{0}C. The amount of cDNA used for each PCR was 10 ng in a 10 μL reaction volume. The PCR products were analyzed by electrophoresis through 2% agarose gels and visualized by Gel Red staining. Each biological replicate of cDNA sample was run for three times. The primers used for amplifying the proteins are given in supplemental Table S1. β actin was used as a housekeeping gene.

II.2.9. Enzyme assays. Control and diabetic kidney homogenate (50μg) was used to carry out following functional assays-

II.2.9.a. Total protease activity assay. Total protease activity in the control and diabetic homogenised kidney protein lysate was measured by azocasein assay

(Brock et. al., 1982). The principle of this assay is the hydrolysis of azocasein by proteases resulting in release of azo-molecule with a unique absorption at 450 nm. The assay was carried out by incubating 50 μg protein lysate with 200 μL of 1% azocasein in 0.2 M Glycine-NaOH (pH 10.0) at 37 °C for 30 min. The reaction was terminated by the addition of 300 μL of 5% trichloroacetic acid. The assay mixture was centrifuged at 13 000× g for 10 min, then an equal volume of 1.0 N NaOH was added to the supernatant and absorbance was measured at 450 nm.

II.2.9.b. In-gel protease assay. Control and diabetic homogenised kidney protein lysate (50 μg each) was separated on 12% native PAGE containing 0.1% gelatin at 4^0 C (Solomon et al., 1999). Gel was incubated in carbonate-bicarbonate buffer pH 10.5 at 37^0 C for 1 h. Protease specific negative staining were visualized with CBB-R250 by incubating overnight at room temperature and then scanned by densitometer GS800 (Bio-Rad).

II.2.9.c. Proteasomal activity assay. Proteasome activity assay kit (Abcam) was used for measuring proteasome activity in control and diabetic kidney protein lysate. The assay is based on the proteolytic release of fluorescent AMC from AMC-tagged peptide. Proteasome specific inhibitor MG-132 facilitates differential measurement of proteasome specific activity over non-specific total proteolytic activity. Protein lysate (50 μg) was incubated with 0.1 nmol of AMC tagged peptide at 37° C for 30 minutes. Fluorescence intensity of AMC was recorded by excitation with 350 nm and emission at 440 nm in a Varian Carry eclipse fluorescence spectrophotometer. For *in vitro* proteasome, 1μg proteasome was modified with 5mM methylglyoxal for 3 h at 37° C. Proteasomal activity was measured as described above.

II.2.9.d. SOD assay. SOD activity was measured according to the protocol described previously (Beauchamp et al., 1971). The principle of this assay is based on the ability of O_2^- to reduce NBT into blue precipitate. In brief, 50μg control and diabetic crude kidney homogenate was added to an assay mixture

(50mM phosphate buffer, pH 7.8, 13mM L-methionine, 75μM NBT, 20μM riboflavin, 0.01M EDTA and distilled water). One set of tubes were illuminated by white light source from a distance of 30 cm for 30 min and another set of tubes was kept in dark for 30 min. The controls had the reaction mixture without enzyme extract placed under light as well as in dark. Absorbance was recorded at 560 nm.

II.2.9.e. LDH assay. LDH catalyses the conversion of pyruvate to lactate through oxidation of NADH, the assay determines the depletion of NADH by measuring absorbance at 340nm resulting from the oxidation of NADH. 50μg control and diabetic crude kidney homogenate was added to an assay mixture (2.8ml 0.2M tris HCL pH 7.3, 0.1ml 6.6 mM NADH, 0.1ml 30mM Na-pyruvate). The controls had the reaction mixture without NADH. (http://www.worthington-biochem.com/ldh/assay.html)

II.2.9.f. ADH assay. Ethanol is converted to acetaldehyde by alcohol dehydrogenase, during which NADH is oxidized by 1-methoxy-5-methyl phenazinium methyl sulphate reducing tetrazolium system to produce the purple-colored MTT formazan. 50μg control and diabetic crude kidney homogenate was added to an assay mixture (3.7nM NAD, 0.2M tris-HCL pH 8.2, 60μM MTT, 100μM MPMS and 10% absolute ethanol). Samples were incubated at 37° C for 1 h. Reaction was stopped using 100μl of stopping reagent (50% DMF and 20% SDS). Absorbance was recorded at 570nm (Zanon et al., 2007).

II.2.9.g. GST assay. GST activity was measured according to the protocol described previously (Habig et al., 1974). Glutathione is transferred by GST to the substrate (1,2 dichloro-4-nitrobenzene) resulting in the formation of glutathione 2,4-dintrobenzene conjugate which is measured by spectrometrically at 340 nm. In brief, 50μg control and diabetic crude kidney homogenate was added in an assay mixture containing 100 mM phosphate buffer pH 7.5, 0.25% ethanol, 5mM

glutathione and 1mM benzene substrate (1,2 dichloro-4-nitrobenzene). Formation of glutathione 2,4-dintrobenzene conjugate was measured.

II.2.10. Determination of aggregation propensity of identified proteins. Amino acid sequences of identified trypsin resistant proteins were retrieved from Uniprot (http://www.uniprot.org/) and further used for prediction of aggregation propensity. Different web servers like Aggrescan (http://bioinf.uab.es/aggrescan/) (Conchillo-Sole et al., 2007), Tango (www.tango.embl.de) (Fernandez-Escamilla et al., 2004), PASTA (www.protein.cribi.unipd.it/pasta) (Trovato et al., 2007) and Waltz (http://waltz.switchlab.org/) (Trovato et al., 2006) were used for predicting and calculating aggregation propensity of proteins, with their default parameters. Homology modelling of these proteins was done by using CPH model server 3.0 (http://www.cbs.dtu.dk/services/CPHmodels/) Predicted structures were validated by Ramchandran plot analysis using RAMPAGE (http://mordred.bioc.cam.ac.uk/~rapper/ rampage. php) and also for overall model quality using ProSA (https://prosa.services.came.sbg.ac.at/prosa.php). Further, AGE modified peptides identified through PLGS analysis and predicted aggregation prone regions were examined for putative identification of common regions between them. These aggregation prone regions were then mapped on the predicted structure using PyMol (**Py**thon based **Mol**ecular viewer).

II.2.11. Statistical analysis. All experiments were performed in triplicates. Statistical analysis was performed by Student's t-test. Data were expressed as mean ± SD. A *p*-value < 0.05 was considered as statistically significant.

II. 3. Results and discussion

II.3.1. Accumulation of PRPs: Consequence of glycation and impaired proteasomal function- Diabetes is associated with accelerated glycation and crosslinking of proteins. The characteristic feature of cross linked proteins is increased stability and resistance for the proteolysis (Bulteau et al., 2001) due to which cells are unable to clear the aggregated proteins and the accumulated aggregates often have toxic effects. This protease resistance property of PRPs was

used for their identification. A similar approach called drug affinity responsive target stability (DARTS) was used to identify drug targets, where in binding of drug to protein causes protease resistance (Lomenick et al., 2009). In this study, an attempt has been made to identify glycation induced PRPs using the DARTS approach. The basic strategy used in this study was masking protease recognition sites of proteins by glucose due to glycation reaction, thereby reducing protease action. This idea is comparable to a well-known concept of DNase resistance of DNA bound by transcription factors. As a proof of concept, *in vitro* study was carried out with glycated and ribosyled BSA. Glycation and ribosylation induced protein aggregation and resistance to trypsin digestion as compared to unmodified BSA (Figure 2.1). These results suggested that glycation induced PRPs can be identified by this approach.
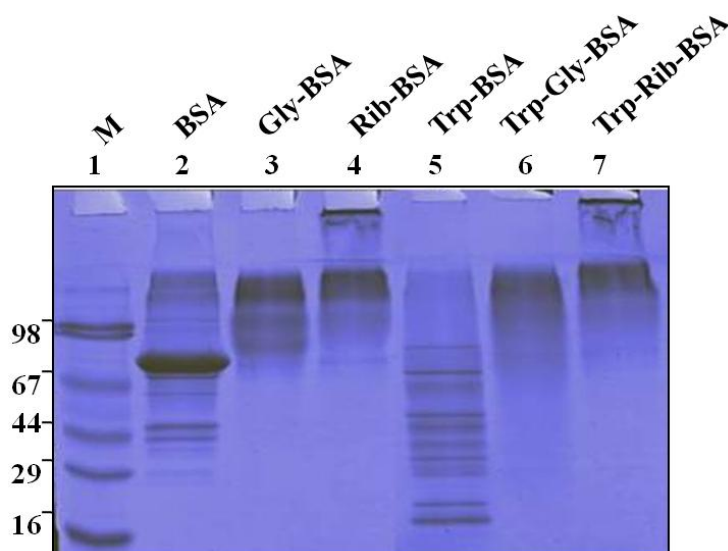
Figure 2.1 *In vitro* evidence on protease resistance of glycated protein. BSA was glycated and ribosylated with glucose and ribose respectively, which showed protease resistance to tryptic digestion. Lane 2, 3 and 4 contains undigested BSA, Gly-BSA and Rib-BSA respectively, whereas lane 5, 6, and 7 contains the same digested with trypsin, Try-BSA, Try-Gly-BSA and Try-Rib-BSA respectively, and Lane 1 contains SDS-PAGE marker. The experiment was repeated independently three times.

Further, the feasibility of these *in vitro* results was demonstrated in complex protein mixtures. A diabetic condition in Wistar rats was induced by STZ and confirmed by measuring blood glucose and HbA1C levels (Table 2.1).

Table 2.1 Blood glucose and HbA1c level of diabetic and control rats

Number of animal	Number of animals survived	Body wt in gms	Glucose mg/dl	HbA1c level
Control (12)	10	246.5± 13.22	73.46 ± 6.18	≤ 5.5
Diabetic (12)	10	162.4± 24.70	335.08 ± 11.56	≥ 8.0

Value in parenthesis indicates the total number of rats in the group and (±) indicates the standard deviations. # Control and diabetic animal groups showed approximately 20% mortality.

Control and diabetic rat kidney proteins were used to identify PRPs after trypsin digestion without reduction and alkylation. Interestingly, control kidney protein was almost completely digested with trypsin, while the diabetic kidney protein showed several protease resistant bands (Figure 2.2 A). These *in vivo* results supported our *in vitro* results, as well as previous studies where long lived proteins such as collagen and amyloid were demonstrated to be protease resistant in diabetic condition (Monnier et al., 1984; Reddy et al., 2002; Schnider et al., 1981; Smith et al., 1994). As protease resistance is induced by glycation, the kidney proteins were characterized for AGE modification by western blot analysis (Figure 2.2 B). Diabetic rat kidney showed relatively more AGE modified proteins than the corresponding control, and also these AGEs modified proteins were relatively resistant to trypsin (Figure 2.2 B). This strongly suggested that accumulation of PRPs in diabetes could be due to AGE modification. AGE modification of proteins is associated with altered protein conformation and function. Under normal physiological condition, misfolded proteins and potentially harmful protein aggregates are ubiquitinated and removed by proteasomal system. However, the oxidative inactivation of proteasome has been reported during aging (Davies et al., 2006; Friguet et al., 2002), glyoxal treated

cells (Bulteau et al., 2001), Alzheimer's disease (Riederer et al., 2011) etc. Analysis of protein ubiquitination and proteasome activity reveals the basis for the accumulation of AGE modified PRPs in the diabetic rat kidney. As proteasome targets ubiquitin marked proteins, its reduced function will slowly build up ubiquitinated proteins in cells. It was remarkable to notice relatively more ubiquitinated proteins in the diabetic rat kidney than in the control group. The protease resistant fragments in diabetes were also found to be ubiquitinated (Figure 2.2 C). Interestingly, most of the AGE modified proteins were uniquitinated.
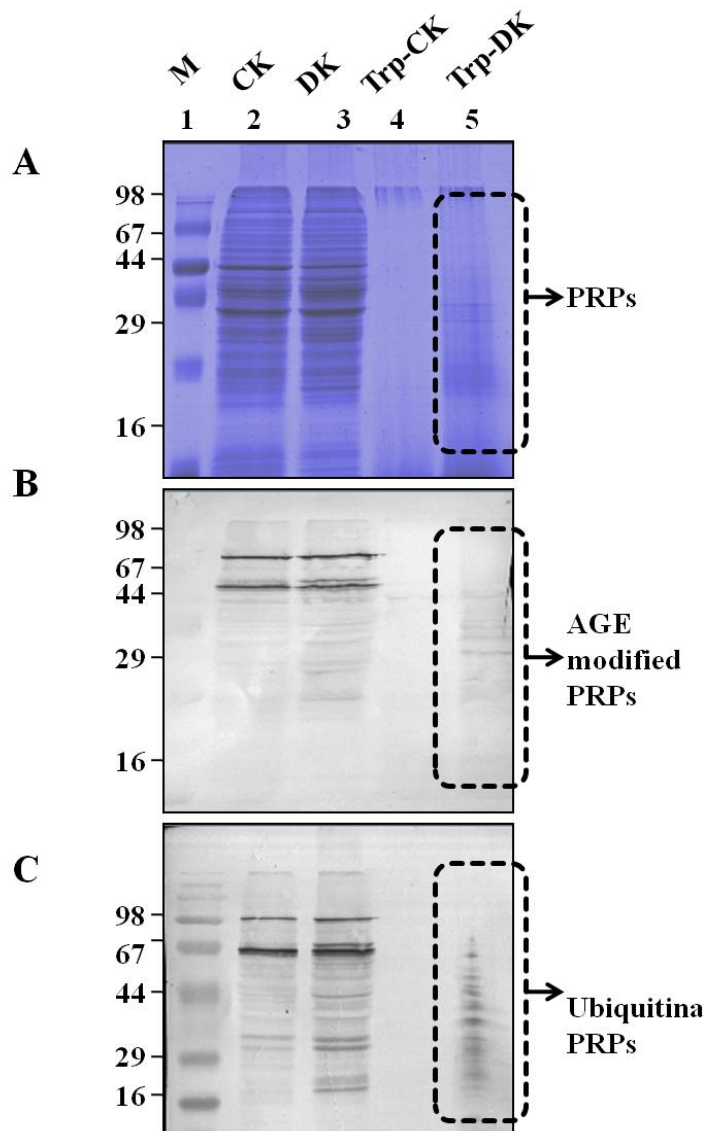
Figure 2.2 AGE and ubiquitin modification of PRPs. The protein lysate of control (CK) and diabetic (DK) rat kidney was separated on SDS-PAGE with and without tryptic digestion. Western blot analysis was performed with anti-AGE or anti-ubiquitin antibodies for detection of PRPs with AGE and ubiquitin modification. **A.** SDS-PAGE: Lane 2 and 3 showing undigested control (CK) and diabetic (DK) rat kidney lysate whereas lane 4 and 5 contains the same digested with trypsin (Try-CK, Try-DK). The same samples were immunoblotted with **B.** Anti-AGE and **C.** Anti-ubiquitin antibody, respectively. The experiment was repeated independently three times.

Further, the detection of ubiquitinated PRPs has driven us to investigate total protease and proteasomal activity from control and diabetic kidney homogenate. Azocasein assay (Figure 2.3 A) and in-gel protease assay (Figure 2.3 B) showed significantly decreased total protease activity in the diabetic kidney than control. Chymotrypsin-like activity of proteasome was considerably decreased in the diabetic condition (Figure 2.3 C), as this was selectively inhibited by carbonyl compounds in the cell culture (Queisser et al., 2010). Inhibition of chymotrypsin like activity of proteasome by carbonyl compound was demonstrated by *in vitro* modification of proteasome with methylglyoxal (Figure 2.3 D). This suggested that the decreased proteasome activity in diabetic kidney could be due to AGE modification. Collectively, these results indicate that accumulation of PRPs in the diabetic rat kidney is a consequence of AGE modification and reduced proteasomal activity.
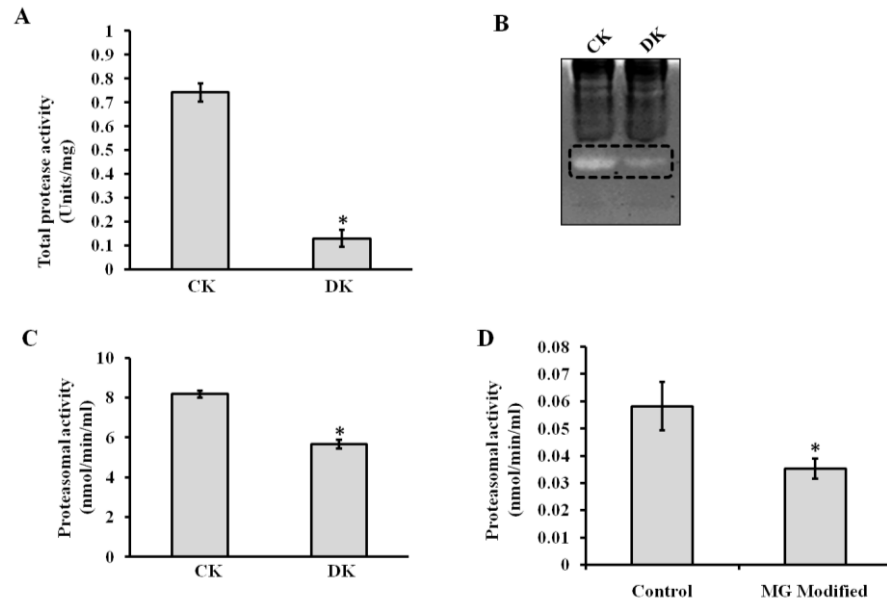
Figure 2.3 Total protease and proteasomal activity. Control (CK) and diabetic (DK) rat kidney protein lysate was assessed for total protease activity by **A.** Azocasein assay and **B.** In- gel protease assay. These assays demonstrated that total protease activity is significantly reduced in DK. Formation of fluorescent AMC from AMC-tagged peptide was determined to assess **C.** Proteasomal activity of rat kidney homogenate of CK and DK, and **D.** *In vitro* MGO modified proteasome activity. Bars represent means ± SE from three independent experiments. *$P < 0.05$.

II.3.2. Identification and characterization of PRPs for glycation and ubiquitin modifications- Mass spectrometry has been extensively used to identify and characterize proteins modified by glycation (Lapolla et al., 2006) and ubiquitination (Kaiser et al., 2005). Therefore, PRPs detected as AGE modified and ubiquitinated by western blotting were identified and characterized by mass spectrometry. About 18 PRPs were identified with a confidence of > 95% and found to be involved in various cellular processes are listed in Table 2.2.

Table 2.2 Detailed information of mass spectrometrically identified proteins

Acc.No.	Protein name	MW (KDa)	pI	PLGS Score	Peptides (whole database)	Peptides (Single database)	Unique peptides	Coverage (%)
D3ZGY4	Glyceraldehyde 3 phosphate dehydrogenase	35800	7.737	1133.457	3	52	3	12.9129
P63039	60 kDa heat shock protein mitochondrial	60917	5.8044	48.5405	6	113	7	15.1832
P56574	Isocitrate dehydrogenase NADP	50934	8.851	137.8497	10	95	35	25.885
P07895	Superoxide dismutase Mn mitochondrial	24658	9.0509	101.7715	3	47	10	10.3604
P51635	Alcohol dehydrogenase NADP	36482	6.9456	95.5803	2	82	23	7.6923
F1LP05	ATP synthase subunit alpha	59775	9.572	155.1342	11	169	1	19.5298
P10719	ATP synthase subunit beta	56318	5.019	51.5456	6	66	10	17.2023
P04764	Alpha enolase	47098	6.1377	45.9096	5	122	00	11.7512
P16617	Phosphoglycerate kinase	44509	7.9043	97.3903	9	88	23	27.5779
P42123	L lactate dehydrogenase B chain	36589	5.6274	70.4556	3	94	17	10.241
P04636	Malate dehydrogenase mitochondrial	35660	8.8239	84.2337	4	86	7	16.2722
P04903	Glutathione S transferase alpha 1	25542	9.1703	384.1361	11	81	00	21.1712
P00884	Fructose bisphosphate aldolase B	39593	8.4326	78.8326	1	131	3	3.5714

Acc.No.	Protein name	MW (KDa)	pI	PLGS Score	Peptides (whole database)	Peptides (Single database)	Unique peptides	Coverage (%)
P06685	Sodium potassium transporting ATPase subunit alpha 1	112554	5.1398	114.518	11	178	16	10.4594
P10860	Glutamate dehydrogenase 1 mitochondrial	61377	7.9801	56.1638	5	123	23	14.3369
Q68FU3	Electron transfer flavoprotein subunit beta	27670	7.83	57.4798	2	60	19	12.9412
Q5XIF6	Tubulin alpha 4A chain	49892	4.5903	246.3592	15	73	11	33.1081
Q9WVK7	Hydroxyacyl coenzyme A dehydrogenase mitochondrial	34425	8.8932	100.3093	2	54	19	9.1954

List of unique peptides assigned for each protein, and all peptide sequences and their score are listed in **Supplemental Table S1 and S2** respectively.

(Note: All supplemental information is provided in CD enclosed with thesis)
All these 18 proteins were further confirmed for the presence of different AGE modification and ubiquitination in MS^E analysis. A characteristic representative MS/MS annotation of glycation modification, Imidazolon A (ImiA) with increase in mass of 144.03 Da and ubiquitin modification with increase in mass of 114.04 Da of GAPDH is depicted in Figure 2.4.A. and Figure 2.4.B. Similarly, total 238 glycation and ubiquitin modifications were manually validated for all 18 proteins (Table 2.3). (See **supplementary Figure S1 and Table S3; provided in CD**).
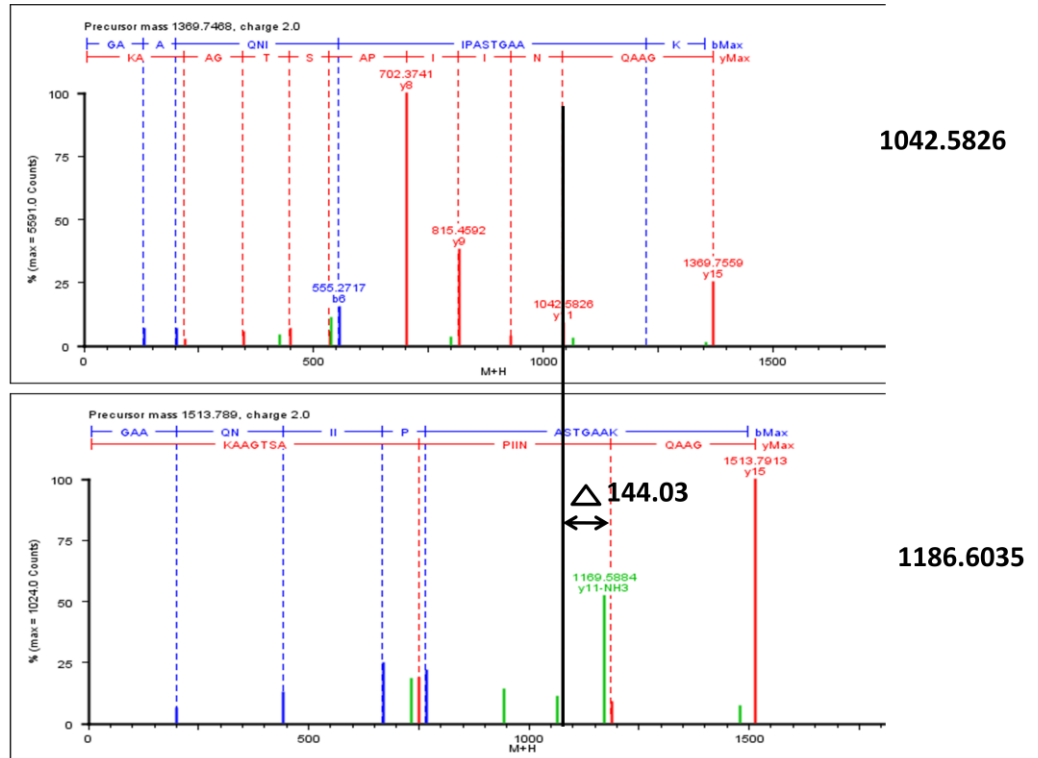
199-213   GAAQNIIPASTGAAK(ImiA) : 144.03

Figure 2.4.A A representative MS/MS annotation of glycation modification of Imidazolan A (Imi A) showing increase in mass of 144.03 Da

702.3741

816.4489

196-213   (R)DGRGAAQNIIPASTGAAK(Ubi)(A)
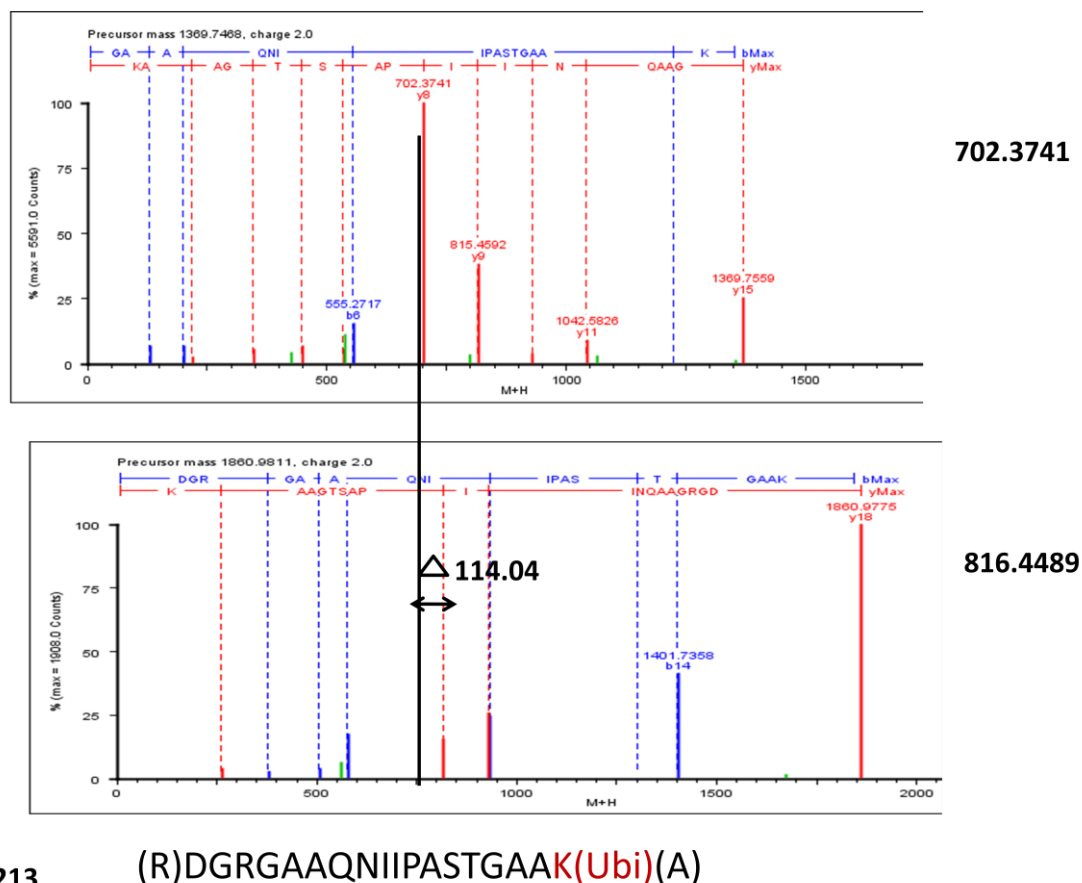
Figure 2.4.B A representative MS/MS annotation of Ubiquitin modification (Ubi) showing increase in mass of 114.04 Da

Table 2.3 Mass spectrometrically identified proteins detected by Anti-AGE and Anti-ubiquitin antibody.

Acc.No.	Protein name	No. of AGE modifications	No. of Ubiquitin modifications
D3ZGY4	Glyceraldehyde 3 phosphate dehydrogenase	7	2
P63039	60 kDa heat shock protein mitochondrial	14	4
P56574	Isocitrate dehydrogenase NADP	11	1
P07895	Superoxide dismutase Mn mitochondrial	11	1
P51635	Alcohol dehydrogenase NADP	9	1

Acc.No.	Protein name	No. of AGE modifications	No. of Ubiquitin modifications
F1LP05	ATP synthase subunit alpha	14	4
P10719	ATP synthase subunit beta mitochondrial	6	3
P04764	Alpha enolase	6	2
P16617	Phosphoglycerate kinase	13	4
P42123	L lactate dehydrogenase B chain	10	3
P04636	Malate dehydrogenase mitochondrial	8	1
4903	Glutathione S transferase alpha 1	18	2
P00884	Fructose bisphosphate aldolase B	12	3
P06685	Sodium potassium transporting ATPase subunit alpha 1	17	2
P10860	Glutamate dehydrogenase 1 mitochondrial	10	4
Q68FU3	Electron transfer flavoprotein subunit beta	11	2
Q5XIF6	Tubulin alpha 4A chain	7	1
Q9WVK7	Hydroxyacyl coenzyme A dehydrogenase mitochondrial	12	2

Furthermore, identified PRPs were additionally validated by western blotting using specific antibodies for few representative proteins (Figure 2.5). It was interesting to identify some of these proteins involved in energy metabolism such as ENO, GST, GAPDH, ICDH and MDH as modified by various glycation modifications, common to our previous study (Chougale et al., 2012). Hence, these results provided additional evidence that the protease resistance of these proteins is due to a variety of AGE modifications. In addition to these proteins, stress response proteins such as 60 kDa HSP, Mn-SOD were identified as PRPs in

the diabetic rat kidney. Few other PRPs involved in cytoskeletal organization and transport were also identified.
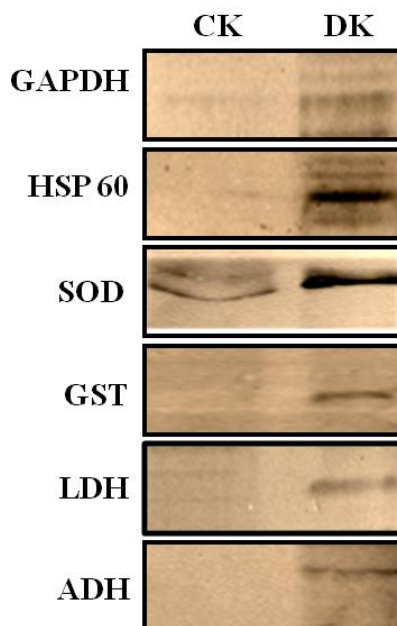
Figure 2.5 Validation of LC-MS^E identified PRPs by western blotting. Protein lysate of Control (CK) and diabetic (DK) rat kidney was digested with trypsin, and separated on SDS-PAGE, followed by immunoblotting with antibodies against GAPDH, HSP 60, SOD, GST, LDH and ADH. Presence of these proteins in DK after trypsin digestion confirmed the identification of PRPs by mass spectrometry. The experiment was repeated independently three times.

II.3.3. PRPs exhibited reduced functional activity - Mn-SOD, LDH, ADH and GST were selected as a representative of oxidative stress, energy metabolism and detoxification respectively for the functional analysis. The activity of all these enzymes was significantly affected in diabetic condition (Figure 2.6 A-D). The activity of Mn-SOD was reported to be reduced in leukocytes of diabetic patients (Uchimura et al., 1999). In normal physiological condition SOD plays a central role in scavenging free radicals, reduced SOD function may increase oxidative stress. Our results with ADH were comparable with previous study of glycation of sorbitol dehydrogenase decreasing its activity (Hoshi et al., 1996). With respect to GST, our results were consistent with the earlier reports where impaired GST activity in liver microsomes and mitochondria was observed in diabetic rats (Traverso., 2002). As GSTs constitute one of the major components of the phase

II drug-metabolizing enzyme and antioxidant systems, its reduced activity may lead to diabetic complications by causing a disturbance in xenobiotic metabolism. Glycation induced inactivation of LDH was observed both in isolation and in cell lysates previously (Morgan et al., 2002). These effects could be due to the direct adduction of the free- or protein-bound carbonyls with the target enzyme.
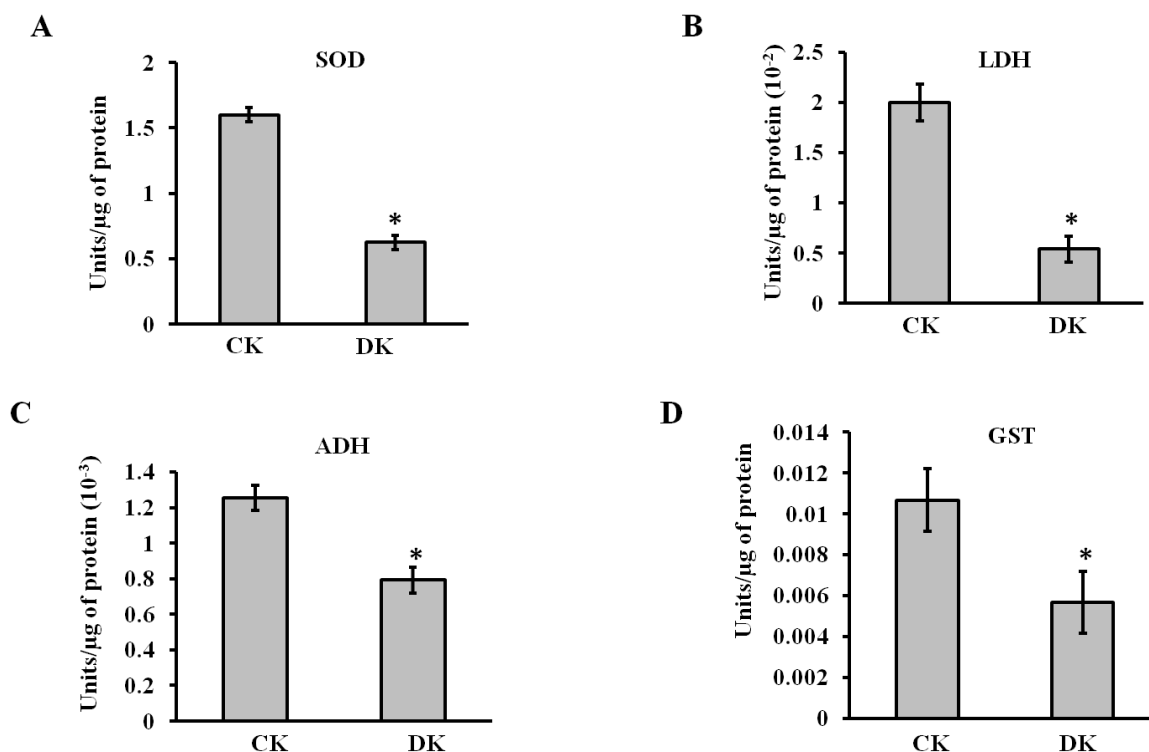
Figure 2.6 Functional assays of identified PRPs. The enzymatic activities of **A.** SOD, **B.** LDH, **C.** ADH, and **D.** GST were analyzed for control (CK) and diabetic (DK) rat kidney protein lysate. In DK, significant reduction in enzymatic activity was observed. Bars represent means ± SE from three independent experiments. *$P < 0.05$.

II.3.4. Prediction of aggregation hotspots in PRPs - Protein aggregation is implicated in the development of Alzheimer's, Parkinson's diseases and in diabetes through crosslinking of proteins. In this study, identified PRPs were assumed to be aggregated due to glycation reaction. *In silico* analysis was done to predict the regions of a polypeptide chain that were prone to β-sheet aggregation and amyloid formation. Aggregation prone regions of the identified PRPs are listed in Table 2.4. It was remarkable to find that some of the aggregation prone

regions had glycation modification sites identified by LC-MS^E. The aggregation prone regions containing glycation modifications were mapped onto their structure in representative PRPs (Figure 2.7). The finding of glycation modification sites in the aggregation prone region suggests that the increased protein cross-linking and aggregation in diabetes could be due to AGE modification.

Table 2.4 *In silico* analysis of aggregation prone regions in PRPs.

Bold and italicized regions had glycation modification

Identified proteins	Predicted aggregation prone regions
Glyceraldehyde 3 phosphate dehydrogenase	35-47, 114-121, *158-181*, *214-232*, 301-314
60 kDa heat shock protein mitochondrial	*17-31*, 60-76, *138-142*, 240-250, 253-258, *397-405*, 464-481
Isocitrate dehydrogenase NADP	60-72, 74-84, 105-114, 142-150, *186-197*, 246-253, 297-308, 322-336, *369-377*
Superoxide dismutase Mn mitochondrial	1-6, 97-105, *134-146*, 179-194, 200-211, 214-218
Alcohol dehydrogenase NADP	*31-46, 72-81*, 102-114, *145-161*, 173-179, 233-238, *247-261, 269-282*
ATP synthase subunit alpha	1-11, 74-80, 112-125, *218-227*, 241-252, 339-367, *407-417*
ATP synthase subunit beta mitochondrial	61-72, 82-86, *139-149, 202-235*, 263-271, 282-290, 303-310, 316-332, 384-395, 435-443, 504-511
Alpha enolase	21-35, *105-121*, 149-154, 165-172, 223-232, 276-287, 307-316, 363-370, 381-393
Phosphoglycerate kinase	16-26, 81-101, 112-122, *175-185*, 235-254, 363-375

Identified proteins	Predicted aggregation prone regions
L lactate dehydrogenase B chain	22-47, ***88-98***, ***124-129***, 131-139, 141-152, 173-179, 200-212, 294-301
Malate dehydrogenase mitochondrial	27-35, 40-61, 91-98, 134-157, 164-180, ***235-260***
Glutathione S transferase alpha 1	***6-10***, ***67-79***, 101-112, 147-151, 156-171
Fructose Bisphosphate aldolase B	61-69, ***98-110***, 249-261, 267-273, 281-290, 353-364
Sodium potassium transporting ATPase subunit alpha 1	91-117, 130-150, 244-249, ***253-263,*** 303-332, 388-393, 750-760, 771-798, 802-817, 865-879, 802-817, 916-936, 949-971, 994-1001
Glutamate dehydrogenase 1 mitochondrial	104-120, 160-177, 300-328, ***355-363, 418-425,*** 427-447, 550-558
Electron transfer flavoprotein subunit beta	1-20, 117-127, ***218-228***
Tubulin alpha 4A chain	1-12, 64-71, 148-158, 166-172, 189-193, ***226-243***, 312-323, 327-333, ***335-347***, 372-383, ***399-410***
Hydroxyacyl coenzyme A dehydrogenase mitochondrial	21-45, 47-55, 106-122, 153-173, ***215-233,*** 259-272
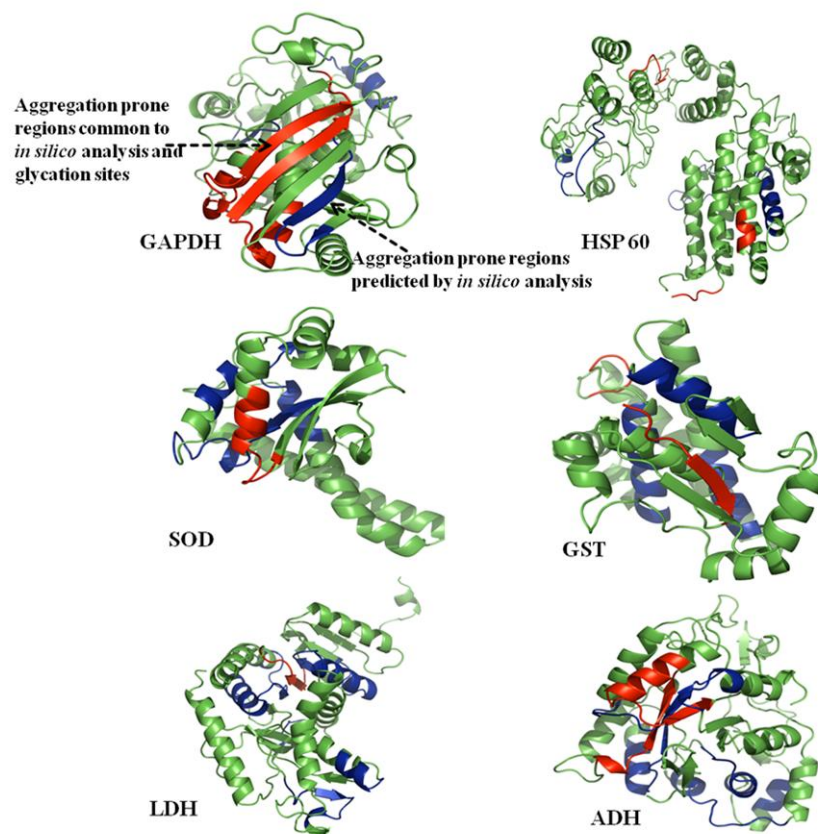
Figure 2.7 Prediction of aggregation prone regions. Protein structures of rat GAPDH, HSP 60, SOD, GST, LDH and ADH were modeled by CPH 3.0 model server and analyzed using PyMol. Aggregation prone regions in these proteins were predicted *in silico* using Aggrescan, Tango, PASTA and Waltz web servers (blue colour). The regions common to aggregation prone sequences and glycation sites were highlighted in the red colour, indicating that most of the glycation sites were overlapping with predicted aggregation hotspots.

II.3.5. Gene expression analysis of PRPs - Western blotting (Figure 2.9 A) and semiquantitative RT-PCR (Figure 2.9 B) study revealed the upregulation of GAPDH, HSP60, SOD, GST, LDH and ADH at both protein as well as mRNA level respectively in diabetic rat kidneys. Beta-actin (housekeeping gene) showed equivalent expression at the mRNA level of control as well as diabetic kidney tissue (Figure 2.8). Increased expression of GAPDH has been observed in diabetic rat liver (Johnson et al., 2009). HSP70 which is involved in stress response has

also been observed to be upregulated in the circulation of diabetic patients and correlates positively with the chronicity of disease (Nakhjavani et al., 2010). The mRNA levels of Mn-SOD found to be increased in the rat embryos as a response to maternal diabetes (Cederberg et al., 2000). Increased expression of GST in renal proximal tubules in the early stages of diabetes in the Akita mouse model has been detected by mRNA, western blot and immunohistochemical analysis (Fujita et al., 2001). Dramatic increase in LDH mRNA level has been reported in chronic hyperglyceamia induced in Sprague-Dawley rats by partial pancreatectomy (Jonas et al., 1999). Increased brain protein level of ADH has been observed in Alzheimer's disease due to elevated carbonyls (Balcz et al., 2001). As we have shown that the biological function of PRPs was decreased due to AGE modification in diabetic condition, the cells possibly have increased expression of these proteins to compensate for the loss of activity. Indeed, it has been studied that inactivation of sorbitol dehydrogenase by glycation reaction was associated with increased mRNA and protein levels in the liver of STZ-induced diabetic rats (Hoshi et al., 1996). In addition to this, decreased proteasomal activity and decreased removal of these proteins contributes to their stability and may lead to cross-linking and aggregation (Figure 2.10). These results provided insight into the probable cause of protease resistance and its consequences leading to diabetic complications.
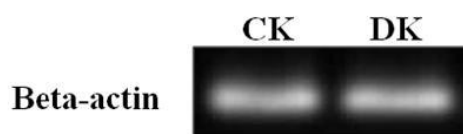
Figure 2.8 Gene expression analysis of Beta-actin (House keeping gene) by semi-quantitative RT-PCR
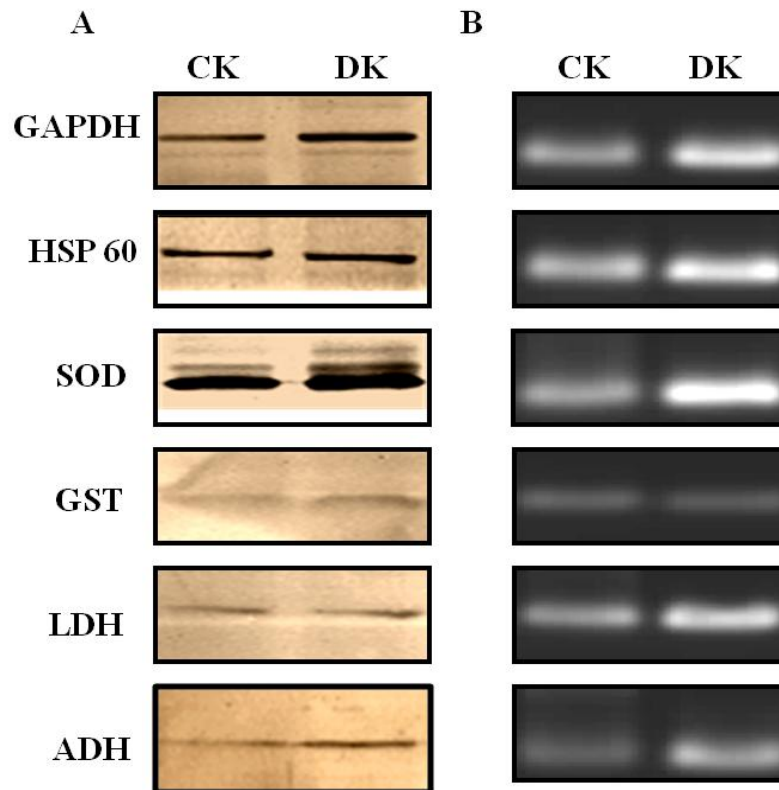
Figure 2.9 Expression analysis of PRPs. A. Protein expression of GAPDH, HSP 60, SOD, GST, LDH and ADH in control (CK) and diabetic (DK) rat kidney was measured by the Western blot analysis. **B.** The same proteins were analysed at the transcript level by performing Semi-quantitative RT-PCR using total RNA isolated from control and diabetic rat kidney tissues. All samples were analyzed on 1% agarose gels containing gel red. Both analysis showed upregulation of PRPs in diabetic condition. Results shown are representative of three independent experiments.
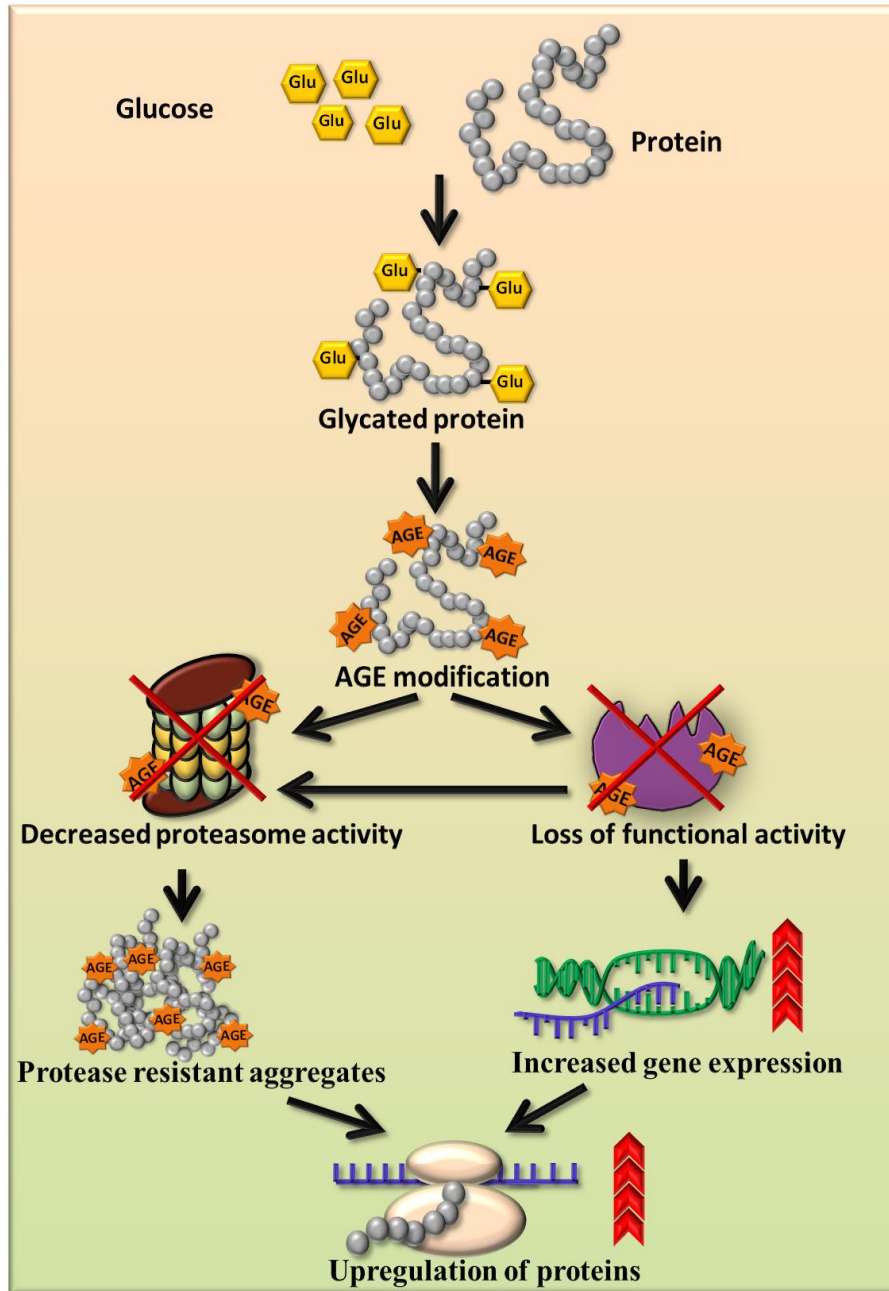
Figure 2.10 Schematic diagram for accumulation of PRPs and upregulation of proteins. The proposed model shows that AGE modification and impairment in proteasomal activity results in accumulation of protease resistant aggregates. AGE modification causes loss of functional activity of enzymes, which is compensated by increased gene expression. Hence, the inability of proteasome to remove protease resistant aggregates and decreased enzyme activity may cause upregulation of proteins in the diabetic condition.

CHAPTER III

Protriptyline, an anti-depressant inhibits protein cross linking and multiple targets of Alzheimer's disease

III.1. Introduction

Alzheimer's disease (AD) is the foremost cause of dementia in the ageing population affecting over 35 million people worldwide. According to World Alzheimer Report 2013, this number is expected to increase by two fold in 2030. AD is a progressive neurodegenerative disorder that leads to the irreversible loss of neurons, intellectual abilities and eventually to death within a decade of diagnosis. Although the molecular bases of AD pathogenesis remains incompletely elucidated, the disease has been recognized as a multifactorial syndrome involving various molecular and cellular processes such as protein aggregation, oxidative stress, cell cycle deregulation and neuroinflammation (Roberson et al., 2006).

There are currently several plausible hypotheses for AD pathogenesis. Cholinergic hypothesis states that the reduced cholinergic neurotransmission leads to the degeneration of cholinergic neurons and hence synaptic failure and cognitive dysfunction (Bartus et al., 1982). Following this, Acetylcholinesterase (AChE) was validated as a therapeutic target to reduce the degradation of acetylcholine in the synapse. AChE inhibitors (AChEIs) are effective in temporarily restoring cholinergic function, and constitute the majority of AD drugs currently available in the market (Alzheimer's Association: FDA-approved treatments for Alzheimers, 2012). However, they are incapable of delaying or preventing neurodegeneration (Small, 2005; Terry et al., 2003).

A variety of biochemical, genetic and pathological studies describe pivotal roles of the Amyloid β (Aβ) peptide in the pathogenesis of AD. "Amyloid hypothesis," describes the altered synthesis, aggregation and accumulation of Aβ which results in amyloid plaque formation (Hardy et al., 2002). While extracellular deposits of amyloid plaques are highly neurotoxic, recent studies have also implicated soluble, oligomeric aggregates of Aβ in neurotoxicity (Haass et al., 2007). Therefore, a key therapeutic strategy for the treatment of AD involves the development of drugs targeted at inhibiting Aβ production, aggregation, destabilization and clearance of preformed fibrils (Golde, 2006). A

crucial step in Aβ production is the specific N-terminal enzymatic cleavage of the membrane embedded Amyloid Precursor Protein (APP) by the transmembrane aspartyl protease, β-secretase (BACE-1) (Selkoe, 1999; Citron, 2002; Hussain, 2004; Hills et al., 2007). Therefore, inhibiting BACE-1 has been considered as another attractive approach to prevent Aβ neurotoxicity. It is noteworthy that no inhibitors of Aβ aggregation or BACE-1 activity have reached the market yet, despite strong evidence of the causative roles of Aβ in AD.

We further point out that Aβ is transported through a Receptor for Advanced Glycation End products (RAGE) and cause neuronal damage. Long-lived proteins are preferentially modified to form Advanced Glycation End products (AGE), and the stability of Aβ makes it an ideal substrate for non-enzymatic glycation and formation of AGEs (Vitek et al., 1994). In a recent study, it has been shown that Aβ-AGE formation may intensify the neurotoxicity whereas inhibition of this process significantly rescued the early cognitive deficit in mice (Li et al., 2014). Therefore, glycated Aβ has been considered as a more suitable ligand for RAGE, as it aggravates neuronal deterioration (Li et al., 2014). Hence inhibiting glycation of Aβ may be a valuable therapeutic strategy for AD. However, there has been no concerted effort to explore the inhibition of Aβ glycation as a therapeutic strategy.

Efforts to target AChE inhibition (Anand et al., 2013); Aβ production (Zhang et al., 2012); Aβ aggregation (Schen et al., 2012); tau phosphorylation and aggregation (Götz et al., 2012) have been investigated largely in isolation, despite the complex nature of AD etiology. Recently, drug discovery in AD has gradually inclined towards development of "Multi-Target-Directed Ligands" (MTDLs) (Youdim et al., 2005; Zhang et al., 2005; Cappelli et al., 2005; Lee et al., 2014) which are efficient in treating complex diseases because of their ability to target multiple modes of disease pathogenesis. Further, to evaluate MTDLs for the AD treatment, "drug repositioning" seems to be an appealing strategy, as this approach has several advantages, including reduced time and cost necessary for clinical trials. Priority candidate drugs for hypertension, retinoid therapy, diabetes and antibiotics with sufficient supporting evidences have been considered for

repositioning in AD (Corbett et al., 2012). However, to the best of our knowledge, repositioning drugs for multiple targets in AD is scarce. In this study, an *in silico* screening of 140 FDA approved drugs for neurological treatment was done against the primary targets of AD therapeutics, namely, acetylcholinesterase, β-secretase, and Aβ aggregation. Further *in vitro* studies showed that amongst selected molecules, the tricyclic antidepressant protriptyline exhibited significant inhibition of AChE, as well as inhibition of other targets of AD. In addition, protriptyline was also found to inhibit glycation mediated Aβ aggregation. Mechanistic insights into protriptyline binding and inhibition of AChE, Aβ, and BACE-1 activity were described in detail with molecular dynamics simulation studies.

III. 2. Materials and methods

Materials. All chemicals were procured from sigma unless and otherwise stated.

III.2.1. *In silico* Screening. Structures of 140 FDA approved antiepileptics, psycoleptics, analgesics, psycoanaleptics, anti-Parkinson and other nervous system drugs were obtained from DrugBank (http://www.drugbank.ca/) database and optimized for their 3D coordinates using Marvin Sketch Tool (http://www.chemaxon.com). Three dimensional structures of Human acetylcholinesterse (PDB ID: 1B41), β-secretase (PDB ID: 2HM1) and Aβ peptide (PDB ID: 1ZOQ) were accessed from RCSB PDB. Protein structures were energy minimized using Swiss PDB viewer (http://spdbv.vital-it.ch/). AutoDock 4.2 software (Morris et al., 2009) was used to convert receptor and ligand from *.pdb to *.pdbqt format and to set other docking parameters. Grid map was set around the active site of acetylcholinesterase (Ser203, Glu334 and His447), β-secretase (Asp32 and Asp228) and KLVFF (residue 17 to 21) region of Aβ protein involved in aggregation. Virtual screening was carried out using AutoDock Vina software and the Lamarckian genetic algorithm as a searching procedure (Trott et al., 2010). Binding energy obtained for each complex was represented in heat map format using MeV software packages

(http://www.tm4.org/mev/) (Saeed et al., 2006). The gradient ruler is an indicator of interaction strength. Molecules showing strong binding against all the selected targets were selected for further *in vitro* and molecular simulation studies.

III.2.2. Acetylcholinesterase Inhibition Assay. The modified method of Ellman et al. was adopted to measure AChE activity (Ellman et al., 1961). Briefly, 25 µl (0.3 U/ml) AChE from Electric eel fish (*Electrophorus electricus*) was incubated with and without different concentrations of drugs selected from Molecular Docking studies. The reaction was carried out for 15 min at 25°C. 500 µl of 5, 5-dithiobis (2-nitrobenzioc) acid DTNB (3 mM) was then added and reaction was initiated by the addition of 100µl substrate acetyl thiocholine iodide (ATCI) (15 mM). Total volume of the reaction was made up to 1 ml by Tris buffer, pH 8.0. ATCI hydrolysis was measured by colored product formation, 5-thio-2-nitrobenzoate anion by reaction between DTNB and thiocholine, a hydrolysis product of ATCI. The formation of the colored product was measured at 405 nm wavelength after 30 min. The background was determined from negative controls (omission of AChE enzyme).

III.2.3. Isothermal Titration Calorimetry. ITC was performed using Microcal Auto-iTC instrument (GE Healthcare). 40 injections of 2 µl protriptyline (Stock =2.2 mM) was titrated against 0.3 U/µl solution of AChE. Experiments were carried out at 25 °C in a Tris buffer, pH 8.0. Reference titration was carried out by injecting the same concentration of protriptyline into buffer. Reference titration was subtracted from experimental titration. Origin 6.0 software was used to derive affinity constants (K_d), the molar reaction enthalpy (ΔH) and the stoichiometry of binding (N), by fitting the integrated titration peaks.

III.2.4. Fluorescence Analysis of AchE-Protriptyline Interaction. AchE-protriptyline interaction was also studied by measuring tryptophan fluorescence using Varioscan plate reader. AChE was excited at 280 nm and emission was scanned from 300 nm to 500 nm. Titration of enzyme with protriptyline was performed by the addition of different concentrations of inhibitor (10 nM-100

nM) to a fixed concentration (0.2U/μl) of enzyme solution. Background buffer and inhibitor spectra were subtracted and graphs were smoothed.

III.2.5. β–secretase Inhibition Assay. BACE-1 activity was studied in accordance with the manufacturer's instructions (Sigma). To test the effect of protriptyline on BACE-1 activity, 1.8 U of BACE-1 enzyme and 10 μM of β-secretase specific peptides conjugated to fluorogenic reporter molecules were incubated with or without various concentrations of protriptyline for 2 h at 37°C. Negative control included all the reactants except BACE-1 enzyme. After 2 h, fluorescence emission was measured at 405 nm upon excitation at 320 nm.

III.2.6. Inhibition Kinetics for AChE and BACE-1. Michaelis–Menten constant (K_m) was determined by measuring the activities of AChE and BACE-1 using various concentrations of ATCI (100 μM-1000 μM) and BACE-1 substrate (0.25 μM-6 μM) respectively. Lineweaver-Burk double reciprocal plot was plotted in order to determine the K_m. The protriptyline inhibition kinetics was analyzed over a range of concentration (50 μM–1500 μM) and (10 μM–150 μM) for AChE and BACE-1 respectively. The IC_{50} of protriptyline for both the enzymes was calculated by determining the inhibitor concentration at which the enzyme activity is 50% inhibited. The K_i was calculated directly from IC_{50} value using Cheng-Prussoffs classical equation (Copeland et al., 1995).

$$K_i = \frac{IC_{50}}{1 + S / K_m}$$

In order to determine the type of inhibition, AChE and BACE-1 were incubated with 60 μM and 15 μM protriptyline concentrations respectively and assayed at increasing concentrations of AChE substrate (ATCI, 100 μM-1000 μM) and BACE-1 substrate (1 μM-10 μM) respectively. The reciprocals of reaction rate (1/v) for each inhibitor concentration were plotted against the reciprocals of the substrate concentrations (1/S). Mode of inhibition by protriptyline was determined from the graphical representation.

III.2.7. Inhibition of Aβ Aggregation. Aβ$_{13-22}$ peptide (HHQKLVFFAE), the aggregation prone region of Aβ, was synthesized from ThermoFisher Scientific. Synthetic Aβ$_{13-22}$ peptide was dissolved in 10% ammonium hydroxide and sonicated for 5 min. It was then diluted in 10 mM PBS, pH 7.0 to a final concentration of 200 μM. 100 μM of Aβ$_{13-22}$ was incubated with and without various concentrations of protriptyline in 10 mM PBS, pH 7.0 at 37°C for a week and these samples were further used for aggregation inhibition assays.

III.2.8. Glycation Inhibition Assay. Anti-glycation activity of protriptyline was studied using insulin, BSA and Aβ. 1.5 mg/ml insulin and 0.1 M glucose were incubated with various concentrations of protryptiline in 10 mM PBS, pH 7.0 for 7 days. These samples were further used to study glycation inhibition by MALDI (Golegoankar et al., 2010). BSA glycation reaction was performed in a similar manner with 1mg/ml BSA concentration and inhibition was studied by AGE fluorescence and Thioflavin T assay. In Aβ glycation studies, 100 μM Aβ$_{13-22}$ and 0.1 M glucose were incubated with and without various concentrations of protriptyline in 10 mM PBS, pH 7.0 for 7 days. These samples were further used to study glycation mediated Aβ aggregation by different assays.

III.2.9. Thioflavin T Assay. Thioflavin T assay was performed on 7th day of incubation. 50 μl (25 μM) of Aβ$_{13-22}$ was mixed with 150μl of Thioflavin T (ThT) stock solution (50 μM ThT in PBS pH 7.0) and placed in 96-well plate (black with flat bottom, Cornings). Fluorescence emission was measured at 460-550 nm upon excitation at 440 nm. To account for background fluorescence, the fluorescence intensity measured from each control solution without Aβ was subtracted from each solution containing Aβ$_{13-22}$. Similarly, Thoflavin T assay was performed for aggregation kinetics of Aβ$_{13-22}$ and Aβ$_{13-22}$ glycation with and without protriptyline.

III.2.10. Light Scattering Analysis. Inhibition of aggregation/ glycation mediated aggregation of Aβ was detected by static light scattering method using a Perkin-Elmer Luminescence spectrometer LS50B. Both excitation and emission

wavelengths were set at 400 nm. Excitation and emission slit width was set to 10 nm and 2.5 nm, respectively. Scattering was recorded for 60 sec.

III.2.11. Circular Dichroism Spectroscopy. The far UV CD spectra (wavelength range of 190-250 nm) of amyloid (20 µg/ml) with and without protriptyline were recorded on a Jasco-J815 spectropolarimeter at ambient temperature. Each CD spectrum was accumulated from three scans at 50nm/min with cell path length of 0.1 cm. Contribution due to buffer was corrected in all spectra and observed values were converted to mean residual ellipticity (MRE) in deg cm^2 dmol^{-1} defined as

$$MRE = \frac{M\theta_\lambda}{10dcr}$$

Where M is the molecular weight of the protein, θ_λ is CD in millidegree, d is the path length in cm, c is the protein concentration in mg/ml and r is the number of amino acid residues in the protein. Secondary structure content of the amyloid with and without protriptyline was calculated using the CDPro software (http://lamar.colostate.edu/~sreeram/CDPro/main.html).

III.2.12. Atomic Force Microscopy. For atomic force microscopy (AFM) analysis, 10 µl of each sample was deposited on a piece of freshly cleaved mica disk. The disk was washed with water and dried overnight. The sample was mounted onto a Multimode scanning probe microscope equipped with a Nanoscope IV controller from Veeco Instrument Inc., Santa Barbara, CA. All the AFM measurements were done under ambient conditions using the tapping-mode AFM probes model - Tap190Al purchased from Budget Sensors. The radii of tips used in this study were less than 10 nm, and their height was ~ 17 µm. The cantilever used had a resonant frequency of ca. 162 kHz and nominal spring constant of ca. 48 N/m with a 30 nm thick aluminium reflex coating on the back side of the cantilever of the length 225 µm. For each sample, three locations with a surface area of 20 × 20 µm^2 and 10 × 10 µm^2 for amyloid and protriptyline treated amyloid were imaged with a frequency of 1 Hz and at a resolution of 512 × 512 dpi. Representative images were selected for comparative studies.

III.2.13. Measurement of Glycation Associated Fluorescence. Glycation associated fluorescence of Aβ was measured in amyloid, glycated amyloid treated with or without protryptiline at 370 nm excitation and emission was scanned from 400-550nm.

III.2.14. BA*p*NA Assay. Activity of Bovine trypsin was estimated using enzyme-specific chromogenic substrate BA*p*NA (Tamhane et al., 2005). In brief, 10 μg Bovine trypsin was incubated with and without 100 μM, 200 μM, 500 μM protriptyline at 37 ^{o}C for 15 min and volume was made up to 150 μl with 0.1 M Tris-HCl pH 7.8. Further, 1 ml BA*p*NA was added to the reaction mixture and incubated for 10 min at 37°C. The reaction was terminated by addition of 200μl of 30% acetic acid and absorbance was measured at 410nm.

III.2.15. ADAM17 Assay. ADAM17 assay kit (Enzo Life Sciences) was used to study the effect of protriptyline on ADAM17. Briefly, ADAM17 and fluorogenic peptide (substrate) was incubated with and without 100 μM protriptyline at 37°C for 10 min. The negative controls had the reaction mixture without enzyme. Fluorescence was measured at 328 nm and 420 nm for excitation and emission respectively.

III.2.16. Molecular Dynamics Simulations. All simulations in this study were carried out with the NAMD2.9 package (Kale et al., 1999), using the CHARMM22 all-atom force field with CMAP correction for the proteins (MacKerell et al., 1998; 2004). Force field parameters for protriptyline were generated using the SwissPARAM tool, (Zoete et al., 2011) and refined via electronic structure calculations using Gaussian03. This strategy has been used in several recent studies (Hill et al., 2012; Mabanglo et al., 2012; Caulfield et al., 2011). Simulations were carried using a time step of 2 fs in the isothermal-isobaric (NPT) ensemble at a temperature of 310 K and a pressure of 1 atmosphere. Each system was sampled for a total duration of 60 ns with multiple trajectories. The SHAKE algorithm (Ryckaert et al., 1977) was used to constrain bond lengths involving hydrogen atoms. Constant temperature was maintained with Langevin dynamics with a collision frequency of 1 ps^{-1}, and constant

pressure was maintained using the Langevin piston Nose-Hoover method (Feller et al., 1995). Three-dimensional orthorhombic periodic boundary conditions were employed and full electrostatics calculated with the particle-mesh Ewald method (Essmann et al., 1995). A non-bonded cutoff distance of 12 Å was employed, which were smoothened at a distance of 10.5 Å.

III.2.16.a. AChE System setup. Initial coordinates for the AChE molecules were derived from the X-ray crystallographic structure of the enzyme complexed with fasciculin-II (Kryger et al., 2000) reported in the PDB database (PDB ID 1B41). Fasciculin was deleted from the structure, and the missing residues were added with the *Modeller* software. Protriptyline was docked with the catalytic site residues (Ser199, Glu330, His443) using Autodock. The resultant system was immersed in a box of equilibrated TIP3P water molecules (Jorgensen et al., 1983), maintaining a minimum distance of 14 Å from the box edge to each atom. Seven sodium counter ions were added at random positions within the simulation box.

III.2.16.b. Aβ System setup. Amyloid β (Aβ) is an intrinsically unstructured peptide whose high aggregation propensity makes it forbiddingly difficult to report the monomeric structure with purely experimental means in fully aqueous environment. However, NMR studies have reported the monomeric structure in mixtures of organic solvent and water (Tomaselli et al., 2006). Our initial structure was generated by heating and quenching full length Aβ (PDB ID 1ZOQ) in water. Heating this structure in 100% water for 2 ns at 600 K resulted in a random coil state, which was quenched at 310 K and four independent 100 ns trajectories were generated. Two of the trajectories resulted in monomeric structures with significant anti-parallel beta sheet content in the C-terminal region and marginal helicity in the N-terminal region, in excellent agreement with recent reports of the important conformations in the Aβ ensemble (Lin et al., 2012; Sgourakis et al., 2007). Five protriptyline molecules were placed randomly in the vicinity of the monomeric structure thus obtained, and the resilting system placed in an equilibrated box of TIP3P water in a manner similar to AChE. The protriptyline-Aβ dimer complex was obtained by adding an incoming monomer at a distance of 25 Å from the center of mass of the protriptyline bound monomeric

state. Chloride counter ions were added in each case to maintain charge neutrality. The free monomer and dimer complexes were simulated separately with equivalent protocols.

III.2.16.c. BACE1 System setup. The initial co-ordinates of human β-secretase (BACE-1) were obtained from PDB ID 2HM1, which is a 2.2 Å resolution crystallographic structure of the protein bound with hydroxyethylamine (Freskos et al., 2007). The latter was removed, missing residues added with *Modeller*, and the active residues Asp32 and Asp228 of the resultant structure was docked with protriptyline. Previous studies point out that Asp228 of the active site of beta secretase is protonated (Xiong et al., 2004). Asp protonation was done accordingly in our setup. His residues were protonated in order to mimic the experimental conditions of pH 5.0, and the system was immersed in an equilibrated box of TIP3P water as the other systems. Three sodium counter ions were added at random positions.

III.2.16.d. Asphericity (I_γ) analysis. The minimum (I_{min}) and the maximum (I_{max}) values of the principle moments of intertia of the protein were first calculated for every snapshot using the VMD software (Humphrey et al., 1996), and the asphericity was obtained as,

$$I_\gamma = 1 - \frac{I_{min}}{I_{max}}$$

For a perfectly spherical object, I_{min} and I_{max} are equal, leading to an I_γ value of 0.0 Thus, higher values of I_γ denote deviations from spherical gemoetry, or greater asphericity.

III.2.16.e. Inter-residue contact maps analysis. A pair of residues belonging to different peptide units was considered to make contact if their centers of mass approached within 7.0 Å of each other. The inter-residue contact maps were obtained by calculating the contact probabilities of each inter-protein residue pair from the simulated snapshots.

III.2.16.f. Secondary Structure analysis. Secondary structures reported are calculated within the VMD package using the algorithm STRIDE (Frishman et al., 1995).

III.2.17. Cell culture. Murine neuro2a neuroblastoma cells were purchased from NCCS, Pune, India. The cells were maintained in Dulbecco's modified Eagle's medium (DMEM) and 10% Fetal Bovine Serum (FBS). Cells were maintained at 37 ºC in humidified air containing 5% CO_2 and were grown in monolayer cultures.

III.2.17.a. Cell viability. Cell viability following exposure to protriptyline was measured by MTT reduction assay. Neuro 2a (N2a) neuroblastoma cells were seeded at a cell density of $1x10^4$ cells per well in a 96 well plate. After the cells adhered and attained their morphology, they were serum starved for 24 h prior to treatment with various concentrations of protriptyline in triplicate for 15 h. After incubation, cells were given one wash with PBS and 100ul fresh serum free media was added. 20 ul of 5mg/ml MTT (dissolved in PBS) was added to each well and incubated in dark at 37^0C until violet formazan crystals were observed. Media from each well was discarded and crystals were dissolved in 100 ul DMSO. Absorbance was measured at 555 nm using Biorad iMark microplate reader.

III.2.17.b. Determination of AChE inhibition in cultured cells. Equal numbers of cells were seeded in 25 cm^2 flasks (1.5 million). Cells were allowed to adhere and attain their morphology. Cells were serum starved for 24 h and treated with 25 and 60 μM protriptyline concentration for 16 h. Cells were trypsinised and given two washes with icecold PBS. Pellet was suspended in PBS and sonicated for 20 min. Centrifugation was done for 60 min at 16000 rpm. Protein in the supertanent was collected and estimated by Bradford's method. Acetylcholinesterase assay was done by taking equal amount of protein and performed as mentioned above by Ellman's assay.

III.2.18. Statistical Analysis. All the experiments were performed independently three times. Student's t-test was used for statistical analysis. Data were expressed as mean ± SD. A p-value < 0.05 was considered as statistically significant.

III.3. Results and discussion

III.3.1. Tricyclic Antidepressant Drugs Display Strong Binding Against Various Targets of AD *In silico*. - Multi-target-directed ligands (MTDLs) are likely to offer promising approaches for treatment of a disease as complex as AD (Youdim et al., 2005; Zhang et al., 2005; Cappelli et al., 2005). The structures of 140 ligands were docked with the major targets of AD viz. AChE, BACE-1 and Aβ aggregation. Ligands were scored based on electrostatic and hydrophobic contributions to the binding energy (Kitchen et al., 2004). Furthermore, polar interactions were considered by H-bonding interactions analysis. Docking scores were used to rank ligands, depending on presence of number of H-bond donors and acceptors within the active sites (Kellenberger et al., 2004). Binding energy scores represented in the Heatmap (Figure 3.1 A) displayed variability in interactions of the ligands to the three targets of AD (see **Supplementary Table S4** for binding affinity values; **provided in CD**). There were several ligands that showed noteworthy interaction with at least two targets, but only few of them had strong interaction with all the targets. It was observed that five antidepressant drugs protriptyline, amytriptyline, maprotiline, doxepin and nortriptyline, which are tricyclic secondary amines showed strong binding affinity and broad specificity toward multiple targets of AD (Figure 3.1 B).
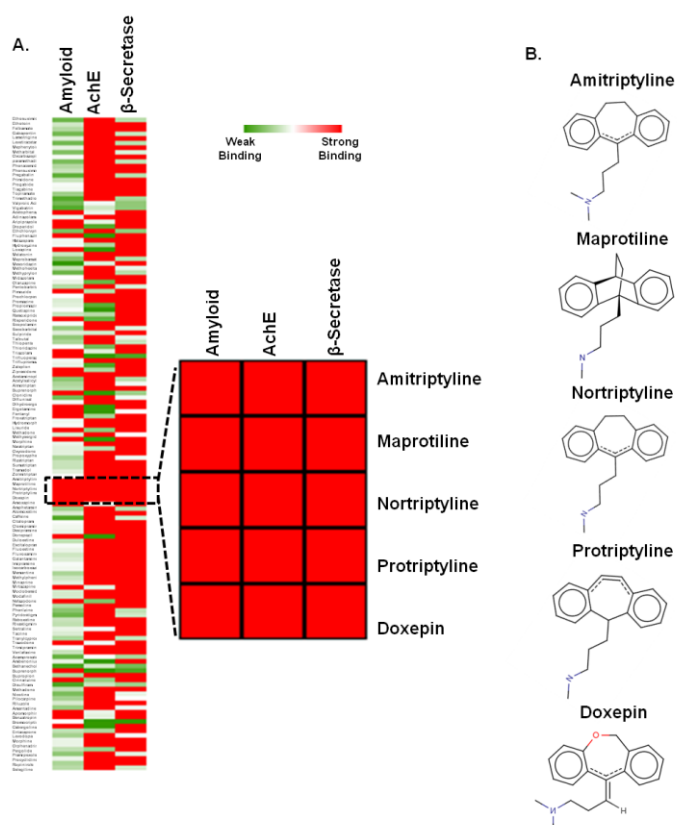
Figure 3.1 Virtual screening by docking. A. Heat map analysis of binding constants of 140 FDA approved nervous system drugs screened against Aβ, AChE and β-secretase by Autodock 4.2. Five ensquared drugs were zoomed, showing higher affinity to all the above mentioned targets**. B.** Chemical structures of the five drugs. All are tricyclic anti-depressant drugs.

III.3.2. Protriptyline Inhibits AChE Activity by Inducing Conformational Change in The Active Site - AChE currently remains the foremost therapeutic target for AD and the current treatment and management of AD mainly involves use of acetylcholinesterase inhibitors (Small et al., 2005; Terry et al., 2003). Therefore, protriptyline, amitriptyline, maprotiline, doxepin and nortriptyline were assessed initially against AChE inhibition. While all the five drugs displayed inhibitory activity against this target (Figure 3.2 A), protriptyline displayed highest inhibition, with the least IC_{50} of about 0.06 mM. In comparison, the other ligands displayed relatively higher IC_{50} values; the values corresponding to maprotiline, doxepin, nortriptyline and amitriptyline were 0.1 mM, 0.480 mM,

0.135 mM and 0.6 mM, respectively. Hence, the inhibitory activity of protriptyline against the other targets of AD was evaluated in detail in the remaining study.

The assessment of strong inhibitory activity of protriptyline was consolidated by enzyme kinetic studies, which suggested competitive inhibition of AChE by protriptyline (Figure 3.2 B). The apparent K_m for ACHI was determined to be ~0.025 mM by Lineweaver-Burk plot and it was found to be increased in the presence of protriptyline. The inhibition constant K_i was determined from Cheng-Prusoff's equation and found to be ~0.001 mM. Thermodynamic studies of protriptyline-AChE interaction was carried out using Isothermal titration calorimetry (ITC) as it is one of the most widely used quantitative technique for direct measurement of the enthalpy change when two species interact, allowing the determination of heat of association, stoichiometry, and binding affinity from a single experiment (Campoy et al., 2005; Shoemaker et al., 2007). The raw data and corresponding thermogram of the binding experiment is depicted in Figure 3.2 C. Binding was strongly exothermic and showed 1:1 stoichiometry for AChE and protriptyline. The spontaneity of the process is evidenced by a negative change in the enthalpy, ΔH, and a positive change in the entropy, ΔS. Kinetic and ITC data demonstrated the binding of single molecule of protriptyline to the active site of AChE. The active site of AChE comprises two subsites; the anionic subsite (Trp82, Glu198, Tyr333) and the esteratic subsite (Ser199, Glu330 and His443) (Tai et al., 2007). Strong binding propensity of protriptyline to both the subsites of AChE was evidenced via the MD studies (Figure 3.2 D and 3.2 E). The mean interaction strengths of protriptyline with the anionic sub-sites is -31.3 ($\pm$ 9.1) kcal mol^{-1} and -19.4 ($\pm$5.0) kcal mol^{-1} with the esteratic subsite (Figure 3.2 F). Breakup of the interactions into the non-bonded components showed that electrostatics plays a relatively stronger role than van der Waals interactions in protriptyline binding with active site. The mean interaction strengths of active site residues with the ligand are provided in Table 3.1.

Tabel 3.1 Acetylcholinesterase-protriptyline interaction energy calculations.
Interaction energy of ligand with active site residues averaged over last 20 ns of all simulated trajectories. Interaction strengths are in kcal mol^{-1} unit. Standard deviations are provided within braces.

	Cataytic/Esteratic subsite			Anionic subsite		
	443 His	330 Glu	199 Ser	82 Trp	198 Glu	333 Tyr
TBE	-13.0(4.0)	-5.9(2.9)	0.5 (0.9)	-7.2(2.7)	-21.2(8.0)	-2.8(1.2)
EE	-9.3 (5.0)	-5.5 (2.8)	0.6 (0.9)	-4.6 (2.0)	-20.9 (7.9)	0.3 (0.6)
vDWE	-3.3 (1.2)	-0.4 (0.3)	-0.05(0.03)	-2.6(1.6)	-0.2 (0.1)	-3.0 (1.0)

TBE: Total Binding Energy; EE: Electrostatic Energy; vDWE: van der Waal's Energy

Protriptyline-AChE interaction was also studied by fluorescence spectrometry. A significant shift in the tryptophan fluorescence emission spectra was observed upon protriptyline binding suggested that the drug induces conformational change in AChE, thereby in its functional abilities. The fluorescence intensity of AChE exhibited an emission maximum at a wavelength, λ_{max}, of 325 nm in the unbound state. However, titration of the native enzyme with increasing concentrations of inhibitor resulted in a concentration-dependent quenching of the tryptophanyl fluorescence (Figure 3.2 G). A progressive red shift in the emission spectrum with increasing concentration of protriptyline suggested the conformation change in enzyme.

The evidence of structural distortion was supported by the MD simulation data. In Figure 3.2 H, we compare the backbone root mean squared deviation (RMSD) of the active site residues in the free and protriptyline bound state for a sample MD simulation trajectory. The higher RMSD in the latter is a distinct demonstration of the perturbative effect of the ligand on the active site structure. This structural distortion is supported by changes in the inter-residue distances of the active site residues (Table 3.2).

Table 3.2 inter-residue distances between active site of AChE residues averaged over last 20 ns of free (vertical) and ligand bound (horizontal) simulated trajectories. Distances are in Å unit. Standard deviations are provided within braces.

	Trp82	Glu198	Tyr333	Ser199	Glu330	His443
Trp82	-	12.4 (0.5)	14.9 (1.03)	14.9 (0.6)	16.0 (0.6)	5.9 (0.6)
Glu198	12.8 (0.4)	-	15.8 (0.7)	4.1 (0.3)	9.8 (0.4)	9.6 (0.8)
Tyr333	14.0 (0.8)	14.1 (1.0)	-	14.5 (0.5)	9.6 (0.5)	11.1 (0.8)
Ser199	12.7 (0.4)	3.8 (0.1)	12.2 (1.1)	-	8.4 (0.4)	11.5 (0.8)
Glu330	17.5 (0.6)	9.9 (0.4)	8.9 (1.1)	8.8 (0.4)	-	10.5 (0.9)
His443	6.5 (0.3)	8.0 (0.3)	9.5 (0.8)	7.8 (0.3)	10.3 (0.8)	-

Distinct increases in several of the inter-residue distances are noted, especially in the distances involving Tyr333 and His443. The sharpest increase in the mean inter-residue distance is found for two residues belong to the esteratic subsite, namely Ser199 and His443 that play critical roles in the hydrolysis of acetylcholine. The increase from 7.8 Å in the free state to 11.5 Å in the bound state strongly suggests that protriptyline binding directly affects the catalytic ability of AChE. Further, we found protriptyline binding at the active site to be commensurate with an increase in its solvent accessibility. The solvent accessible surface area, or SASA, was calculated by running a spherical probe of 1.8 Å radius around the surface and calculating the area covered by the probe / calculated in the standard manner (Copeland et al., 1995). In Figure 3.2 I, we have presented histograms of the SASA obtained from the MD trajectories of the free and protriptyline bound AChE. The active site SASA increased from 1533 ($\pm$ 38.9) $Å^2$ to 1623 ($\pm$ 33.0) $Å^2$ upon protriptyline binding. Hence, our study revealed that protriptyline inhibits AChE, one of the important targets in AD pathology, by binding to the active site and causing conformational change.
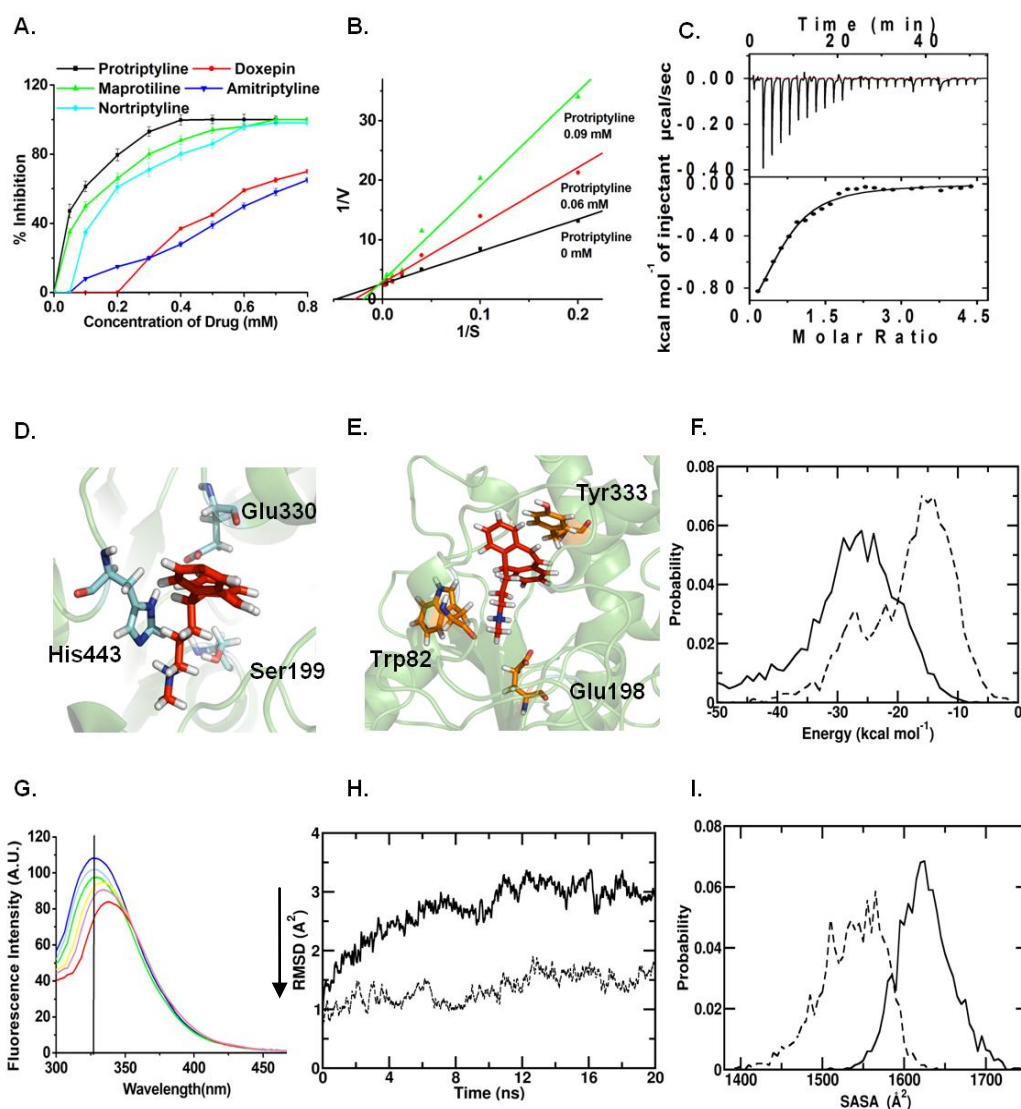
Figure 3.2 Protriptyline inhibits AChE activity. A. Determination of IC50 values of five drugs for AChE by using 0.05-0.8 mM concentration range of all the drugs **B.** Estimation of the kinetic constants by Lineweaver–Burk analysis. AChE inhibition by protriptyline showed competitive inhibition. **C.** Isothermal Titration Calorimetric analysis of protriptyline – AChE interactions. The upper panel shows the raw data in the form of heat effect during titration and the lower panel shows corresponding thermogram representing the best fit curve **D.** Snapshot of drug binding with catalytic subsite of AChE **E.** snapshot of drug binding with anionic subsite of AChE **F.** Distribution of protriptyline –anionic subsite (solid line) and protriptyline –esteratic subsite (broken line) non-bonded (nonb) interaction energy; data are averaged over last 20 ns **G.** Fluorescence quenching of AChE by protriptyline **H.** Evolution of the backbone RMSD for the protriptyline bound (solid line) and free (broken line) AChE active sites from MD

trajectories **I.** SASA distributions of active sites for protriptyline bound (solid line) and free (broken line) AChE active sites from MD trajectories

III.3.3. Protriptyline Inhibits Aβ Self-Assembly - Recent studies suggest that the $K_{16}LVFF_{20}$ segment in the Aβ sequence is crucial for the peptide's oligomeric properties as well as fibrillogenetic behavior (Jana et al., 2012; Santini et al., 2004; Balbach et al., 2000; Bernstein et al., 2005; Tjernberg et al., 1996). The sequence HHQKLVFFAE corresponding to Aβ_{13-22} was used for our *in vitro* amyloid aggregation inhibition studies.

β-sheet rich structures are a common feature of amyloid aggregates (Chimon et al., 2007) and bind to the molecule Thioflavin T (ThT). Therefore, ThT fluorescence assays are frequently used to monitor aggregation of amyloidogenic peptides (Levine et al., 1993). In Figure 3.3 A, we present ThT fluorescence as a function of time for Aβ_{13-22} in the absence or presence of 10 μM protriptyline. It is observed that the lag time corresponding to the nucleation phase is increased from ~25 to about ~50 h in the presence of protriptyline. The data further shows a dramatic inhibition in the growth phase in the presence of protriptyline. The fluorescence intensity corresponding to the saturation phase was further lowered in the presence of protriptyline, demonstrating the ability of protriptyline to reduce Aβ aggregation. Static light scattering experiments were performed to investigate the relative decrease in average molecular mass of Aβ aggregates in the presence of protriptyline (Figure 3.3 B). As expected, protriptyline reduced the light scattering in a concentration dependent manner. Furthermore, Far-UV CD spectra of the Aβ_{13-22} were recorded with and without protriptyline to monitor any possible alterations in secondary structural propensities (Figure 3.3 C). CDPro analysis comparing the spectra obtained at the two conditions showed that protriptyline treatment reduced β-sheet formation and increased overall helicity. The reduced β-sheet formation by CD analysis corroborated the Thioflavin T results. We further performed atomic force microscopy (AFM) experiments on the peptide aggregates formed with and without protriptyline treatment. The results of an AFM scans for Aβ_{13-22} incubated

for 7 days with and without protriptyline over scanning areas of 10μm × 10μm and 20μm × 20μm are compared in Figure 3.3 D.
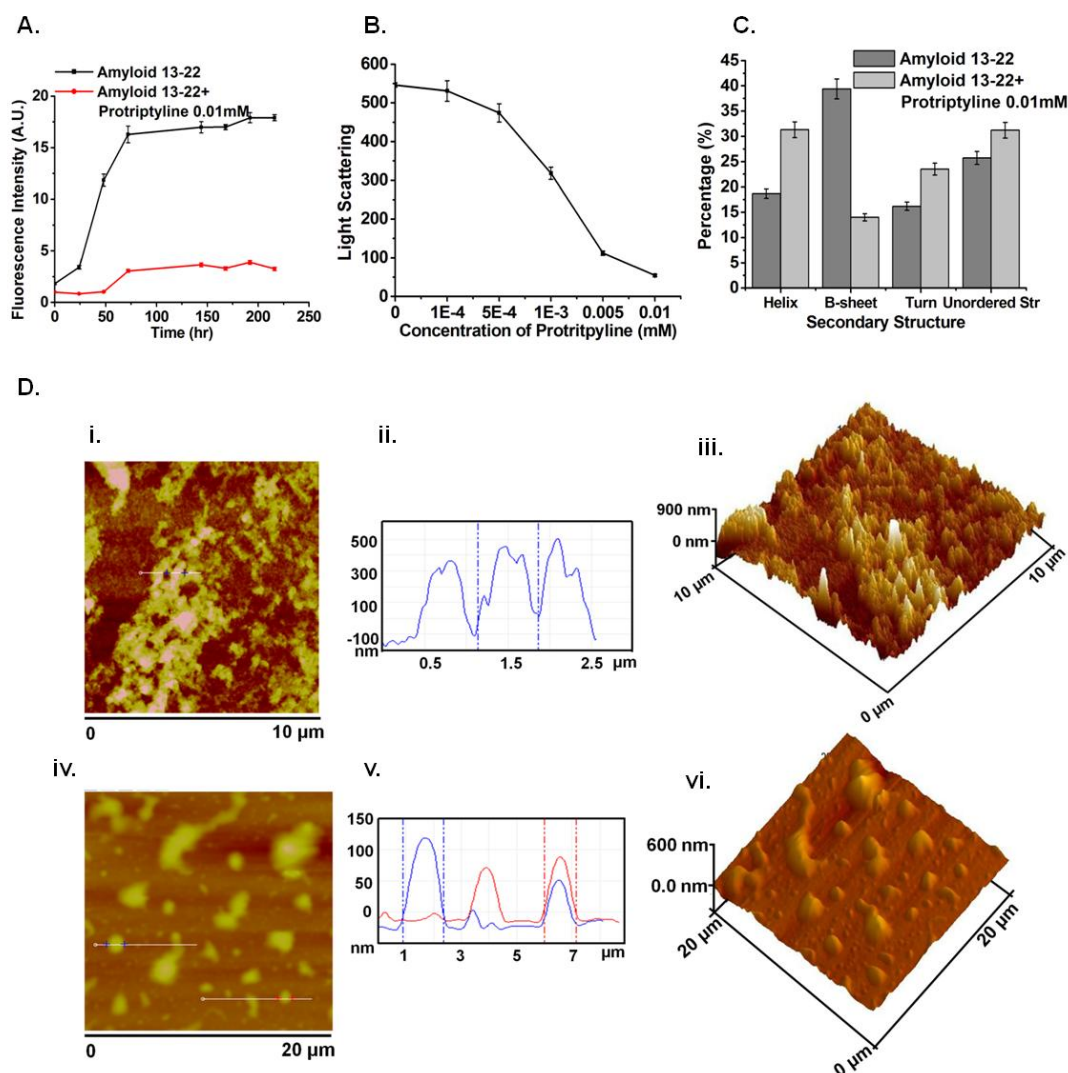
Figure 3.3 Inhibition of Aβ aggregation by protriptyline. Aβ $_{13-22}$ aggregation in the absence and presence of protriptyline was investigated by **A.** Thioflavin T assay **B.** Light scattering **C.** CD analysis **D.** Atomic Force Microscopy images [i and iv] of aggregated amyloid and Amyloid + protriptyline (0.010mM) in 10 × 10 μm^2 and 20 × 20 μm^2 surface area respectively. It is also represented in Line profile [ii and v] and 3D images [iii and vi].

First, the AFM profiles suggested a distinct reduction in the fibrillar density and a high degree of size dispersion resulting from protriptyline treatment. Further, the line profile and 3D AFM images showed that the average height of the $A\beta_{13-22}$ aggregates was ~400 nm, with the maximum height reaching ~600 nm. The height of the aggregates reduced to ~100 nm in case of protriptyline treated samples. It was quite convincing from the AFM images that the amyloid protein is aggregated and protriptyline treated sample protein showed decreased aggregation.

For a molecular level insight into the inhibitory action of protriptyline on $A\beta$ self-assembly, we performed MD simulations of $A\beta$ dimerisation in the absence and presence of protriptyline molecules. A β-sheet rich full-length monomer was considered for these studies. A single protriptyline molecule was found to bind to the $A\beta$ monomer with a mean binding strength of -84.0 (±34.0) kcal mol^{-1} (Figure 3.4). The mean monomer-monomer interaction strength obtained at the end of multiple independent trajectories over a combined total simulation time of 60 ns was -249.1 (±87.1) kcal mol^{-1}. In the presence of protriptyline, however, the monomer-monomer interaction weakened significantly, with a mean value of only -69.7 (±31.5) kcal mol^{-1}.
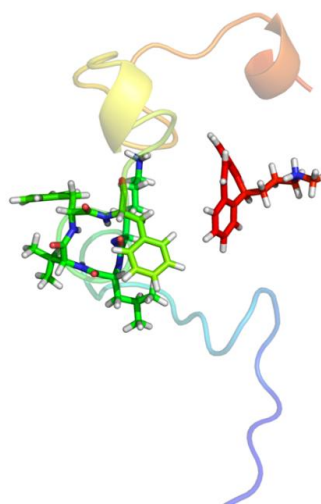
Figure 3.4 Snapshot of drug binding with Aβ monomer. Central hydrophobic core are in line representation (Green color) and protriptyline is represented in red color.

In Figure 3.5 A, we have depicted evolution of monomer-monomer interaction over simulation time for sample simulations in the absence and in the presence of protriptyline; the distributions of these interactions, along with distribution of the protriptyline-dimer interaction is depicted as an inset. The weakening of the inter-monomer interactions due to protriptyline binding results in the formation of complexes that are less compact compared to the pure dimeric forms. In Figure 3.5 B, we compare distributions of asphericities I_γ, of the pure and protriptyline-bound dimer complexes; I_γ value of 0.0 denotes perfect sphericity while increasing values denote increased asphericity. The protriptyline bound dimer complexes have a wider distribution and a higher mean value of I_γ; the mean asphericity values of the free and protriptyline -bound complexes are 0.2 and 0.5, respectively. Further, the mean radii of gyration (R_g) of these complexes were found to be 13.0 ($\pm$0.1) and 16.5 (1.0) Å, respectively. The difference in dimeric compactness upon protriptyline binding is evident from representative snapshots depicted in Figures 3.5 C and 3.5 D.

In order to evaluate the effects of protriptyline binding on the inter-monomer associations, we have analyzed the nature of inter-residue contacts. The average numbers of inter-residue side-chain cross-contacts were reduced upto 46% upon protriptyline binding. Here, as in previous studies (Lee et al., 2011), we have defined two residues to be in contact if the maximum separating distance of their side-chains does not exceed 7 Å. In Figures 3.5 E and 3.5 F, we compare the inter-residue contact probabilities for the free and protriptyline-bound complexes from the MD data. The largest numbers of contacts between the KLVFF regions are lost upon protriptyline binding. However, we note the emergence of a small extent of extraneous contacts, particularly involving the N- and C-terminal regions of the different monomeric units.

Further the effect on the secondary structural propensities of the Aβ units due to protriptyline binding was investigated. Protriptyline was found to reduce β-sheet and induce higher helical propensities in the monomeric form of Aβ. Figures 3.5 G and 3.5 H represent residue-wise β-sheet and helical propensities of the free and protriptyline-bound dimeric complexes, respectively, from the MD data. A

sharp decrease in β-sheet propensity is found uniformly along the Aβ sequence, including in the residue span H$_{13}$HQKLVFFAE$_{22}$. The decrease in β-sheet propensity is accompanied with an overall increase in helical conformations. Sharp increase in helicity was observed near the N-terminal and KLVFF regions. The alterations to secondary structural propensities thus observed from MD analysis are an excellent corroboration of the CD and ThT binding data.
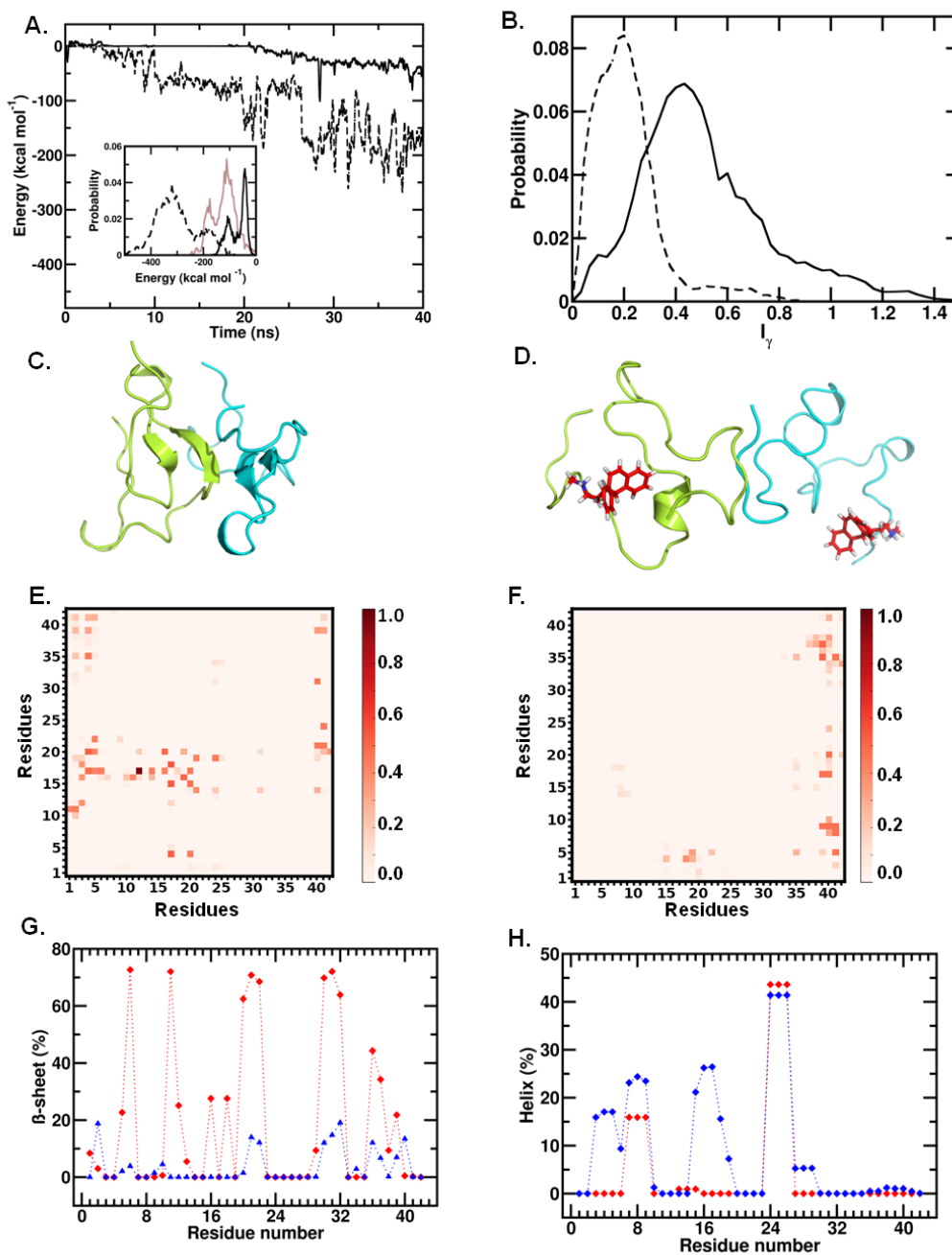
Figure 3.5 Destabilization of amyloid dimer by protriptyline. A. Evolution of monomer-monomer interaction strength over time for free dimer (broken line) and protriptyline-bound dimer (solid line) *Inset.* Distributions of the interactions from multiple trajectories, and the dimer interactions with protriptyline (in brown) **B.** Distributions of the asphericity for free (in broken line) and protriptyline-bound (solid line) dimer **C.** Representative snapshot of free, and D) protriptyline-bound dimer **E.** Residue-residue contact probabilities for free dimer, and **F.** protriptyline-bound dimer **G.** Residue-wise Beta sheet percentages for free dimer (in red) and protriptyline-bound dimer (in blue) **H.** Residue-wise helical percentages for free dimer (in red) and protriptyline-bound dimer (in blue).

III.3.4. Protriptyline Inhibits β-Secretase Activity - β-secretase is a key enzyme required for Aβ production. Hence, β-secretase inhibition is an attractive target for countering AD (Citron et al., 2002; Hussain et al., 2004; Hills et al., 2007). β-secretase assay demonstrated decreased activity with increasing concentrations of protriptyline having IC50 ~0.025mM (Figure 3.6 A). Protriptyline inhibited β-secretse by competitive inhibition as depicted by Lineweaver-Burk plot (Figure 3.6 B). Apparent K_m and K_i of β-secretase were calculated as mentioned above for AChE and found to be 0.0025mM and 0.005mM respectively. Apparent K_m of β-secretase was increased in the presence of protriptyline Competitive inhibition was evidenced by MD simulation analysis that illustrated protriptyline binds strongly at the active site of BACE-1 comprised of Asp32 and Asp228 (Figure 3.6 C). The mean binding strength required for protriptyline to bind to the active site is -29.5 ($\pm$7.0) kcal mol^{-1}. The centre of mass distance between the two residues increases from 5 Å to 8 Å as a result of protriptyline binding (Figure 3.6 D).
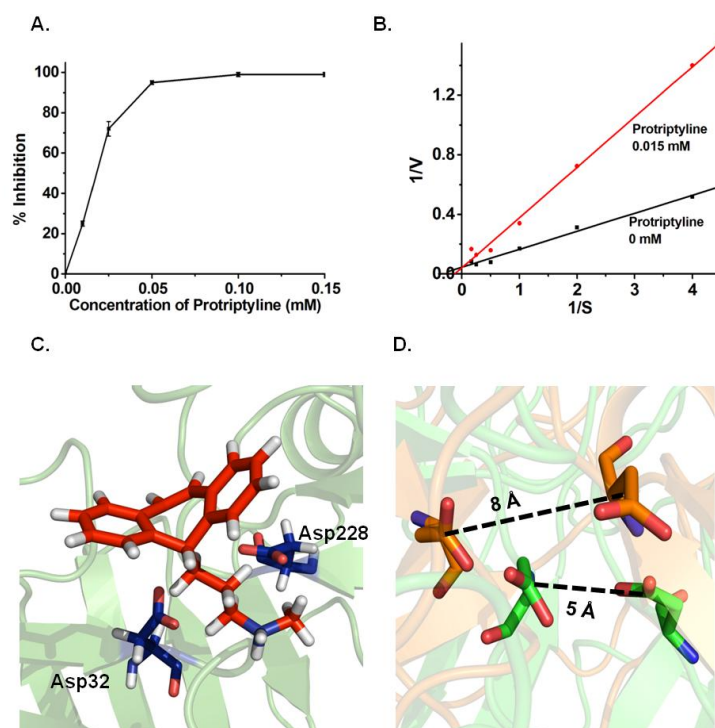
Figure 3.6 β-secretase (BACE-1) inhibition by protriptyline. A. Determination of IC50 of β-secretase by using various concentrations of protriptyline. The sigmoidal curve indicates the best fit for the percentage inhibition data obtained **B.** Lineweaver-Burk analysis to estimate the kinetic constants. It showed competitive inhibition. **C.** Snapshot of drug binding with active site of β-secretase. Active site residues in beta secretase are in line representation. **D.** Active site of β-secretase. The structures from unbound (green) and ligand bound (orange) simulations are shown after all - atom superimposition. Snapshots are generated using PyMol.

The comparison of the root mean squared deviation (RMSD) of C_α atoms of the active site in the unbound state with the protriptyline bound state indicated structural distortion of the arrangement of the active site (Figure 3.7 A). The binding was also found to induce significant alterations to the local secondary structural propensity around the active site (Figure 3.7 B). Therefore, inhibition of β-secretase by protriptyline is an extra benefit as it prevents Aβ generation. And even if there is some production, protriptyline will obstruct it to get aggregate.
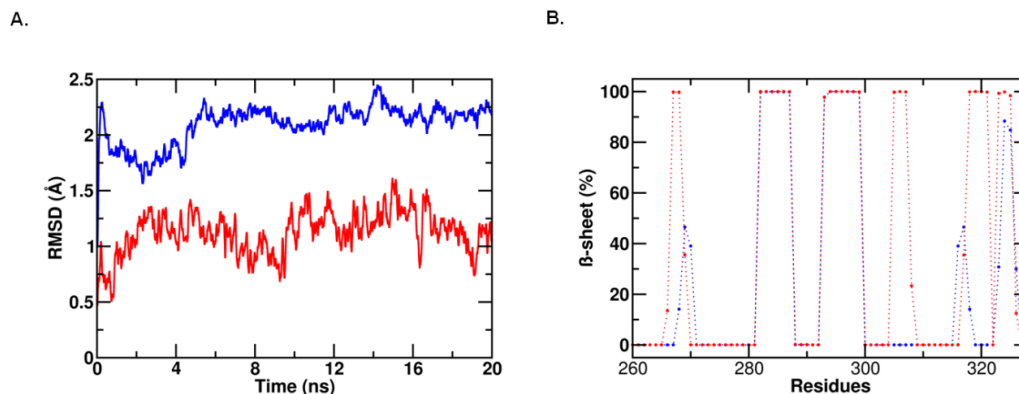
Figure 3.7 A. Root mean square deviation (RMSD) of active site regions of β-secretase in unbound (red) and ligand bound (blue) simulated trajectory **B**. Comparison of residue wise percentage of beta from unbound (red) and ligand bound (blue) simulated trajectory

III.3.5 Protriptyline Inhibits Glycation Associated Aggregation of Aβ - AD is also referred as type III diabetes (Steen et al., 2005) and its pathogenesis has been correlated with the extent of glycation (Li et al., 2012). Recent studies suggested glycated Aβ is more neurotoxic than native Aβ (Vitek et al., 1994); therefore the effect of protriptyline on glycation of Aβ was investigated. Glycated proteins emit fluorescence at 440 nm upon excitation at 370 nm. Fluorescence assay illustrated that Aβ undergoes glycation. The increase in glycation associated fluorescence was reduced by protriptyline in a concentration dependent manner (Figure 3.8 A). Glycation enhances the aggregation and also alters the secondary structure of proteins. Static light scattering was used to study glycation induced protein aggregation. Concentration dependent decrease in light scattering was observed (Figure 3.8 B). Further, it was studied by Thioflavin T fluorescence assay. Kinetics of aggregation displayed increased Thioflavin T fluorescence during glycation reaction. Lag phase for Aβ and glycated Aβ aggregation was increased in the presence of protriptyline with decreased Thioflavin T fluorescence (Figure 3.8 C).
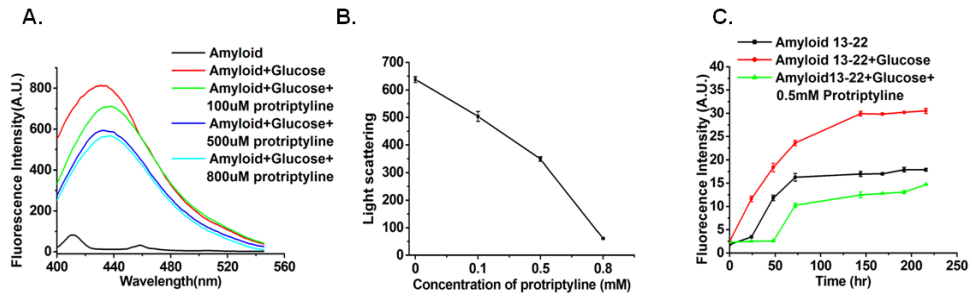
Figure 3.8 Protriptyline inhibits glycation. A. Fluorescence emmission of Aβ and glycated Aβ in presence of various concentration of protriptyline **B.** Light scattering and **C.** Kinetics of amyloid aggregation by Thioflavin T of Aβ$_{13-22}$ and glycated Aβ$_{13-22}$ in the absence and presence of protriptyline.

Furthermore, glycation inhibition activity of protriptyline was confirmed with other proteins such as insulin and BSA. MALDI-TOF-MS based *in vitro* insulin glycation inhibition assay showed the glycated insulin peak, marked by an arrow. The intensity of glycated peak was observed to be reduced with increasing protriptyline concentrations (Figure 3.9). Similarly, inhibition of BSA glycation was proved by AGE fluorescence and Thioflavin T fluorescence. Concentration dependent decrease in BSA glycation was observed (Figure 3.10).
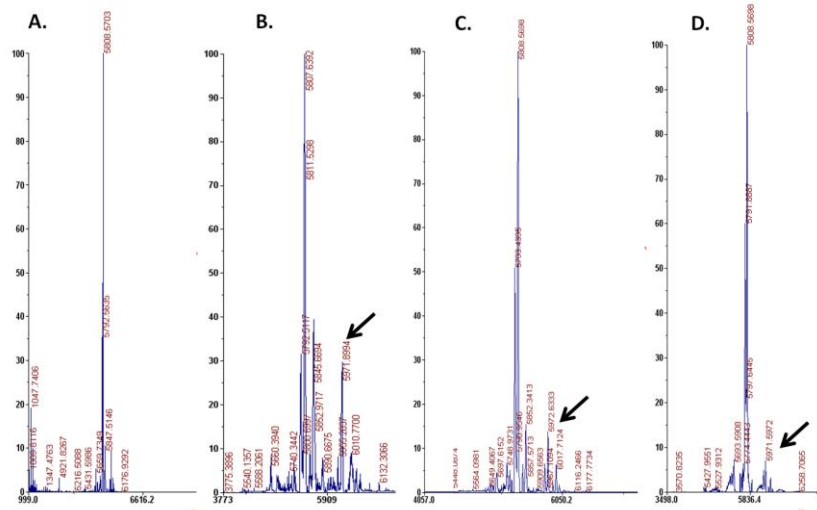
Figure 3.9 Insulin glycation inhibition assay. A. Control insulin **B.** Glycated insulin **C.** glycation inhibition in presence of 500 μM and **D.** 1000 μM

protriptyline. These spectra were acquired on a positive reflector mode by MALDI-TOF-MS. Glycated peaks are shown by black arrow
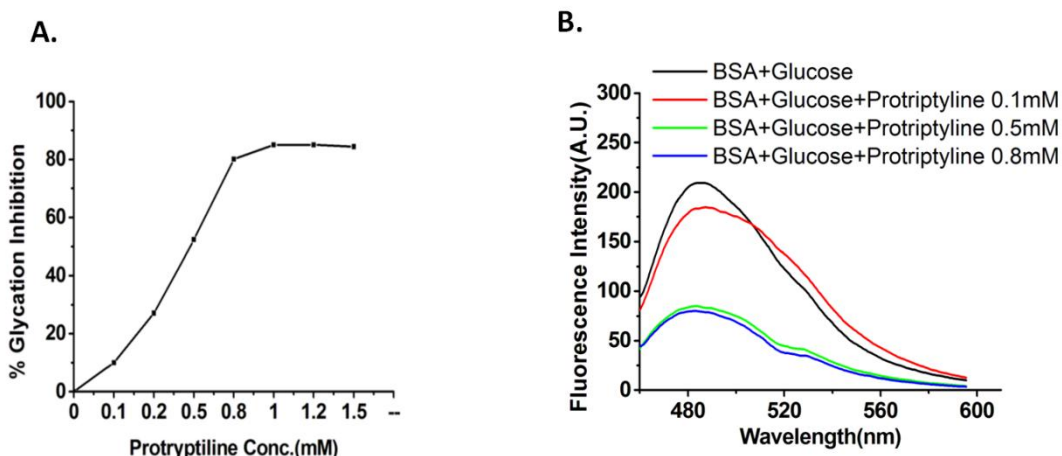
Figure 3.10 BSA (Bovine Serum Albumin) glycation inhibition assay. Glycation inhibition of BSA was studied by **A.** Measurement of AGE fluorescence, % glycation inhibition was plotted and **B.** Thioflavin T fluorescence assay, concentration dependent decrease in thioflavin T fluorescence was observed.

III.3.6. Protriptyline Does Not Affect Other Proteases - Protriptyline inhibited multiple targets of AD, therefore we further studied the influence of this drug on enzymes such as trypsin and α-secretase. It was interesting to observe that it was not able to inhibit trypsin activity even at high concentration as 0.1 and 0.5mM (Figure 3.11 A). For ADAM 17, protriptyline was found to be a weak inhibitor. It was showing ~3% inhibition at 0.1 mM and ~25% inhibition at 0.5mM (Figure 3.11 B). It suggested that protriptyline is not a non-specific inhibitor as it was not able to inhibit other proteases.
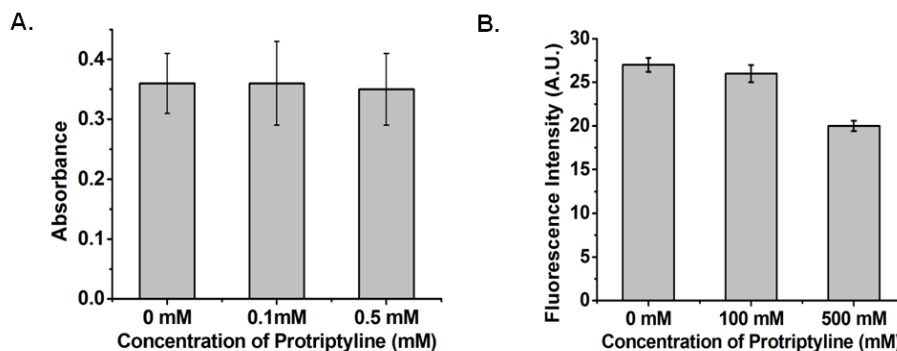
Figure 3.11 Protriptyline Does Not Affect Other Proteases. Effect of protriptyline on **A.** Trypsin **B.** ADAM 17 activity. Specific synthetic substrate BA*p*NA and fluorogenic peptide was used for analyzing activity on trypsin and ADAM 17, respectively. Trypsin activity was unaffected, while ADMA 17 showed weak inhibition in presence of protriptyline

III.3.7 Cell viability and AChE activity in neuro2a cells - The effect of various concentrations of protriptyline (25-500 µM) was tested on neuro2a neuroblastoma cells. Cell viability was assessed by MTT assay and reported as percent of cell viability (The viability percent of more than 90% was considered as accepted viability). It was observed that there was more than 90% viability upto 150 µM protriptyline and drastic reduction in viability was observed at 200-500 µM protriptyline concentrations (Figure 3.12 A). Furthermore, to confirm the *in vitro* results, the effect of protriptyline was checked on acetylcholinesterase activity. The protein extract from protriptyline treated cells was used for assessment and it was observed that the AChE activity was reduced with increasing concentrations of protriptyline (Figure 3.12 B).

B.
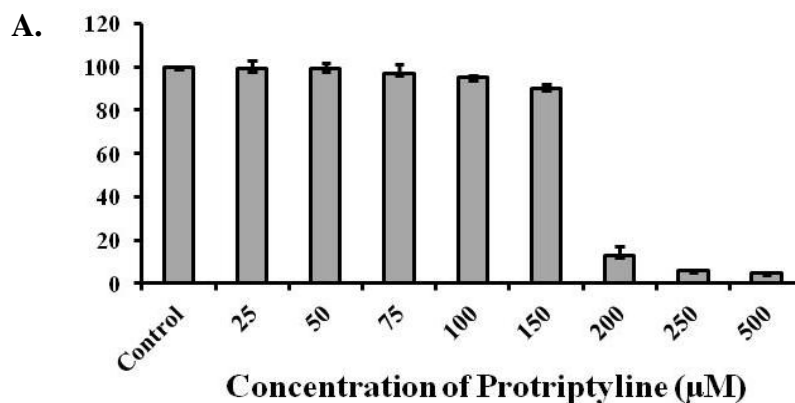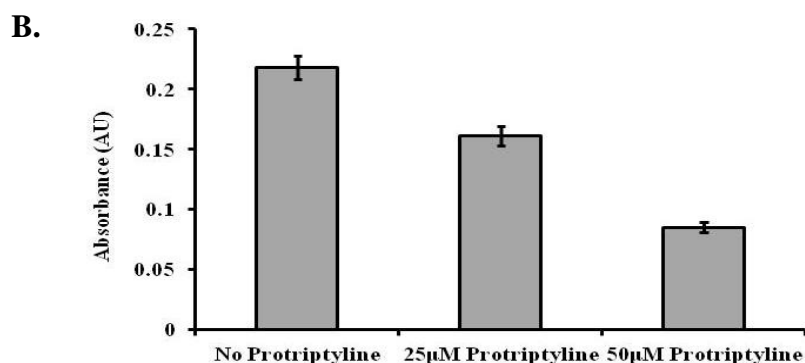
Figure 3.12 Cell viability and AChE activity in neuro2a cells. A. Effect of various concentrations of protriptyline (25-500 µM) on cell viability was assessed by MTT assay **B.** AChE activity was measured by treating neuro2a cells for 15 h with 25 and 60 µM protriptyline concentrations

III.4. Conclusion

The multifactorial nature of AD makes its treatment complex and unmanageable. The discovery of molecules that can inhibit multiple pathways of the disease should significantly advance therapeutic strategies. In this study, we investigated the efficacy of the tricyclic antidepressant, protriptyline, against important AD targets. Our *in vitro* and *in silico* investigations established the inhibitory effects of the drug on AChE, amyloid aggregation, BACE-1 and glycation (Figure 3.13). Protriptyline was able to inhibit AChE and β-secretase by binding at the active site and causing conformational changes. In addition, it strongly prevented self-assembly of Aβ and glycated Aβ. It is a FDA approved drug for the treatment of depression, narcolepsy, Attention Deficit Hyperactivity Disorder (ADHD) and headaches and its ability to cross blood brain barrier (BBB) is an additional advantage, which is a crucial requirement of molecules used for intra-cranial diseases. Furthermore, as there is high prevalence rate (30-50%) of AD and depression co-morbidity, the use of antidepressants can be a rational complementary therapy for AD treatment. Therefore, antidepressant activity of this drug could be an added advantage when dealing with AD complications related to depression. To the best of our knowledge, this is the first study in which

an anti-depressant drug has been shown to inhibit multiple targets of AD. Our results strongly ratify protriptyline as a promising candidate for AD therapy, and its further evaluation in animal and clinical studies.
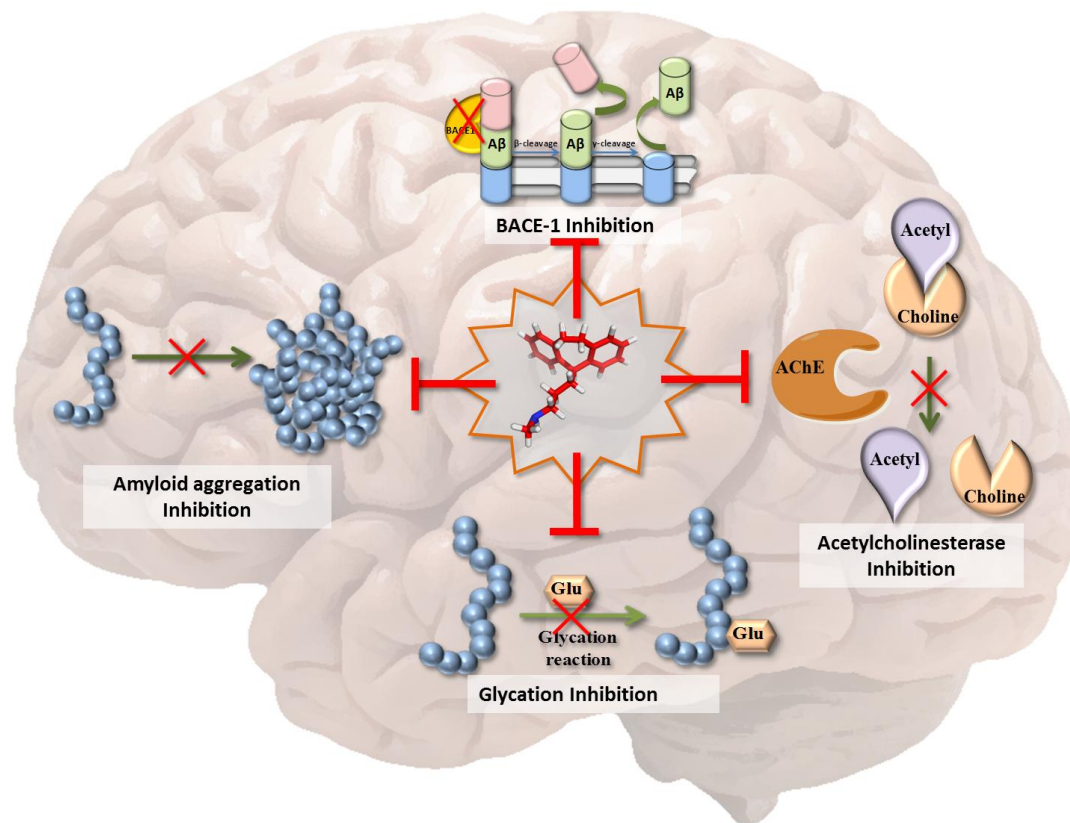
Figure 3.13 Protriptyline as MTDL. The scheme represents that protriptyline (at the center) is able to inhibit key targets of AD pathogenesis such as AChE, BACE-1 (β-secretase), Amyloid aggregation and glycation induced amyloid aggregation.

CHAPTER IV

Tolbutamide, an anti-diabetic drug promotes glycation

IV. 1. Introduction

Diabetes is a metabolic disorder characterized by elevated levels of plasma glucose. Prolonged glucose in diabetes results in several complications such as retinopathy, nephropathy, neuropathy and cardiovascular diseases (Schlienger JL, 2013). One of the major causes of these complications is protein glycation and formation of advanced glycation end products (Singh et al., 2014). Glycation is a non-enzymatic reaction between carbonyl group of glucose and free amino group of protein, which further undergoes structural rearrangement to form advanced glycation end products (AGEs) (Brownlee et al., 1984). Glycation of plasma proteins such as albumin, globulins, and fibrinogen have adverse effects which may include altered drug binding in plasma, free radical generation and activation of platelets (Negre-Salvayre et al., 2009). Albumin is one of the most abundant plasma proteins having concentration of 3.5 -5.5 g/dl in humans. Albumin is also a major carrier protein, able to bind and transport endogeneous solutes and broad range of drugs (Colmenarejo et al., 2003). Drug binds albumin selectively at two main sites namely, Sudlow site I and Sudlow site II (Sudlow et al., 1975). Site I, also called as warfarin binding site, is located on sub-domain IIA of albumin. Bulky heterocyclic compounds, for instance coumarins, sulfonamides, and salicylate, bind to this site (Moser et al., 2006; Dockal et al., 2000; Joseph et al., 2009). Sub-domain IIIA contains Sudlow site II, which binds to aromatic carboxylic acids and profens (Dockal et al., 2000). The binding of drug to the albumin affect its pharmacologic and pharmacokinetic properties such as bioavailability, metabolism, and excretion (Ascoli et al., 2006). Binding of some drugs also induces conformational change in the albumin (Wang et al., 2012). There are numerous reports suggesting the conformational change in the albumin upon interaction with the drugs such as Phenothiazine Drugs, hydroxycinnamic acids, Troxerutin, tenoxicam, imipramine hydrochloride etc. (Wang et al., 2012; Bai et al., 2009; Trnková et al., 2010; Malik et al., 2012).

Sulfonylureas are commonly used drugs for the management of type II diabetes, either alone or in combination with other drugs. Among the sulfonylurea drugs, tolbutamide was the first to be used for the treatment of diabetes (Jakoby et

al., 1995). Earlier reports have suggested that tolbutamide has very high affinity for serum albumin and ~ 90% drug found to be protein bound in circulation (Joseph et al., 2011). It is possible that the binding of tolbutamide may change the conformation of albumin, and may influence its glycation. Albumin has been reported to be one of the heavily glycated plasma proteins due to its abundance, larger half-life (21 days) and more lysine and arginine residues, the hotspots of glycation (Philippe et al., 2011). Therefore, in this study, we have investigated the effect of tolbutamide on albumin conformation using BSA as a model protein (Joseph et al., 2011). We have found that the binding of tolbutamide, a first generation sulfonylurea, induces significant conformational change in the albumin. It was proved by thioflavin T assay, ANS assay, and CD analysis. Molecular dynamic simulations suggested that the binding of tolbutamide increases the solvent accessibility of lysine residues of albumin. Furthermore, the change in conformation of albumin facilitates increased glycation, which was observed by AGE fluorescence and the results were corroborated by mass spectrometric analysis. This study suggested that tolbutamide enhances albumin glycation by inducing conformational change in the protein.

IV. 2. Materials and methods

IV. 2. 1. Fluorescence quenching. BSA-tolbutamide interaction was also studied by measuring tryptophan fluorescence. BSA was titrated with tolbutamide by the addition of different concentrations of drug (1-50 μM) to a fixed concentration of BSA solution. Tryptophan fluorescence was measured by excitation at 280 nm and emission was scanned from 300 nm to 500 nm. Background buffer and inhibitor spectra were subtracted and graphs were smoothened.

IV. 2. 2. Reaction for study of tolbutamide-BSA binding. 200 μM tolbutamide was incubated with 50 mg/ml BSA in 0.2 M phosphate buffer, pH 7.4 for 24 h. Only drug and buffer served as a negative control. These samples were further used for Thioflavin T, ANS and CD analysis.

IV. 2. 3. Circular Dichroism Spectroscopy. The far UV CD spectra (in wavelength range of 190-250 nm) of BSA (20 μg/ml) with or without various

concentrations of tolbutamide (0.1, 0.2, 0.3 M) was recorded using Jasco-J815 spectropolarimeter at ambient temperature. Each CD spectrum was accumulated from three scans at 50nm/min with cell path length of 0.1 cm. Contribution due to buffer was corrected in all spectra and observed values were converted to mean residual ellipticity (MRE) in deg cm^2 dmol^{-1} defined as

$$MRE= M\theta_\lambda/10dcr$$

Where M is the molecular weight of the protein, θ_λ is CD in millidegree, d is the path length in cm, c is the protein concentration in mg/ml and r is the number of amino acid residues in the protein. Secondary structure content of the BSA with and without tolbutamide was calculated using the CDPro software (http://lamar.colostate.edu/~sreeram/CDPro/main.html).

IV. 2. 4. ANS binding studies. Fluorescence measurements were performed with 1-anilino-8-naphthalenesulphonate (ANS) to determine binding of tolbutamide to BSA after 24 h at RT. ANS is hydrophobic dye which binds to solvent exposed hydrophobic regions in a protein. The final ANS concentration used was 10 μM, excitation wavelength was 375 nm and emission was monitored between 400 and 550 nm. Spectra were recorded at 100nm/min with slit widths of 7 nm each for excitation and emission monochromators.

IV. 2. 5. Thioflavin T assay. 100 μM BSA with or without tolbutamide was incubated with 20 μM Thioflavin T. Immediately, fluorescence was measured by exciting at 440 nm and emission was scanned from 460 nm to 550 nm on Perkin Elmer LS 50B luminescence spectrometer. Actual fluorescence of protein was measured by subtracting background fluorescence of the drug.

IV. 2. 6. Molecular Dynamic Simulations. Initial coordinates of BSA molecule were taken from the crystallographic structure reported in the PDB database (PDB ID 4F5S). Tolbutamide was docked with BSA using Autodock (Trott et al., 2010). The resultant system was immersed in a box of equilibrated TIP3P water molecules, maintaining a minimum distance of 14 Å from the box edge to each atom. Twenty two sodium counter ions were added at random positions within the

simulation box. For comparison the free protein was also simulated. NAMD2.9 package (Kale et al., 1999) and CHARMM22 all-atom force field with CMAP correction was used for the simulation study (MacKerell et al., 1998; 2004). Force field parameters for tolbutamide were generated using the SwissPARAM tool (Zoete et al., 2011). Simulations were carried using a timestep of 2 fs in the isothermal-isobaric (NPT) ensemble at a temperature of 310 K and a pressure of 1 atmosphere. Each system was sampled for a total duration of 50 ns. The SHAKE algorithm (Ryckaert et al., 1977) was used to constrain bond lengths involving hydrogen atoms. Constant temperature was maintained with Langevin dynamics with a collision frequency of 1 ps^{-1}, and constant pressure was maintained using the Langevin piston Nose- Hoover method (Feller et al., 1995). Three-dimensional orthorhombic periodic boundary conditions were employed and full electrostatics calculated with the particle-mesh Ewald method (Essmann et al., 1995). A non-bonded cutoff distance of 12 Å was employed, which were smoothened at a distance of 10.5 Å.

IV. 2. 7. Glycation Assay. For glycation reaction, 50 mg/ml BSA was incubated with 0.1 M glucose with or without various concentrations of tolbutamide (0.1, 0.2 and 0.3 M) in 0.2 M phosphate buffer, pH 7.4 for 7 days. Glycation associated fluorescence of BSA in all samples was measured at 370 nm excitation and emission was scanned from 400-550 nm.

IV. 2. 8. In-solution Trypsin Digestion. 100 μg protein sample was kept overnight for acetone TCA precipitation after incubation of 15 days. Samples were then washed with chilled acetone and used for digestion. Samples were reduced and alkylated by 10 mM dithiothreitol for 30 min and 55 mM iodoacetamide for 45 min respectively. 2μg trypsin was added and the solution was incubated at 37°C for 16 h. 2 μL of formic acid was added to stop the reaction and then samples were vortexed and centrifuged. The peptides in the supernatant were collected and stored at -80°C until further used.

IV. 2. 9. LC-MS/MS analysis. Tryptic peptides were fractionated using an Accela LC system connected to Q Exactive™ Hybrid Quadrupole-Orbitrap™

Mass Spectrometer (Thermo Scientific). Peptides were injected and resolved by Hypersil Gold column (Thermo Scientific) over a 45 min gradient, using 6 gradient segments (held at 2 % solvent A over 2 min, 2–40% C over 35 min, 40–98% A over 2 min, held at 98% A over 2 min, 98-2% A over 2 min held at 2% A for 2 min) with a flow rate of 350 µl min^{-1}. Solvent A was ACN with 0.1% formic acid and Solvent B was aqueous with 0.1% formic acid. Peptides were ionized by HESI ionization with a capillary temperature of 320°C. Tandem Mass Spectra were acquired using Q Exactive™ Hybrid Quadrupole-Orbitrap™ Mass Spectrometer was controlled by Xcalibur software (Thermo Scientific). The Orbitrap was set to analyse the survey scans at 17,500 resolutions in the mass range *m/z* 350 to 1800 and the top five multiply charged ions in each duty cycle selected for MS/MS fragmentation using higher-energy collisional dissociation (HCD).

IV. 2. 10. Data processing and analysis. The raw data files were processed using Proteome Discoverer software 1.4 (Thermo Scientific) and searched against the UniProt BSA sequence using the SEQUEST HT v1.3 algorithm. Peptide precursor mass tolerance was set at 10 ppm, and MS/MS tolerance was set at 0.6 Da. Search criteria included Hexose- 162.053, Carboxyethyl lysine- 72.021, Carboxymethyl lysine- 58.005, MOLD- 49.008 on lysine residues and Imidazolone B- 142.027, Argpyrimidine- 80.026 on Arginine residues as variable modifications and carbamidomethylation of cysteine (+57.021) as static modification. Searches were performed with full tryptic digestion and a maximum of 2 missed cleavages were allowed. Peptide data was filtered to satisfy false discovery rate (FDR) of 5%. Annotation threshold was set at 5% of base peak and match tolerance was set at 0.05 Da.

IV. 2. 11. Statistical analysis. Statistical analysis was performed by Student's t-test. Data are expressed as mean ± SD. A p-value <0.05 was considered as statistically significant.

IV. 3. Results and discussion

Binding of tolbutamide to BSA was studied by fluorescence quenching assay. Figure 4.1 A shows the fluorescence spectra of BSA in the absence and presence of tolbutamide. The fluorescence spectra of BSA showed maximum fluorescence intensity at 340 nm. It was observed that the fluorescence intensity of BSA decreases with increasing concentration of tolbutamide. Further the number of binding sites of tolbutamide on BSA was calculated by using following equation (Hu et al., 2006):

$$\log [(F0-F)/F] = \log K + n \log[Q]$$

Where K and n are binding constant and binding site number, respectively

The graph of log [(F0-F)/F] vs log [Q] was plotted in Figure 4.1 B, in which the intercept and slope indicated the binding constant and binding number for tolbutamide to BSA, respectively. The binding constant was found to be 3.2. Further, it was observed that three molecules of tolbutamide interact with single molecule of BSA. These results are very well in accordance with the previous studies that showed three binding sites of tolbutamide on human serum albumin (Michael et al., 1995).

A. **B.**
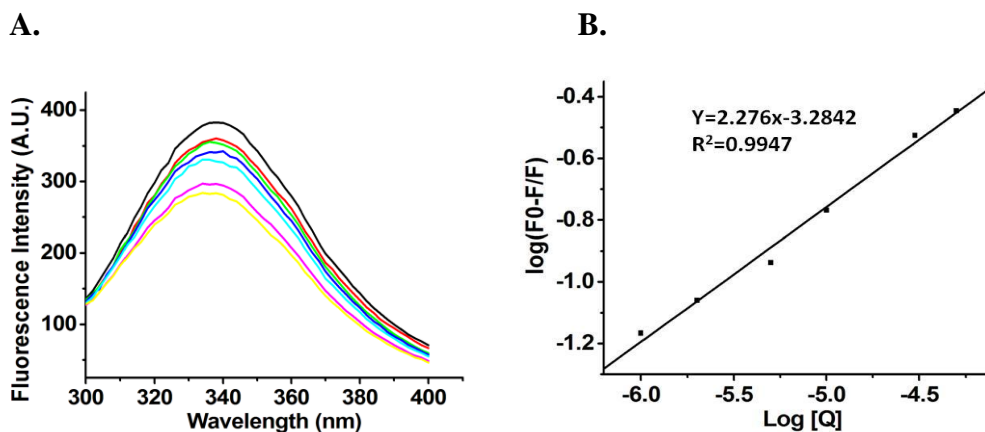
Figure 4.1 A. Tolbutamide-BSA interaction study by fluorescence spectroscopy **B.** Plot of log [F0-F/F] vs log [Q] to determine binding number and binding constant.

The change in the BSA conformation due to binding of tolbutamide was studied by CD spectroscopy, ANS and Thioflavin-T assay. CD spectra of BSA illustrated minima at 208 nm and a characteristic of α-helix at 222 nm (Greenfield et al., 1969). It was observed that increasing concentration of tolbutamide, minima at these wavelengths was decreasing (Figure 4.2 A). Secondary structure analysis by CDPro software demonstrated that α-helix content decreases and β-sheets increase with increasing concentration of tolbutamide. The turn and unordered structures did not differ much in presence of tolbutamide (Figure 4.2 B). Furthermore, 8-Anilinonaphthalene-1-sulfonic acid (ANS), a commonly used fluorescent probe was utilized to study conformational changes induced by ligand binding to proteins (Yoshimura et al., 1993). A blue shift in the fluorescence emission maxima and increase in the fluorescence intensity signifies the hydrophobicity of a binding site. ANS showed emission maxima at 525 nm while ANS bound to BSA with various concentrations of tolbutamide (0.1 M, 0.2 M and 0.3 M) showed blue shift with emission maxima at 470 nm. Concentration dependent increase in fluorescence intensity was observed indicating that the hydrophobicity in BSA increases with increasing concentration of tolbutamide (Figure 4.2 C). In addition to this, Thioflavin-T assay was performed to confirm the conformational change. Thioflavin T is a commonly used benzothiazole dye to diagnose amyloid fibrils that display increased fluorescence upon binding to amyloid fibrils (Khurana et al., 2005). It was observed that binding of Thioflavin-T to BSA showed emission maxima at 480nm. Its fluorescence increased with increasing concentration tolbutamide (Figure 4.2 D). As Thioflavin-T displays enhanced fluorescence upon binding to β-sheet rich structures, increased fluorescence in tolbutamide incubated BSA suggested that binding of tolbutamide induces conformational change in the albumin by increasing β-sheets. Hence, the Thioflavin-T assay results support the CD analysis and ANS assay results indicating that tolbutamide induces conformation change by increasing β-sheets.
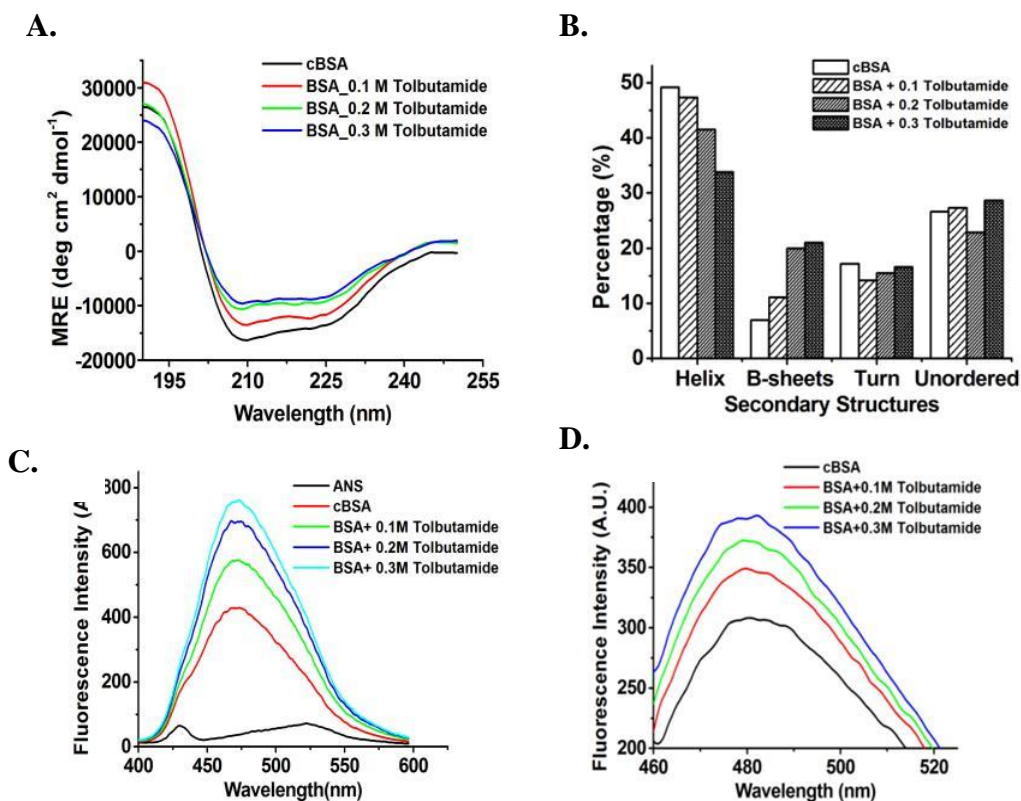
Figure 4. 2 Investigation of change in conformation due to tolbutamide binding A. CD spectra **B.** CD Pro analysis **C.** ANS assay and **D.** Thioflavin-T assay of BSA without and with various concentrations of tolbutamide

As tolbutamide is an anti-diabetic drug and being used chronically to treat diabetes, change in conformation brought by tolbutamide may influence the glycation of albumin. Therefore, molecular dynamic simulations were carried out to study the exposure of lysine residues, hotspots of glycation, after tolbutamide treatment. Solvent Accessible Surface Area (SASA) of lysine residues increased from 19800 ($\pm$81.7) Å^2 to 20050 ($\pm$75.0) Å^2 upon tolbutamide binding (Figure 4.3 A). Increment of solvent exposure of lysine residues is an indication of conformational change of BSA upon ligand binding. The more exposure of lysine residues of BSA in the presence of tolbutamide increases the probability of glucose to react with it and hence increases the chance of glycation. The validation of this result was done by *in vitro* glycation of BSA in the presence of tolbutamide. AGE specific fluorescence was increased in presence of tolbutamide (Figure 4.3 B). Additionally, the increase in glycation was confirmed

by LC-MS/MS analysis using high resolution accurate mass spectrometer (Q-Exactive). Mass spectrometric data was analyzed by Proteome Discoverer. The peptides with glycation modification and good fragmentation pattern were selected. As expected the numbers of glycated peptides were more in glycated BSA, and this number increased in the presence of tolbutamide. The numbers of modified peptides were increased with increasing tolbutamide concentration (Figure 4.3 C). Furthermore, the extent of modification in tolbutamide treated BSA was quantified by extracted ion chromatograms. For example, a representative hexose modified peptide (m/z 928.0021) was selected. Its MS/MS fragmentation pattern is shown in figure 4.4 A. Extracted ion chromatogram (XIC) of its selected fragment ion (m/z 201.0872) represents the area of that fragment ion in different samples. Area for the fragment ion was increased in case of glycated BSA and was further enhanced with increasing tolbutamide concentration (Figure 4.4 B).
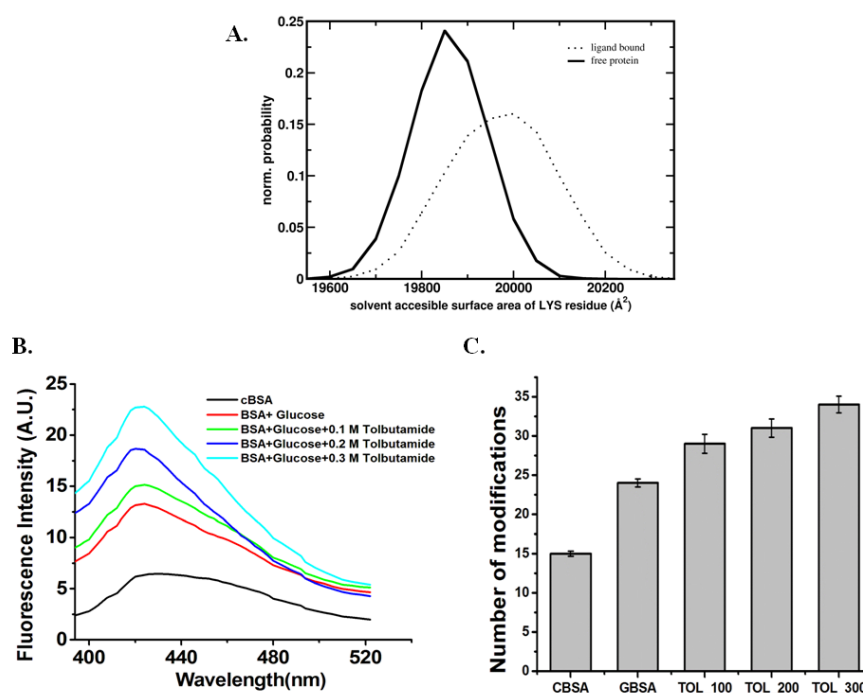
Figure 4.3 Glycation in the presence of tolbutamide A. Solvent Accessible Surface Area (SASA) analysis of lysine residues of BSA before and after tolbutamide treatment by MD simulations **B.** AGE specific fluorescence assay **C.** A bar graph representing number of glycation modifications on BSA in the absence and presence of tolbutamide by LC-MS analysis

A.

B.
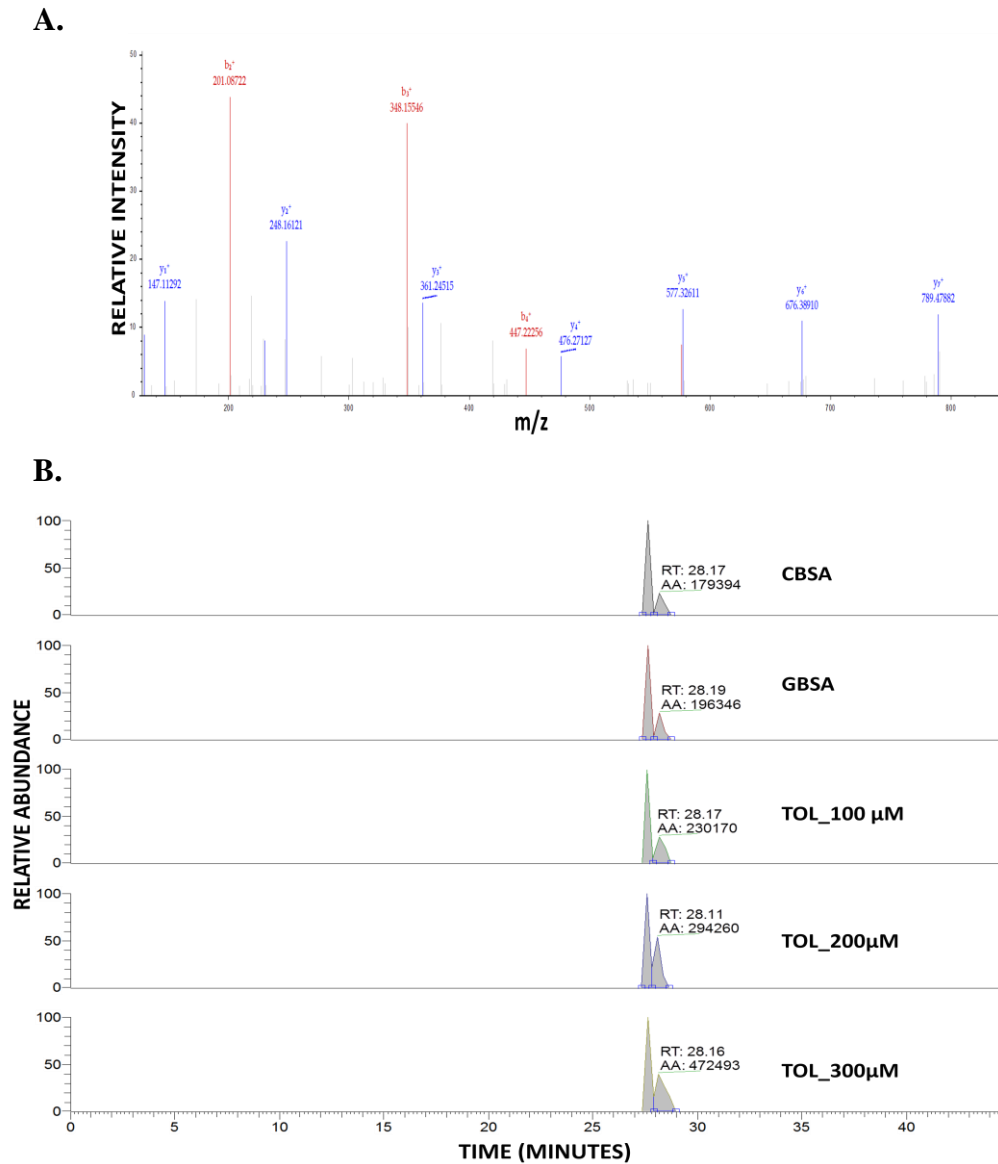
Figure 4.4 Detection of hexose modified peptide in tolbutamide treated BSA A. MS/MS fragmentation of modified peptide (m/z 928.0021) in sample **B.** Extracted ion chromatogram (XIC) of selected fragment ion (m/z 201.0872) of glucose modified peptide in control and tolbutamide treated BSA

IV. 4. Conclusion. In our study, we have studied the effect of tolbutamide on the most abundant plasma protein, albumin. Tolbutamide induces the conformation change in BSA. Binding of tolbutamide increases the hydrophobicity and β-sheets. Moreover, tolbutamide was also found to enhance the solvent accessibility of lysine residues; site of glycation. The exposure of sites for glycation promotes the glycation reaction as evidenced by AGE specific fluorescence and LC-MS/MS analysis. Therefore in conclusion, the altered BSA structure exposes the sites for glycation and hence promotes this reaction. As a result, prolonged use of tolbutamide may have adverse effects.

V. Summary and future perspectives

SUMMARY AND FUTURE PERSPECTIVES

This thesis deals with the different aspects of protein crosslinking such as its identification, characterization, induction and inhibition. We did the proteomic analysis for identification and characterization of glycation induced protein aggregates in diabetic rat kidney. We have showed that AGE modification and impairment in proteasomal activity, a central protein degrading machinery of the cell, results in accumulation of protease resistant aggregates. AGE modification causes loss of functional activity of enzymes, which is compensated by increased gene expression. Both the inability of proteasome to remove protease resistant aggregates and decreased enzyme activity may cause up regulation of proteins in the diabetic condition. This study provided insight into the probable cause of protease resistance and its consequences leading to diabetic complications.

As accumulation of protein aggregates causes harm to the cells, the thesis further dealt with its inhibition. We have found a molecule, protriptyline, which will inhibit the protein crosslinking. Protriptyline was found to be MTDL i.e. multi-target directed ligand for AD treatment. Our *in vitro* and *in silico* investigations established the inhibitory effects of the drug on AChE, amyloid aggregation, BACE-1 and glycation. Protriptyline was able to inhibit AChE and β-secretase by binding at the active site and causing conformational changes. In addition, it strongly prevented self-assembly of Aβ and glycated Aβ. It is a FDA approved drug for the treatment of depression, narcolepsy, Attention Deficit Hyperactivity Disorder (ADHD) and headaches and its ability to cross blood brain barrier (BBB) is an additional advantage, which is a crucial requirement of molecules used for intra-cranial diseases. Furthermore, as there is high prevalence rate (30-50%) of AD and depression co-morbidity, the use of antidepressants can be a rational complementary therapy for AD treatment. Therefore, antidepressant activity of this drug could be an added advantage when dealing with AD complications related to depression. To the best of our knowledge, this is the first study in which an anti-depressant drug has been shown to inhibit multiple targets of AD. Our results strongly ratify protriptyline as a promising candidate for AD therapy. In future studies, this molecule can be studied in great detail in

Alzheimer's animal models and also in diabetic animals to prove its efficacy as a crosslink inhibitor in both the disease conditions. If the results are promising, it can be further studied at the clinical level.

Furthermore, we have showed that tolbutamide induces crosslinking in BSA by increasing glycation. We have studied the effect of tolbutamide on the most abundant plasma protein, albumin. Tolbutamide induces the conformation change in BSA. Binding of tolbutamide increases the hydrophobicity and β-sheets. Moreover, tolbutamide was also found to enhance the solvent accessibility of lysine residues, site of glycation. The exposure of sites for glycation promotes the glycation reaction as evidenced by AGE specific fluorescence and LC-MS/MS analysis. Therefore in conclusion, the altered BSA structure due to tolbutamide binding exposes the sites for glycation and hence promotes this reaction. As a result, prolonged use of tolbutamide can have adverse effects. Although we have proved it in vitro, it is necessary to show it in vivo by using diabetic models. Also, it is very important to study the effect of other drugs used in the treatment of chronic diseases on the proteins and their further consequences.

VI. Bibliography

VI. Bibliography

Aboukhatwa, M., Dosanjh, L., and Luo, Y. Antidepressants are a rational complementary therapy for the treatment of Alzheimer's disease. *Mol. Neurodegener.* **5**, 10

Ahmad, W., Li, L., and Deng, Y. (2008) Identification of AGE-precursors and AGE formation in glycation-induced BSA peptides. *BMB Rep.* **41**, 516-22

Akira, K., Amano, M., Okajima, F., Hashimoto, T., and Oikawa, S. (2006) Inhibitory effects of amlodipine and fluvastatin on the deposition of advanced glycation end products in aortic wall of cholesterol and fructose-fed rabbits. *Biol. Pharm. Bull.* **29**, 75-81

Alzheimer's Association: FDA-approved treatments for Alzheimers. https://www.alz.org/national/documents/topicsheet_treatments.pdf 2012.

Amos, A. F., McCarty, D. J., and Zimmet, P. (1997) The rising global burden of diabetes and its complications: estimates and projections to the year 2010. *Diabet. Med.* **14 Suppl 5**, S1-85

Anand, P., and Singh, B. A review on cholinesterase inhibitors for Alzheimer's disease. *Arch. Pharm. Res.* **36**, 375-399

Ascoli, G. A., Domenici, E., and Bertucci, C. (2006) Drug binding to human serum albumin: abridged review of results obtained with high-performance liquid chromatography and circular dichroism. *Chirality* **18**, 667-679

Ashburn, T. T., and Thor, K. B. (2004) Drug repositioning: identifying and developing new uses for existing drugs. *Nat. Rev. Drug. Discov.* **3**, 673-683

Austin, G. E., Mullins, R. H., and Morin, L. G. (1987) Non-enzymic glycation of individual plasma proteins in normoglycemic and hyperglycemic patients. *Clin. Chem.* **33**, 2220-2224

Babu, P. V., Sabitha, K. E., and Shyamaladevi, C. S. (2008) Effect of green tea extract on advanced glycation and cross-linking of tail tendon collagen in streptozotocin induced diabetic rats. *Food. Chem. Toxicol.* **46**, 280-285

Bai, H. X., Liu, X. H., Yang, F., Yang, X. R. (2009) Interactions of Human Serum Albumin with Phenothiazine Drugs: Insights from Fluorescence Spectroscopic Studies. *Jnl. Chinese. Chemical. Soc.* **56,** 696–702

Balbach, J. J., Ishii, Y., Antzutkin, O. N., Leapman, R. D., Rizzo, N. W., Dyda, F., Reed, J., and Tycko, R. (2000) Amyloid fibril formation by A beta 16-22, a seven-residue fragment of the Alzheimer's beta-amyloid peptide, and structural characterization by solid state NMR. *Biochemistry* **39**, 1374-1375

Balcz, B., Kirchner, L., Cairns, N., Fountoulakis, M., and Lubec, G. (2001) Increased brain protein levels of carbonyl reductase and alcohol dehydrogenase in Down syndrome and Alzheimer's disease. *J. Neural Transm. Suppl.* **61**, 193-201

Bartus, R. T., Dean, R. L., 3rd, Beer, B., and Lippa, A. S. (1982) The cholinergic hypothesis of geriatric memory dysfunction. *Science* **217**, 408-414

Beauchamp, C., and Fridovich, I. (1971) Superoxide dismutase: Improved assays and an assay applicable to acrylamide gels. *Anal. Biochem.* **44**, 276-287

Bernstein, S. L., Wyttenbach, T., Baumketner, A., Shea, J. E., Bitan, G., Teplow, D. B., and Bowers, M. T. (2005) Amyloid beta-protein: monomer structure and early aggregation states of Abeta42 and its Pro19 alloform. *J. Am. Chem. Soc.* **127**, 2075-2084

Bhonsle, H. S., Korwar, A. M., Kote, S. S., Golegaonkar, S. B., Chougale, A. D., Shaik, M. L., Dhande, N. L., Giri, A. P., Shelgikar, K. M., Boppana, R., and Kulkarni, M. J. (2012) Low plasma albumin levels are associated with increased plasma protein glycation and HbA1c in diabetes. *J. Prot.Res.* **11**, 1391-1396

Biemel, K. M., Reihl, O., Conrad, J., and Lederer, M. O. (2001) Formation pathways for lysine-arginine cross-links derived from hexoses and pentoses by Maillard processes: unraveling the structure of a pentosidine precursor. *J. Biol. Chem.* **276**, 23405-23412

Booth, A. A., Khalifah, R. G., Todd, P., and Hudson, B. G. (1997) In vitro kinetic studies of formation of antigenic advanced glycation end products (AGEs). Novel inhibition of post-Amadori glycation pathways. *J. Biol. Chem.* **272**, 5430-5437

Brock, F. M., Forsberg, C. W., and Buchanan-Smith, J. G. (1982) Proteolytic activity of rumen microorganisms and effects of proteinase inhibitors. *Appl. Environ. Microbiol.* **44**, 561-9.

Brownlee, M. (2001) Biochemistry and molecular cell biology of diabetic complications. *Nature.* **414,** 813-20

Brownlee, M., Vlassara, H., and Cerami, A. (1984) Nonenzymatic glycosylation and the pathogenesis of diabetic complications. *Ann. Intern. Med.* **101**, 527-537

Brownlee, M., Vlassara, H., Kooney, A., Ulrich, P., and Cerami, A. (1986) Aminoguanidine prevents diabetes-induced arterial wall protein cross-linking. *Science* **232**, 1629-1632

Bulteau, A. L., Verbeke, P., Petropoulos, I., Chaffotte, A. F., and Friguet, B. (2001) Proteasome inhibition in glyoxal-treated fibroblasts and resistance of glycated glucose-6-phosphate dehydrogenase to 20s proteasome degradation *in vitro*. *J. Biol. Chem.* **276**, 45662-45668

Burcham, P. C., Raso, A., Thompson, C., and Tan, D. (2007) Intermolecular protein cross-linking during acrolein toxicity: efficacy of carbonyl scavengers as inhibitors of heat shock protein-90 cross-linking in A549 cells. *Chem. Res. Toxicol.* **20**, 1629-1637

Campion, D., Dumanchin, C., Hannequin, D., Dubois, B., Belliard, S., Puel, M., Thomas-Anterion, C., Michon, A., Martin, C., Charbonnier, F., Raux, G., Camuzat, A., Penet, C., Mesnage, V., Martinez, M., Clerget-Darpoux, F., Brice, A., and Frebourg, T. (1999) Early-onset autosomal dominant Alzheimer disease: prevalence, genetic heterogeneity, and mutation spectrum. *Am. J. Hum. Genet.* **65**, 664-670

Cappelli, A., Gallelli, A., Manini, M., Anzini, M., Mennuni, L., Makovec, F., Menziani, M. C., Alcaro, S., Ortuso, F., and Vomero, S. (2005) Further studies on the interaction of the 5-hydroxytryptamine3 (5-HT3) receptor with arylpiperazine ligands. development of a new 5-HT3 receptor ligand showing potent acetylcholinesterase inhibitory properties. *J. Med. Chem.* **48**, 3564-3575

Carbone, D. L., Doorn, J. A., Kiebler, Z., Ickes, B. R., and Petersen, D. R. (2005) Modification of heat shock protein 90 by 4-hydroxynonenal in a rat model of chronic alcoholic liver disease. *J. Pharmacol. Exp. Ther.* **315**, 8-15

Caulfield, T., and Medina-Franco, J. L. Molecular dynamics simulations of human DNA methyltransferase 3B with selective inhibitor nanaomycin A. *J. Struct. Biol.* **176**, 185-191

Cederberg, J., Galli, J., Luthman, H., and Eriksson, U. J. (2000) Increased mRNA levels of Mn-SOD and catalase in embryos of diabetic rats from a malformation-resistant strain. *Diabetes.* **49**, 101-107

Cervantes-Laurean, D., Schramm, D. D., Jacobson, E. L., Halaweish, I., Bruckner, G. G., and Boissonneault, G. A. (2006) Inhibition of advanced glycation end product formation on collagen by rutin and its metabolites. *J. Nutr. Biochem.* **17**, 531-540

Chimon, S., Shaibat, M. A., Jones, C. R., Calero, D. C., Aizezi, B., and Ishii, Y. (2007) Evidence of fibril-like beta-sheet structures in a neurotoxic amyloid intermediate of Alzheimer's beta-amyloid. *Nat. Struct. Mol. Biol.* **14**, 1157-1164

Choei, H., Sasaki, N., Takeuchi, M., Yoshida, T., Ukai, W., Yamagishi, S., Kikuchi, S., and Saito, T. (2004) Glyceraldehyde-derived advanced glycation end products in Alzheimer's disease. *Acta. Neuropathol.* **108**, 189-93

Chougale, A. D., Bhat, S. P., Bhujbal, S. V., Zambare, M. R., Puntambekar, S., Somani, R. S., Boppana, R., Giri, A. P., and Kulkarni, M. J. (2012) Proteomic

analysis of glycated proteins from streptozotocin-induced diabetic rat kidney. *Mol. Biotech.* **50,** 28-38

Citron, M. (2002) Beta-secretase as a target for the treatment of Alzheimer's disease. *J. Neurosci. Res.* **70**, 373-379

Colmenarejo, G. (2003) In silico prediction of drug-binding strengths to human serum albumin. *Med. Res. Rev.* **23**, 275-301

Conchillo-Sole, O., de Groot, N. S., Aviles, F. X., Vendrell, J., Daura, X., and Ventura, S. (2007) AGGRESCAN: a server for the prediction and evaluation of "hot spots" of aggregation in polypeptides. *BMC Bioinformatics.* **27,** 8:65

Copeland, R. A., Lombardo, D., Giannaras, J., Decicco, C. P. (1995) Estimating ki values for tight binding inhibitors from dose-response plots. *Bioorganic & Medicinal Chemistry Letters* **5**, 1947-1952

Corbett, A., Pickett, J., Burns, A., Corcoran, J., Dunnett, S. B., Edison, P., Hagan, J. J., Holmes, C., Jones, E., Katona, C., Kearns, I., Kehoe, P., Mudher, A., Passmore, A., Shepherd, N., Walsh, F., and Ballard, C. Drug repositioning for Alzheimer's disease. *Nat. Rev. Drug Discov.* **11**, 833-846

Coughlan, M. T., Forbes, J. M., and Cooper, M. E. (2007) Role of the AGE crosslink breaker, alagebrium, as a renoprotective agent in diabetes. *Kidney. Int. Suppl.* **106**, S54-60

Culbertson, S. M., Enright, G. D., and Ingold, K. U. (2003) Synthesis of a novel radical trapping and carbonyl group trapping anti-AGE agent: a pyridoxamine analogue for inhibiting advanced glycation (AGE) and lipoxidation (ALE) end products. *Org. Lett.* **5**, 2659-2662

Cummings, J. L., Vinters, H. V., Cole, G. M., and Khachaturian, Z. S. (1998) Alzheimer's disease: etiologies, pathophysiology, cognitive reserve, and treatment opportunities. *Neurology* **51**, S2-17

Davies, K. J. A., and Shringarpure, R. (2006) Preferential degradation of oxidized proteins by the 20S proteasome may be inhibited in aging and in inflammatory neuromuscular diseases. *Neurology.* **66**, S93-S96

Dockal, M., Chang, M., Carter, D. C., and Ruker, F. (2000) Five recombinant fragments of human serum albumin-tools for the characterization of the warfarin binding site. *Protein Sci.* **9**, 1455-1465

Du, X., Zhang, T., Li, R., and Wang, K. (2001) Nature of cerium(III)- and lanthanum(III)-induced aggregation of human erythrocyte membrane proteins. *J. Inorg. Biochem.* **84**, 67-7

Dukic-Stefanovic, S., Schinzel, R., Riederer, P., and Munch, G. (2001) AGES in brain ageing: AGE-inhibitors as neuroprotective and anti-dementia drugs? *Biogerontology* **2**, 19-34

Dyer, D. G., Dunn, J. A., Thorpe, S. R., Bailie, K. E., Lyons, T. J., McCance, D. R., and Baynes, J. W. (1993) Accumulation of Maillard reaction products in skin collagen in diabetes and aging. *The Journal of clinical investigation* **91**, 2463-2469

Ellman, G. L., Courtney, K. D., Andres, V., Jr., and Feather-Stone, R. M. (1961) A new and rapid colorimetric determination of acetylcholinesterase activity. *Biochem. Pharmacol.* **7**, 88-95

Essmann, U., Perera, L., Berkowitz, M. L., Darden, T., Lee, H. (1995) A smooth particle mesh Ewald method. *J. Chem. Phys.* **103**, 8577-8593

Feller, S. E., Zhang, Y., Pastor, R. W., Brooks, B. R. (1995) Constant pressure molecular dynamics simulation: The Langevin piston method. *J. Chem. Phys.* **103**, 4613-4621

Fernandez-Escamilla, A. M., Rousseau, F., Schymkowitz, J., and Serrano, L. (2004) Prediction of sequence-dependent and mutational effects on the aggregation of peptides and proteins. *Nat. Biotech.* **22**,1302-1306

Feuerstein, G. Z., Zaleska, M. M., Krams, M., Wang, X., Day, M., Rutkowski, J. L., Finklestein, S. P., Pangalos, M. N., Poole, M., Stiles, G. L., Ruffolo, R. R., and Walsh, F. L. (2008) Missing steps in the STAIR case: a Translational Medicine perspective on the development of NXY-059 for treatment of acute ischemic stroke. *J. Cereb. Blood. Flow. Metab.* **28**, 217-219

Figueroa-Romero, C., Sadidi, M., and Feldman, E. L. (2008) Mechanisms of disease: the oxidative stress theory of diabetic neuropathy. *Rev. Endocr. Metab. Disord.* **9**, 301-14

Freskos, J. N., Fobian, Y. M., Benson, T. E., Moon, J. B., Bienkowski, M. J., Brown, D. L., Emmons, T. L., Heintz, R., Laborde, A., McDonald, J. J., Mischke, B. V., Molyneaux, J. M., Mullins, P. B., Bryan Prince, D., Paddock, D. J., Tomasselli, A. G., and Winterrowd, G. (2007) Design of potent inhibitors of human beta-secretase. Part 2. *Bioorg. Med. Chem. Lett.* **17**, 78-81

Friguet, B., Bulteau, A. L., Chondrogianni, N., Conconi, M., and Petropoulos, I. (2000) Protein Degradation by the Proteasome and Its Implications in Aging. *Ann. N. Y. Acad. Sci.* **908**, 143-154

Frishman, D., and Argos, P. (1995) Knowledge-based protein secondary structure assignment. *Proteins* **23**, 566-579

Fujita, H., Haseyama, T., Kayo, T., Nozaki, J., Wada, Y., Ito, S., and Koizumi, A. (2001) Increased expression of glutathione S-transferase in renal proximal tubules in the early stages of diabetes: a study of type-2 diabetes in the Akita mouse model. *Exp. Nephrol.* **9**, 380-6

Furberg, C. D., and Pitt, B. (2001) Withdrawal of cerivastatin from the world market. *Curr. Control. Trials. Cardiovasc. Med.* **2**, 205-207

glycation end-products: vesperlysines A, B, and C are formed as cross-linked products in the Maillard reaction between lysine and protein with glucose. *Biochem. Biophys. Res. Commun.* **6**, 227–230

Goldberg, A. L. (2003) Protein degradation and protection against misfolded or damaged proteins. *Nature.* **426**, 895-899

Golde, T. E. (2006) Disease modifying therapy for AD? *J. Neurochem.* **99**, 689-707

Golegaonkar, S. B., Bhonsle, H. S., Boppana, R., and Kulkarni, M. J. Discovery of rifampicin as a new anti-glycating compound by matrix-assisted laser desorption/ionization mass spectrometry-based insulin glycation assay. *Eur. J. Mass. Spectrom. (Chichester, Eng)* **16**, 221-226

Gotz, J., Ittner, A., and Ittner, L. M. Tau-targeted treatment strategies in Alzheimer's disease. *Br. J. Pharmacol.* **165**, 1246-1259

Greenfield, N., and Fasman, G. D. (1969) Computed circular dichroism spectra for the evaluation of protein conformation. *Biochemistry* **8**, 4108-4116

Gulyaeva, N., Zaslavsky, A., Lechner, P., Chlenov, M., McConnell, O., Chait, A., Kipnis, V., and Zaslavsky, B. (2003) Relative hydrophobicity and lipophilicity of drugs measured by aqueous two-phase partitioning, octanol-buffer partitioning and HPLC. A simple model for predicting blood-brain distribution. *Eur. J. Med. Chem.* **38**, 391-396

Haan, M. N. (2006) Therapy Insight: type 2 diabetes mellitus and the risk of late-onset Alzheimer's disease. *Nat. Clin. Pract. Neurol.* **2**, 159-166

Haass, C., and Selkoe, D. J. (2007) Soluble protein oligomers in neurodegeneration: lessons from the Alzheimer's amyloid beta-peptide. *Nat. Rev. Mol. Cell. Biol.* **8**, 101-112

Habig, W. H., Pabst, M. J., and Jakoby, W. B. (1974) Glutathione S-Transferases-First enzymatic step in mercapturic acid formation. *J. Biol. Chem.* **249**, 7130-7139

Hammes, H. P., Du, X., Edelstein, D., Taguchi, T., Matsumura, T., Ju, Q., Lin, J., Bierhaus, A., Nawroth, P., Hannak, D., Neumaier, M., Bergfeld, R., Giardino, I., and Brownlee, M. (2003) Benfotiamine blocks three major pathways of hyperglycemic damage and prevents experimental diabetic retinopathy. *Nat. Med.* **9**, 294-299

VI. Bibliography

Hardy, J., and Selkoe, D. J. (2002) The amyloid hypothesis of Alzheimer's disease: progress and problems on the road to therapeutics. *Science* **297**, 353-356

Harrison, C. Signatures for drug repositioning. *Nat. Rev. Genet.* **12**, 668

Havliš, J., Thomas, H., Šebela, M., and Shevchenko, A. (2003) Fast-response proteomics by accelerated in-gel digestion of proteins. *Anal. Chem.* **75**, 1300-1306

Hegde, P., Chandrakasan, G., and Chandra, T. (2002) Inhibition of collagen glycation and crosslinking in vitro by methanolic extracts of Finger millet (Eleusine coracana) and Kodo millet (Paspalum scrobiculatum). *J. Nutr. Biochem.* **13**, 517

Hill, E. H., Stratton, K., Whitten, D. G., and Evans, D. G. Molecular dynamics simulation study of the interaction of cationic biocides with lipid bilayers: aggregation effects and bilayer damage. *Langmuir* **28**, 14849-14854

Hills, I. D., and Vacca, J. P. (2007) Progress toward a practical BACE-1 inhibitor. *Curr. Opin. Drug. Discov. Devel.* **10**, 383-391

Homko, C. J., and Khandelwal, M. (1996) Glucose monitoring and insulin therapy during pregnancy. *Obstetrics and gynecology clinics of North America.* **23**, 47-74

Hoshi, A., Takahashi, M., Fujii, J., Myint, T., Kaneto, H., Suzuki, K., Yamasaki, Y., Kamada, T., and Taniguchi, N. (1996) Glycation and inactivation of sorbitol dehydrogenase in normal and diabetic rats. *Biochem. J.* **318**, 119-23

Hu, Y. J., Liu, Y., Zhao, R. M., Dong, J. X., Qu, S.S. (2006) Spectroscopic studies on the interaction between methylene blue and bovine serum albumin. *J.*

Humphrey, W., Dalke, A., and Schulten, K. (1996) VMD: visual molecular dynamics. *J. Mol. Graph.* **14**, 33-38

Hurle, M. R., Yang, L., Xie, Q., Rajpal, D. K., Sanseau, P., and Agarwal, P. Computational drug repositioning: from data to therapeutics. *Clin. Pharmacol. Ther.* **93**, 335-341

Hussain, I. (2004) The potential for BACE1 inhibitors in the treatment of Alzheimer's disease. *IDrugs* **7**, 653-658

Jakoby, M. G. t., Covey, D. F., and Cistola, D. P. (1995) Localization of tolbutamide binding sites on human serum albumin using titration calorimetry and heteronuclear 2-D NMR. *Biochemistry* **34**, 8780-8787

Jakus, V., Hrnciarova, M., Carsky, J., Krahulec, B., and Rietbrock, N. (1999) Inhibition of nonenzymatic protein glycation and lipid peroxidation by drugs with antioxidant activity. *Life. Sci.* **65**, 1991-1993

Jana, A. K., and Sengupta, N. Adsorption mechanism and collapse propensities of the full-length, monomeric Abeta(1-42) on the surface of a single-walled carbon nanotube: a molecular dynamics simulation study. *Biophys. J.* **102**, 1889-1896

Johnson, D. T., Harris, R. A., French, S., Aponte, A., and Balaban, R. S. (2009) Proteomic changes associated with diabetes in the BB-DP rat. *Am. J. Physiol. Endocrinol. Metab.* **296**, E422-E432

Jonas, J. C., Sharma, A., Hasenkamp, W., Ilkova, H., Patanè, G., Laybutt, R., Bonner-Weir, S., and Weir, G. C. (1999) Chronic Hyperglycemia Triggers Loss of Pancreatic Î² Cell Differentiation in an Animal Model of Diabetes. *J. Biol. Chem.* **274**, 14112-14121

Jorgensen, W. L., Chandrasekhar, J., Madura, J. D., Impey, R. W., Klein, M. L. (1983) Comparison of Simple Potential Functions for Simulating Liquid Water. *J. Chem. Phys.* **79**, 926–935

Joseph, K. S., Anguizola, J., and Hage, D. S. Binding of tolbutamide to glycated human serum albumin. *J. Pharm. Biomed. Anal.* **54**, 426-432

Joseph, K. S., Moser, A. C., Basiaga, S. B., Schiel, J. E., and Hage, D. S. (2009) Evaluation of alternatives to warfarin as probes for Sudlow site I of human serum albumin: characterization by high-performance affinity chromatography. *J. Chromatogr. A* **1216**, 3492-3500

Jung, Y. S., Joe, B. Y., Cho, S. J., and Konishi, Y. (2005) 2,3-Dimethoxy-5-methyl-1,4-benzoquinones and 2-methyl-1,4-naphthoquinones: glycation inhibitors with lipid peroxidation activity. *Bioorg. Med. Chem. Lett.* **15**, 1125-1129

Kaiser, P., and Wohlschlegel, J. (2005) Identification of ubiquitination sites and determination of ubiquitin-chain architectures by mass spectrometry. *Methods Enzymol.* **399**, 266-77

Kale, L., Skeel, R., Bhandarkar, M., Brunner, R., Gursoy, A. (1999) NAMD2: Greater Scalability for Parallel Molecular Dynamics. *Comput. Phys.* **151**, 283-312

Keita, Y., Michailova, M., Kratzer, W., Worner, G., Worner, W., and Rietbrock, N. (1992) Influence of penicillamine on the formation of early non-enzymatic glycation products of human serum proteins. *Int. J. Clin. Pharmacol. Ther. Toxicol.* **30**, 441-442.

Kellenberger, E., Rodrigo, J., Muller, P., and Rognan, D. (2004) Comparative evaluation of eight docking tools for docking and virtual screening accuracy. *Proteins* **57**, 225-242

Khurana, R., Coleman, C., Ionescu-Zanetti, C., Carter, S. A., Krishna, V., Grover, R. K., Roy, R., and Singh, S. (2005) Mechanism of thioflavin T binding to amyloid fibrils. *J. Struct. Biol.* **151**, 229-238

King, H., Aubert, R. E., and Herman, W. H. (1998) Global burden of diabetes, 1995-2025: prevalence, numerical estimates, and projections. *Diabetes Care* **21**, 1414-1431

Kitchen, D. B., Decornez, H., Furr, J. R., and Bajorath, J. (2004) Docking and scoring in virtual screening for drug discovery: methods and applications. *Nat. Rev. Drug. Discov.* **3**, 935-949

Kryger, G., Harel, M., Giles, K., Toker, L., Velan, B., Lazar, A., Kronman, C., Barak, D., Ariel, N., Shafferman, A., Silman, I., and Sussman, J. L. (2000) Structures of recombinant native and E202Q mutant human acetylcholinesterase complexed with the snake-venom toxin fasciculin-II. *Acta Crystallogr. D Biol. Crystallogr.* **56**, 1385-1394

Kuhla, B., Boeck, K., Schmidt, A., Ogunlade, V., Arendt, T., Munch, G., and Luth, H. J. (2007) Age- and stage-dependent glyoxalase I expression and its activity in normal and Alzheimer's disease brains. *Neurobiol. Aging.* **28**, 29-41

Kuzmicki, M., Telejko, B., Szamatowicz, J., Zonenberg, A., Nikolajuk, A., Kretowski, A., and Gorska, M. (2009) High resistin and interleukin-6 levels are associated with gestational diabetes mellitus. *Gynecol. Endocrinol.* **25**, 258-263

Lapolla, A., Fedele, D., Seraglia, R., and Traldi, P. (2006) The role of mass spectrometry in the study of non-enzymatic protein glycation in diabetes: An update. *Mass Spectrom. Rev.* **25**, 775-797

Ledesma, M. D., Medina, M., and Avila, J. (1996) The in vitro formation of recombinant tau polymers: effect of phosphorylation and glycation. *Mol. Chem. Neuropathol.* **27**, 249-58

Lee, C., and Ham, S. Characterizing amyloid-beta protein misfolding from molecular dynamics simulations with explicit water. *J. Comput. Chem.* **32**, 349-355

Lee, S., Zheng, X., Krishnamoorthy, J., Savelieff, M. G., Park, H. M., Brender, J. R., Kim, J. H., Derrick, J. S., Kochi, A., Lee, H. J., Kim, C., Ramamoorthy, A., Bowers, M. T., and Lim, M. H. Rational design of a structural framework with potential use to develop chemical reagents that target and modulate multiple facets of Alzheimer's disease. *J. Am. Chem. Soc.* **136**, 299-310

LeVine, H., 3rd (1993) Thioflavine T interaction with synthetic Alzheimer's disease beta-amyloid peptides: detection of amyloid aggregation in solution. *Protein Sci.* **2**, 404-410

Li, J., Liu, D., Sun, L., Lu, Y., and Zhang, Z. Advanced glycation end products and neurodegenerative diseases: mechanisms and perspective. *J. Neurol. Sci.* **317**, 1-5

Li, J., Liu, D., Sun, L., Lu, Y., and Zhang, Z. Advanced glycation end products and neurodegenerative diseases: mechanisms and perspective. *J. Neurol. Sci.* **317**, 1-5

Li, M., Shang, D. S., Zhao, W. D., Tian, L., Li, B., Fang, W. G., Zhu, L., Man, S. M., and Chen, Y. H. (2009) Amyloid beta interaction with receptor for advanced glycation end products up-regulates brain endothelial CCR5 expression and promotes T cells crossing the blood-brain barrier. *J. Immunol.* **182**, 5778-5788

Li, X. H., Du, L. L., Cheng, X. S., Jiang, X., Zhang, Y., Lv, B. L., Liu, R., Wang, J. Z., and Zhou, X. W. Glycation exacerbates the neuronal toxicity of beta-amyloid. *Cell. Death. Dis.* **4**, e673

Lin, Y. S., Bowman, G. R., Beauchamp, K. A., and Pande, V. S. Investigating how peptide length and a pathogenic mutation modify the structural ensemble of amyloid beta monomer. *Biophys. J.* **102**, 315-324

Lomenick, B., Hao, R., Jonai, N., Chin, R. M., Aghajan, M., Warburton, S., Wang, J., Wu, R. P., Gomez, F., Loo, J. A., Wohlschlegel, J. A., Vondriska, T. M., Pelletier, J., Herschman, H. R., Clardy, J., Clarke, C. F., and Huang, J. (2009) Target identification using drug affinity responsive target stability (DARTS). *Proc. Natl. Acad. Sci. USA*. **106**, 21984-21989

Mabanglo, M. F., Serohijos, A. W., and Poulter, C. D. The Streptomyces-produced antibiotic fosfomycin is a promiscuous substrate for archaeal isopentenyl phosphate kinase. *Biochemistry* **51**, 917-925

MacKerell, A. D., Bashford, D., Bellott, M., Dunbrack, R. L., Evanseck, J. D., Field, M. J., Fischer, S., Gao, J., Guo, H., Ha, S., Joseph-McCarthy, D., Kuchnir, L., Kuczera, K., Lau, F. T., Mattos, C., Michnick, S., Ngo, T., Nguyen, D. T., Prodhom, B., Reiher, W. E., Roux, B., Schlenkrich, M., Smith, J. C., Stote, R., Straub, J., Watanabe, M., Wiorkiewicz-Kuczera, J., Yin, D., and Karplus, M. (1998) All-atom empirical potential for molecular modeling and dynamics studies of proteins. *J. Phys. Chem. B* **102**, 3586-3616

Mackerell, A. D., Jr., Feig, M., and Brooks, C. L., 3rd (2004) Extending the treatment of backbone energetics in protein force fields: limitations of gas-phase quantum mechanics in reproducing protein conformational distributions in molecular dynamics simulations. *J. Comput. Chem.* **25**, 1400-1415

Malik, A. R., Javed, M. K., Zahid, Y., Rizwan, H. K., Kabir, D. (2012) Conformational changes of serum albumin upon complexation with amphiphilic drug imipramine hydrochloride. *J Proteins and proteomics* **3,** 207-215

Mentink, C. J., Hendriks, M., Levels, A. A., and Wolffenbuttel, B. H. (2002) Glucose-mediated cross-linking of collagen in rat tendon and skin. *Clin. Chim. Acta.* **321**, 69-76

Monnier, V. M., Glomb, M., Elgawish, A., and Sell, D. R. (1996) The mechanism of collagen cross-linking in diabetes: a puzzle nearing resolution. *Diabetes* **45 Suppl 3**, S67-72

Monnier, V. M., Kohn, R. R., and Cerami, A. (1984) Accelerated age-related browning of human collagen in diabetes mellitus. *Proc. Natl. Acad Sci. USA.* **81**, 583-7

Morgan, P. E., Dean, R. T., and Davies, M. J. (2002) Inactivation of cellular enzymes by carbonyls and protein-bound glycation/glycoxidation products. *Arch. Biochem. Biophys.* **403**, 259-269

Morris, G. M., Huey, R., Lindstrom, W., Sanner, M. F., Belew, R. K., Goodsell, D. S., and Olson, A. J. (2009) AutoDock4 and AutoDockTools4: Automated docking with selective receptor flexibility. *J. Comput. Chem.* **30**, 2785-2791

Moser, A. C., Kingsbury, C., and Hage, D. S. (2006) Stability of warfarin solutions for drug-protein binding measurements: spectroscopic and chromatographic studies. *J. Pharm. Biomed. Anal.* **41**, 1101-1109

Munch, G., Mayer, S., Michaelis, J., Hipkiss, A. R., Riederer, P., Muller, R., Neumann, A., Schinzel, R., and Cunningham, A. M. (1997) Influence of advanced glycation end-products and AGE-inhibitors on nucleation-dependent polymerization of beta-amyloid peptide. *Biochim. Biophys. Acta.* **1360**, 17-29

Nagasawa, T., Tabata, N., Ito, Y., Aiba, Y., Nishizawa, N., and Kitts, D. D. (2003) Dietary G-rutin suppresses glycation in tissue proteins of streptozotocin-induced diabetic rats. *Mol. Cell. Biochem.* **252**, 141-147

Nakamura, K., Hasegawa, T., Fukunage, Y., Ienaga, K. (1992) Crosslines A and B as candidates for the fluorophores in age-related and diabetes related crosslinked proteins and their diacetates produced by Maillard reactions of a-acetyl-lysine and glucose. *J. Chem. Soc. Commun.* **14**, 992–994

Nakamura, K., Nakezawa, Y., Ienaga, K. (1997) Acid-stable fluorescent advanced

Nakhjavani, M., Morteza, A., Khajeali, L., Esteghamati, A., Khalilzadeh, O., Asgarani, F., and Outeiro, T. (2010) Increased serum HSP70 levels are associated with the duration of diabetes. *Cell Stress and Chaperones.* **15**, 959-964

Negre-Salvayre, A., Salvayre, R., Auge, N., Pamplona, R., and Portero-Otin, M. (2009) Hyperglycemia and glycation in diabetic complications. *Antioxid. Redox. Signal.* **11**, 3079-3109

Peppa, M., Uribarri, J., and Vlassara, H. (2003) Glucose, Advanced Glycation End products, and Diabetes complications: What is new and what works. *Clin. Diabetes.* **21**, 186-187

Photochem. Photobiol. A **179**, 324–329

Portero-OtÃn, M., Pamplona, R., Ruiz, M. C., Cabiscol, E., Prat, J., and Bellmunt, M. J. (1999) Diabetes induces an impairment in the proteolytic activity against oxidized proteins and a heterogeneous effect in nonenzymatic protein modifications in the cytosol of rat liver and kidney. *Diabetes*. **48**, 2215-2220

Qu, X. A., Gudivada, R. C., Jegga, A. G., Neumann, E. K., and Aronow, B. J. (2009) Inferring novel disease indications for known drugs by semantically linking drug action and disease mechanism relationships. *BMC Bioinformatics* **10 Suppl 5**, S4

Queisser, M. A., Yao, D., Geisler, S., Hammes, H.-P., Lochnit, G. n., Schleicher, E. D., Brownlee, M., and Preissner, K. T. (2010) Hyperglycemia Impairs Proteasome Function by Methylglyoxal. *Diabetes*. **59**, 670-678

Rademakers, R., and Rovelet-Lecrux, A. (2009) Recent insights into the molecular genetics of dementia. *Trends Neurosci*. **32**, 451-461

Ramakrishnan, S., Sulochana, K. N., and Punitham, R. (1999) Two new functions of inositol in the eye lens: antioxidation and antiglycation and possible mechanisms. *Indian. J. Biochem. Biophys*. **36**, 129-133

Reddy, G. K. (2004) Cross-linking in collagen by nonenzymatic glycation increases the matrix stiffness in rabbit achilles tendon. *Exp. Diabesity. Res*. **5**, 143-153

Reddy, G. K., Stehno-Bittel, L., and Enwemeka, C. S. (2002) Glycation-induced matrix stability in the rabbit achilles tendon. *Arch. Biochem. Biophys*. **399**, 174-80

Ricard-Blum, S., and Ville, G. (1988) Collagen cross-linking. *Cell. Mol. Biol*. **34**, 581-590

Riederer, B. M., Leuba, G., Vernay, A., and Riederer, I. M. (2011) The role of the ubiquitin proteasome system in Alzheimer's disease. *Exp. Biol. Med. (Maywood)*. **236**, 268-76

Roberson, E. D., and Mucke, L. (2006) 100 years and counting: prospects for defeating Alzheimer's disease. *Science* **314**, 781-784

Rondeau, P., and Bourdon, E. The glycation of albumin: structural and functional impacts. *Biochimie* **93**, 645-658

Rother, K. I. (2007) Diabetes treatment-bridging the divide. *N Engl J Med Apr.* **356,** 1499-1501

Ruggiero-Lopez, D., Lecomte, M., Moinet, G., Patereau, G., Lagarde, M., and Wiernsperger, N. (1999) Reaction of metformin with dicarbonyl compounds. Possible implication in the inhibition of advanced glycation end product formation. *Biochem. Pharmacol.* **58**, 1765-73

Ryckaert, J. P., Ciccotti, G., Berendsen, H. J. C. (1977) Numerical integration of the cartesian equations of motion of a system with constraints: molecular dynamics of n-alkanes. *J. Comput. Phys.* **23**, 327-341

Saeed, A. I., Bhagabati, N. K., Braisted, J. C., Liang, W., Sharov, V., Howe, E. A., Li, J., Thiagarajan, M., White, J. A., and Quackenbush, J. (2006) TM4 microarray software suite. *Methods Enzymol.* **411**, 134-193

Sajithlal, G. B., Chithra, P., and Chandrakasan, G. (1998) Effect of curcumin on the advanced glycation and cross-linking of collagen in diabetic rats. *Biochem. Pharmacol.* **56**, 1607-1614

Saldana, T. M., Siega-Riz, A. M., Adair, L. S., and Suchindran, C. (2006) The relationship between pregnancy weight gain and glucose tolerance status among black and white women in central North Carolina. *Am. J. Obstet. Gynecol.* **195**, 1629-35

Santini, S., Wei, G., Mousseau, N., and Derreumaux, P. (2004) Pathway complexity of Alzheimer's beta-amyloid Abeta16-22 peptide assembly. *Structure* **12**, 1245-1255

Schenk, D., Basi, G. S., and Pangalos, M. N. Treatment strategies targeting amyloid beta-protein. *Cold. Spring. Harb. Perspect. Med.* **2**, a006387

Schlienger, J. L. (2013) Type 2 diabetes complications. *Presse. Med.* **42**, 839-848

Schnider, S.L. and Kohn R.R. (1981) Effects of age and diabetes mellitus on the solubility and nonenzymatic glucosylation of human skin collagen. *J Clin Invest.* **67**, 1630-5

Seidler, N. W., Yeargans, G. S., and Morgan, T. G. (2004) Carnosine disaggregates glycated alpha-crystallin: an in vitro study. *Arch. Biochem. Biophys.* **427**, 110-115

Selkoe, D. J. (1999) Translating cell biology into therapeutic advances in Alzheimer's disease. *Nature* **399**, A23-A31

Sgourakis, N. G., Yan, Y., McCallum, S. A., Wang, C., and Garcia, A. E. (2007) The Alzheimer's peptides Abeta40 and 42 adopt distinct conformations in water: a combined MD / NMR study. *J. Mol. Biol.* **368**, 1448-1457

Shoemaker, B. A., and Panchenko, A. R. (2007) Deciphering protein-protein interactions. Part I. Experimental techniques and databases. *PLoS Comput. Biol.* **3**, 337-344

Singh, V. P., Bali, A., Singh, N., and Jaggi, A. S. (2014) Advanced Glycation End Products and Diabetic Complications. *Korean J. Physiol. Pharmacol.* **18**, 1-14

Skillman, T. G., and Feldman, J. M. (1981) The pharmacology of sulfonylureas. Am. J. Med. **70**, 361-372

Small, D. H. (2005) Acetylcholinesterase inhibitors for the treatment of dementia in Alzheimer's disease: do we need new inhibitors? *Expert. Opin. Emerg. Drugs.* **10**, 817-825

Smith, M. A., Richey, P. L., Taneda, S., Kutty, R. K., Sayre, L. M., Monnier, V. M., and Perry, G. (1994) Advanced Maillard reaction end products, free radicals, and protein oxidation in Alzheimer's disease. *Ann. N. Y. Acad. Sci.* 738, 447-454

Smith, M. A., Taneda, S., Richey, P. L., Miyata, S., Yan, S. D., Stern, D., Sayre, L. M., Monnier, V. M., and Perry, G. (1994) Advanced Maillard reaction end

products are associated with Alzheimer disease pathology. *Proc. Natl. Acad. Sci. USA.* **91**, 5710-5714

Sobal, G., Menzel, E. J., and Sinzinger, H. (2001) Calcium antagonists as inhibitors of in vitro low density lipoprotein oxidation and glycation. *Biochem. Pharmacol.* **61**, 373-379

Solomon, M., Belenghi, B., Delledonne, M., Menachem, E., and Levine, A. (1999) The involvement of cysteine proteases and protease inhibitor genes in the regulation of programmed cell death in plants. *Plant Cell.* **11**, 431-44

Steen, E., Terry, B. M., Rivera, E. J., Cannon, J. L., Neely, T. R., Tavares, R., Xu, X. J., Wands, J. R., and de la Monte, S. M. (2005) Impaired insulin and insulin-like growth factor expression and signaling mechanisms in Alzheimer's disease--is this type 3 diabetes? *J. Alzheimers Dis.* **7**, 63-80

Sudlow, G., Birkett, D. J., and Wade, D. N. (1975) The characterization of two specific drug binding sites on human serum albumin. *Mol. Pharmacol.* **11**, 824-832

Swamidass, S. J. Mining small-molecule screens to repurpose drugs. *Brief. Bioinform.* **12**, 327-35

Swamy, M. S., Tsai, C., Abraham, A., and Abraham, E. C. (1993) Glycation mediated lens crystallin aggregation and cross-linking by various sugars and sugar phosphates in vitro. *Exp. Eye. Res.* **56**, 177-185

Tai, K., Shen, T., Henchman, R. H., Bourne, Y., Marchot, P., and McCammon, J. A. (2002) Mechanism of acetylcholinesterase inhibition by fasciculin: a 5-ns molecular dynamics simulation. *J. Am. Chem. Soc.* **124**, 6153-6161

Tamhane, V. A., Chougule, N. P., Giri, A. P., Dixit, A. R., Sainani, M. N., and Gupta, V. S. (2005) In vivo and in vitro effect of Capsicum annum proteinase inhibitors on Helicoverpa armigera gut proteinases. *Biochim. Biophys. Acta.* **1722**, 156-167

Terry, A. V., Jr., and Buccafusco, J. J. (2003) The cholinergic hypothesis of age and Alzheimer's disease-related cognitive deficits: recent challenges and their implications for novel drug development. *J. Pharmacol. Exp. Ther.* **306**, 821-827

Thornalley, P. J. (1990) The glyoxalase system: new developments towards functional characterization of a metabolic pathway fundamental to biological life. *Biochem. J.* **269**, 1-11

Thornalley, P. J., Langborg, A., and Minhas, H. S. (1999) Formation of glyoxal, methylglyoxal and 3-deoxyglucosone in the glycation of proteins by glucose. *Biochem. J.* **344 Pt 1**, 109-116

Tjernberg, L. O., Näslund, J., Lindqvist, F., Johansson, J., Karlström, A.R. (1996) Arrest of beta-amyloid fibril formation by a pentapeptide ligand. *J. Biol. Chem.* **271**, 8545-8548

Tobinick, E. L. (2009) The value of drug repositioning in the current pharmaceutical market. *Drug. News. Perspect.* **22**, 119-125

Tomaselli, S., Esposito, V., Vangone, P., van Nuland, N. A., Bonvin, A. M., Guerrini, R., Tancredi, T., Temussi, P. A., and Picone, D. (2006) The alpha-to-beta conformational transition of Alzheimer's Abeta-(1-42) peptide in aqueous media is reversible: a step by step conformational analysis suggests the location of beta conformation seeding. *Chembiochem* **7**, 257-267

Traverso, N., Menini, S., Odetti, P., Pronzato, M. A., Cottalasso, D., and Marinari, U. M. (2002) Diabetes impairs the enzymatic disposal of 4-hydroxynonenal in rat liver. *Free Radic. Biol. Med.* **32**, 350-359

Trnkova, L. , Bousova, I. , Kubicek, V. and Drsata, J. (2010) Binding of naturally occurring hydroxycinnamic acids to bovine serum albumin. *Natural Science* **2**, 563-570

Trott, O., and Olson, A. J. AutoDock Vina: improving the speed and accuracy of docking with a new scoring function, efficient optimization, and multithreading. *J. Comput. Chem.* **31**, 455-461

Trovato, A., Chiti, F., Maritan, A., and Seno, F. (2006) Insight into the Structure of Amyloid Fibrils from the Analysis of Globular Proteins. *PLoS Comput. Biol.* **2**, e170

Trovato, A., Seno, F., and Tosatto, S. C. E. (2007) The PASTA server for protein aggregation prediction. *Protein Eng. Des. Sel.* **20**, 521-523

Uchimura, K., Nagasaka, A., Hayashi, R., Makino, M., Nagata, M., Kakizawa, H., Kobayashi, T., Fujiwara, K., Kato, T., Iwase, K., Shinohara, R., Kato, K., and Itoh, M. (1999) Changes in Superoxide Dismutase Activities and Concentrations and Myeloperoxidase Activities in Leukocytes from Patients with Diabetes Mellitus. *J. Diabetes Complications.* **13**, 264-270

Ulrich, P., and Cerami, A. (2001) Protein glycation, diabetes, and aging. *Recent. Prog. Horm. Res.* **56**, 1-21

van Boekel, M. A., van den Bergh, P. J., and Hoenders, H. J. (1992) Glycation of human serum albumin: inhibition by Diclofenac. *Biochim. Biophys. Acta.* **1120**, 201-204

Velazquez Campoy, A., and Freire, E. (2005) ITC in the post-genomic era...? Priceless. *Biophys. Chem.* **115**, 115–124

Verbeke, P., Siboska, G. E., Clark, B. F., and Rattan, S. I. (2000) Kinetin inhibits protein oxidation and glycoxidation in vitro. *Biochem. Biophys. Res. Commun.* **276**, 1265-70

Vernace, V. A., Schmidt-Glenewinkel, T., and Figueiredo-Pereira, M. E. (2007) Aging and regulated protein degradation: who has the UPPer hand? *Aging Cell.* **6,** 599-606

Vitek, M. P., Bhattacharya, K., Glendening, J. M., Stopa, E., Vlassara, H., Bucala, R., Manogue, K., and Cerami, A. (1994) Advanced glycation end products contribute to amyloidosis in Alzheimer disease. *Proc. Natl. Acad. Sci. U S A* **91**, 4766-70

Vitek, M. P., Bhattacharya, K., Glendening, J. M., Stopa, E., Vlassara, H., Bucala, R., Manogue, K., and Cerami, A. (1994) Advanced glycation end products contribute to amyloidosis in Alzheimer disease. *Proc. Natl. Acad. Sci. U S A* **91**, 4766-4770

Vitek, M. P., Bhattacharya, K., Glendening, J. M., Stopa, E., Vlassara, H., Bucala, R., Manogue, K., and Cerami, A. (1994) Advanced glycation end products contribute to amyloidosis in Alzheimer disease. *Proc. Natl. Acad. Sci. U S A* **91**, 4766-4770

Wa, C., Cerny, R. L., Clarke, W. A., and Hage, D. S. (2007) Characterization of glycation adducts on human serum albumin by matrix-assisted laser desorption/ionization time-of-flight mass spectrometry. *Clin. Chim. Acta.* **385**, 48-60

Ward, W. K., Bolgiano, D. C., McKnight, B., Halter, J. B., and Porte, D. Jr. (1984) Dimished B cell secretory capacity in patients with non-insulin-dependent diabetes mellitus. *J. Clin. Invest.* **74,** 1318-1328

Wells-Knecht, K. J., Zyzak, D. V., Litchfield, J. E., Thorpe, S. R., and Baynes, J. W. (1995) Mechanism of autoxidative glycosylation: identification of glyoxal and arabinose as intermediates in the autoxidative modification of proteins by glucose. *Biochemistry* **34**, 3702-3709

Wild, S., Roglic, G., Green, A., Sicree, R., and King, H. (2004) Global prevalence of diabetes: estimates for the year 2000 and projections for 2030. *Diabetes Care* **27,** 1047-1053

Wu, D., Chen, Z., and Liu, X. (2011) Study of the interaction between bovine serum albumin and ZnS quantum dots with spectroscopic techniques. *Spectrochim. Acta A Mol Biomol. Spectrosc.* **84**, 178-183

Xiong, B., Huang, X. Q., Shen, L. L., Shen, J. H., Luo, X. M., Shen, X., Jiang, H. L., and Chen, K. X. (2004) Conformational flexibility of beta-secretase: molecular dynamics simulation and essential dynamics analysis. *Acta Pharmacol. Sin.* **25**, 705-713

Yan, S. D., Yan, S. F., Chen, X., Fu, J., Chen, M., Kuppusamy, P., Smith, M. A., Perry, G., Godman, G. C., Nawroth, P., and et al. (1995) Non-enzymatically glycated tau in Alzheimer's disease induces neuronal oxidant stress resulting in cytokine gene expression and release of amyloid beta-peptide. *Nat. Med.* **1**, 693-699

Yang, Y., and Song, W. Molecular links between Alzheimer's disease and diabetes mellitus. *Neuroscience* **250**, 140-150

Yoshimura, T. (1993) Monitoring protein conformational changes during membrane fusion. *Methods Enzymol.* **221**, 72-82

Youdim, M. B., and Buccafusco, J. J. (2005) Multi-functional drugs for various CNS targets in the treatment of neurodegenerative disorders. *Trends. Pharmacol. Sci.* **26**, 27-35

Zanon, J. P., Peres, M. F. S., and GattÃ¡s, E. A. L. (2007) Colorimetric assay of ethanol using alcohol dehydrogenase from dry baker's yeast. *Enz. Microb. Tech.* **40**, 466-470

Zhang, C. Natural compounds that modulate BACE1-processing of amyloid-beta precursor protein in Alzheimer's disease. *Discov. Med.* **14**, 189-197

Zhang, H. Y. (2005) One-compound-multiple-targets strategy to combat Alzheimer's disease. *FEBS Lett.* **579**, 5260-5264

Zoete, V., Cuendet, M. A., Grosdidier, A., and Michielin, O. SwissParam: a fast force field generation tool for small organic molecules. *J. Comput. Chem.* **32**, 2359-2368

Sneha Balasaheb Bansode
1904, Biochemical Sciences Division
CSIR-National Chemical Laboratory
Dr. Homi Bhabha Road, Pashan
Pune, India 411008
Phone No. : +91-20-25902204/ 9763363220
Email ID: snehabansode@outlook.com
          sb.bansode@ncl.res.in

Educational Qualification

PhD in Biotechnology at University of Pune, India (Working Place: Biochemical Sciences   Division, CSIR-NCL, Pune)
August 2009 to Current; CSIR-National Chemical Laboratory, Pune, India

Master of Science in Biotechnology, University of Pune
2007 to 2009; Vidya Pratishthan's School of Biotechnology, Baramati, India (65.9/100)

Bachelor of Science in Biotechnology, University of Pune
2004 to 2007; Vidya Pratishthan's School of Biotechnology, Baramati, India (67.4/100)

Work Experience

Senior Research Fellow at Biochemical Sciences Division, CSIR-NCL, Pune
August 2011 to Current; Proteomics Group, CSIR-NCL, Pune, India.
Research topic: Study of glycation and drug induced protein cross-linking

Junior Research Fellow at Biochemical Sciences Division, CSIR-NCL, Pune
August 2009 to July 2011; Proteomics Group, CSIR-NCL, Pune, India.
Research topic: Study of glycation and drug induced protein cross-linking

Award and Achievement

Received NCL-RF-Gupta-Pardeshi-Sainani Best Publication Award for highest impact factor in Biological Sciences in CSIR-NCL-2013

Qualified The Joint CSIR- UGC National Eligibility Test for JRF and eligibility for lecturer ship held on 21st December 2008.

Publications

- **Bansode SB**, Chougale AD, Joshi RS, Giri AP, Bodhankar SL, Harsulkar AM, Kulkarni MJ. Proteomic analysis of protease resistant proteins in the diabetic rat kidney. **Mol Cell Proteomics**. 2013 (1):228-36.

- **Bansode SB,** Jana A, Batkulwar KB, Warkad SD, Joshi RS, Sengupta N, Kulkarni MJ. Molecular Investigations of Protriptyline as a Multi-Target Directed Ligand in Alzheimer's Disease. **PLoS ONE (For revision)**

- Bhonsle HS, Korwar AM, Kesavan SK, Bhosale SD, **Bansode SB**, Kulkarni MJ. "Zoom-ln"-A targeted database search for identification of glycation modifications analyzed by untargeted tandem mass spectrometry. **Eur J Mass Spectrom** (Chichester, Eng). 2012;18(6):475-81.

- Golegaonkar S, Pandit A, Shalini S, Jagadeesha Prasad MG, **Bansode SB**, Kulkarni MJ, Mukhopadhyay A. Rifampicin reduces Advanced Glycation End products and activates DAF-16 to increase life span in *Caenorhabditis elegans*. **Aging Cell (For revision**)

- Batkulwar KB, **Bansode SB**, Patil GV, Godbole R, Kazi RS, Chinnathambi S, Dhansekharan S, Kulkarni MJ. Investigation of Phosphoproteome in RAGE signalling. (**Communicated to Proteomics**)

Technical Skills

Proteomic techniques known: LCMS^{E}, MALDI-TOF, 2D Gel electrophoresis, western blotting, ELISA

Biophysical methods: Circular Dichroism, Light Scattering, Fluorescence spectroscopy

Biochemical methods: Enzyme and inhibitor kinetics, zymography and other biochemical methods

Computational Tool: ProteinLynx Global Server, Homology modeling, protein-small molecule docking and other web based bioinformatics tools

Conferences and presentations

- Poster presentation in International Symposium on Proteomics Beyond IDs... and 4th Annual Meeting of Proteomics Society (INDIA), India in November 2012

- Presented project on biomethanation of biogas produced from Mother liquor at university level in AVISHKAR- 2008 at inter-university research project Competition held by University of Pune.

- Participation in 93rd Indian Science Congress, Hyderabad. (Jan- 2006)

References

Dr. Mahesh J. Kulkarni   Dr. Ashok P. Giri
NCL, Pune, India   NCL, Pune, India
mj.kulkarni@ncl.res.in   ap.giri@ncl.res.in